Synthesis and investigation of nanostructured polymer composites based on heterocyclic esters and carbon nanotubes

Liubov Bardash

Année 2011

THESE

présentée

devant l'**INSTITUT DE CHIMIE MACROMOLECULAIRE – KYIV (UKRAINE)**

et

l'**UNIVERSITE CLAUDE BERNARD - LYON 1 – LYON (FRANCE)**

pour l'obtention

du DIPLOME DE DOCTORAT

spécialité « **MATERIAUX POLYMERES et COMPOSITES** »

Soutenance proposée le 28 September 2011

par

Mlle. **Liubov BARDASH**

Synthèse et Caractérisation de Composites Polymères Nanostructurés à Base d'Esters Hétérocycliques Chargés de Nanotubes de Carbone

Directeur de thèse : Mme. Gisèle BOITEUX (France)
M. Alexander FAINLEIB (Ukraine)

JURY:

Mme. Gisèle BOITEUX	Directeur de thèse
M. Jean-Marc SAITER	Rapporteur
Mme. Eliane ESPUCHE	Examinateur
M. Gérard SEYTRE	Examinateur
M. Alexander FAINLEIB	Directeur de thèse
Mme. Tatiana ALEKSEEVA	Rapporteur
M. Yevgen MAMUNYA	Examinateur
M. Vladimir MIKHALCHYK	Rapporteur

UNIVERSITE CLAUDE BERNARD - LYON 1

Président de l'Université	**M. A. Bonmartin**
Vice-président du Conseil d'Administration	M. le Professeur G. Annat
Vice-président du Conseil des Etudes et de la Vie Universitaire	M. le Professeur D. Simon
Vice-président du Conseil Scientifique	M. le Professeur J-F. Mornex
Secrétaire Général	M. G. Gay

COMPOSANTES SANTE

Faculté de Médecine Lyon Est – Claude Bernard	Directeur : M. le Professeur J. Etienne
Faculté de Médecine et de Maïeutique Lyon Sud – Charles Mérieux	Directeur : M. le Professeur F-N. Gilly
UFR d'Odontologie	Directeur : M. le Professeur D. Bourgeois
Institut des Sciences Pharmaceutiques et Biologiques	Directeur : M. le Professeur F. Locher
Institut des Sciences et Techniques de la Réadaptation	Directeur : M. le Professeur Y. Matillon
Département de formation et Centre de Recherche en Biologie Humaine	Directeur : M. le Professeur P. Farge

COMPOSANTES ET DEPARTEMENTS DE SCIENCES ET TECHNOLOGIE

Faculté des Sciences et Technologies	Directeur : M. le Professeur F. Gieres
Département Biologie	Directeur : M. le Professeur F. Fleury
Département Chimie Biochimie	Directeur : Mme le Professeur H. Parrot
Département GEP	Directeur : M. N. Siauve
Département Informatique	Directeur : M. le Professeur S. Akkouche
Département Mathématiques	Directeur : M. le Professeur A. Goldman
Département Mécanique	Directeur : M. le Professeur H. Ben Hadid
Département Physique	Directeur : Mme S. Fleck
Département Sciences de la Terre	Directeur : Mme le Professeur I. Daniel
UFR Sciences et Techniques des Activités Physiques et Sportives	Directeur : M. C. Collignon
Observatoire de Lyon	Directeur : M. B. Guiderdoni
Ecole Polytechnique Universitaire de Lyon 1	Directeur : M. P. Fournier
Ecole Supérieur de Chimie Physique Electronique	Directeur : M. G. Pignault
Institut Universitaire de Technologie de Lyon 1	Directeur : M. le Professeur C. Coulet
Institut de Science Financière et d'Assurances	Directeur : M. le Professeur J-C. Augros
Institut Universitaire de Formation des Maîtres	Directeur : M. R. Bernard

Year 2011

THESIS

presented

in **INSTITUTE OF MACROMOLECULAR CHEMISTRY – KYIV (UKRAINE)**
and
UNIVERSITY CLAUDE BERNARD – LYON 1 – LYON (FRANCE)

for obtaining

DIPLOMA OF CANDIDATE OF SCIENCE

speciality « POLYMERS AND COMPOSITES MATERIALS »

Defence of the thesis will be held on 28 September 2011

by

Ms. **Liubov BARDASH**

Synthesis and Investigation of Nanostructured Polymer Composites Based on Heterocyclic Esters and Carbon Nanotubes

Thesis supervisors : Mr. Alexander FAINLEIB (Ukraine)
Mme. Gisele BOITEUX (France)

JURY:

Mme Gisèle BOITEUX
Mr. Jean-Marc SAITER
Mme. Eliane ESPUCHE
Mr. Gérard SEYTRE
Mr. Alexander FAINLEIB
Mme. Tatiana ALEKSEEVA
Mr. Yevgen MAMUNYA
Mr. Vladimir MIKHALCHYK

AknowledgementS

This research was completed en cotutelle in Institute of Macromolecular Chemistry of the National Academy of Science of Ukraine and Laboratoire des Materiaux Polymeres et Biomateriaux (Laboratory of polymer materials and biomaterials), Ingenierie des Materiaux Polymeres (I.M.P@ Lyon 1) C.N.R.S, Universite Claude Bernard Lyon 1, Universite de Lyon under French Ambassy/Foreign office (Ministère des Affaires Etrangères) grant for PhD students and Région Rhône-Alpes grant "EXPLORADOC 2008-2009"

Gratitudes

I am very much obliged to people whose tolerance and invaluable help made it possible to fulfil this research successfully. They have applied many efforts for goal achievement of this research. Namely they are :

UKRAINIAN SIDE	FRENCH SIDE
Alexander ***FAINLEIB***	*Gisele* ***BOITEUX***
Valery ***KORSKANOV***	*Gerard* ***SEYTRE***
Olga ***GRIGORYEVA***	*Andrzej* ***RYBAK***
Olga ***STAROSTENKO***	*Philippe* ***CASSAGNAU***
Kristina ***GUSAKOVA***	*Flavien* ***MELIS***
Yevgen ***MAMUNYA***	*Olivier* ***GAIN***
Maksym ***IURZHENKO***	*Chantal* ***TOUVARD***
Volodymyr ***LEVCHENKO***	*Sylvie* ***NOVAT***
Inna ***DANILENKO***	*Eliane* ***ESPUCHE***
Olga ***PURIKOVA***	*Jean-Michel* ***LUCAS***
	Pierre ***ALCOUFFE***
	Erisela ***NIKAJ***
	Ahmed ***MESKINI***
	Denis ***DANIRON***

POLISH SIDE
Jacek ***ULAŃSKI***
Remigiusz ***GRYKIEN***
Ireneusz ***GŁOWACKI***
Marcin ***PASTORCZAK***

CONTENT

General Introduction

At the one of the first conferences on nanotechnology that was held at the Institute for Molecular Manufacturing in Palo Alto (California, USA) in October 1989 [1], delegates from Japan announced that for several years their country considers the development of molecular systems as the basis for the XXI century technologies and "if the rest of the world wants to participate in joint development of nanotechnologies it would be better to wake up and start acting". Now you can confidently assert that one of the most promising directions of development of modern science is nanotechnology. Basic on the title of "nanotechnology" one can say that this scientific direction works with objects, which size is in nanoscale (term "nano" means 10^{-9} m). Thus, nanotechnology is the process of obtaining and use of materials that consist of nanoparticles (nanomaterials, nanocrystals, nanocomposites, etc.) [2].

It is well known that nanofilled polymer materials are more efficient and economically sound in comparison with conventional polymers or polymer composites, because they are characterized by significantly enhanced mechanical, thermal, electrical and other properties, even at low (up to several percents) nanofiller loading due to its specific interaction with polymer matrix at the nanoscale. There are many types of nanoparticles that can be the potential nanofillers for polymer systems. For example, inorganic nanoparticles: nanoparticles of gold, silver, calcium phosphate, silicates; molecular nanostructures: dendrimers, carbon nanotubes (CNTs), fullerenes; nanofibers; graphene; natural nanomonocrystals: quartz monocrystals, rock salt, Iceland spar, diamond, topaz etc. [2]. However, since recent time an attention of scientists is focused on the study of structure-properties relationship of CNTs due to their unique properties as well as the CNTs-containing polymer nanocomposites [2-32].

Carbon nanotube is a cylindrical structure with a diameter from one to several tens of nanometers and length up to tens of micrometers, consisting of one or more hexagonal planes of graphite (graphene) rolled up to tubes usually ended by hemispherical head [28]. CNTs are currently the most promising nanomaterial, which can optimize the

characteristics of materials used in various industries (microelectronics, airspace and automotive industries etc.). CNTs are characterized by high elasticity owing the large aspect ratio of length (*L*) and diameter (*D*) (L/*D*>1000) and have high strength (≥ 30 Giga Pa) and Young's modulus (≥ 1 Tera Pa). CNTs can be conductor like metals or semiconductor: they can transport electrons over long distances without significant interruption that makes them more effective than copper [3, 4]. This unique combination of mechanical and electrical properties makes CNTs to be an ideal reinforcing agent for many materials and products including polymers.

Information about the first polymer nanocomposites containing as filler CNTs was published in 1994 by Ajayan et al. [5]. Since that time thousands works presented the results on creation of new CNTs-containing polymer nanocomposites with a unique complex of physical-chemical, mechanical and electrical properties were published [2-28]. In order to create CNTs-containing polymer nanocomposites the most important is to ensure effective dispersion of CNTs in polymer matrix and to achieve high adhesion between nanotubes and polymer, for example, by chemical modification (functionalization) of CNTs surface.

Nanocomposites containing CNTs have already found commercial applications: in the electronics industry for protecting integrated circuits from anti-static shock, in the automotive industry for preventing electrostatic stress in the fuel lines and pumps; for producing ultrastrong threads, nanowires, transparent conductive surfaces, in chemical industry for encapsulation of active molecules, etc. [27, 28]. As the polymer matrix in CNT-containing nanocomposites the various thermoplastic and thermosetting polymers are used. However, recent studies have shown that one of the most promising methods of obtaining polymer/CNTs nanocomposites is their producing from monomers or oligomers (having low viscosity) in the presence of CNTs (i.e. *in situ* synthesis). At such conditions the greatest efficiency of dispersion of nanotubes in polymer matrix formed is achieved and, therefore, one can expect high efficiency from using of CNTs in polymer nanocomposite.

Heterocyclic esters, namely, cyclic oligomers of butylene terephthalate and oligomers of cyanate esters of bisphenols, are a promising class of reactive oligomers for the synthesis of thermostable CNTs-containing polymer nanocomposites with a complex of properties that can be controlled within a wide range by changing synthesis conditions,

content of CNTs, and method of forming of polymer material and so on. At the beginning of the work on this thesis any publications on this subject were not available. So, investigation in this field of nanoscience and nanotechnology, in fact, only launched.

Urgency of the topic. Synthesis of polymer composites is an alternative way to create new polymer materials with a valuable complex of properties that satisfy the requirements of high-tech industries. Search for new or modified monomers and oligomers, as well as fillers of different nature, which enable the controlled regulation of the whole complex of physical, chemical and mechanical properties of polymer materials and composites and, especially, changes in these properties over a wide range, is the urgent task of Macromolecular Chemistry. Over the last decade the interest in nanofillers, and aspecially CNTs, has increased significantly. It is known that using of nanofillers leads to the creation of new nanocomposites having an exceeding complex of properties in comparison with conventional composites. It is economically beneficial as it enables both to save material resources and to reduce the weight of composite product, article, which is important for high-tech industries such as airspace, microelectronics, etc. An additional advantage of CNTs-containing nanocomposites is that depending on the content of CNTs they can be both dielectrics and exhibit electrical conductivity in a wide range with low percolation threshold. In terms of the polymer component, the nanocomposites obtained by *in situ* polymerization of low viscosity oligomers, which usually provides effective dispersion of nanoparticles in a polymer matrix formed are of special interest.

Oligomers of cyanate esters of bisphenols (Cyanate Ester Resins), cyclic oligomers of esters, for example, cyclic oligomers of butylene terephthalate, are perspective oligomers for producing thermostable nanocomposites. These oligomeric esters can be grouped under common name heterocyclic esters. During polycyclotrimerization of dicyanate ester of bisphenol A polycyanurate network (PCN) is formed. Polycyanurates are high crosslink densely polymers with a unique combination of physical and chemical properties, namely high thermal- and heat resistance, high glass transition temperature (T_g > 520 K) and fire resistance, high adhesion to various substrates (metals, carbon-, organic and glass fiber plastics, etc.). PCNs are recognized dielectrics with low value of dielectric constant ($\varepsilon \approx 2.5 \div 3.2$), PCNs does not practically absorb water and so on.

Cyclic oligomers of butylene terephthalate (CBT) easily transform under certain conditions of synthesis to poly(butylene terephthalate) (cPBT) with the properties

attributed to the classical PBT. Review of the literature has shown that research on the synthesis and properties characterization of nanostructured polymer composites of oligomeric heterocyclic esters and carbon nanotubes are only in the beginning stage. So far comprehensive investigations of kinetics of polymerization reactions, as well as of structure-properties relationships for nanocomposites based on PCN and PBT filled with CNTs have not been carried out yet. The influence of the forming method of PBT/CNTs nanocomposites on their morphology and thermal properties was not investigated, the range of changing electrical properties of PBT/CNTs and PCN/CNTs nanocomposites with varying CNTs loading has not been established yet, etc. Therefore, one of the urgent tasks of Macromolecular Chemistry is development of methods of synthesis of polymer nanocomposites from oligomers of heterocyclic esters and carbon nanotubes and establishment of relationship between synthesis conditions, composition and structure and basic physical and chemical properties of the nanostructured materials produced.

Links with scientific programs, plans, themes. This study was performed at Department of Chemistry of Heterochain Polymers and Interpenetrating Polymer Networks of Institute of Macromolecular Chemistry of the National Academy of Sciences of Ukraine (IMC NASU) according to the scientific planes of the Institute in the framework of Ukraine state budjet themes: "Creation of nanostructured and functional polymer materials" (2007-2010); "Development of nanotechnology of production of hybrid organic-inorganic composite nanomaterials with high heat resistance and adhesion strength and low dielectric loss for the elements of aircrafts, space and microelectronics industries" (2010-2014). Part of the work on the thesis was also fulfilled at IMP@LYON1 of University Claude Bernard Lyon 1 (CNRS, France) according to “Agreement for international joint supervision of a thesis” between IMC NASU and University Claude Bernard Lyon 1 and with the concurrence of the Highest Attestation Commission of Ukraine (№ 03-76-07/335 of 05.02.2008).

The aim and the tasks of the research. *The* ***aim of the study*** is to develop the methods of synthesis of heat-resistant polymer nanocomposites from oligomers of heterocyclic esters of different chemical structure in the presence of multiwalled carbon nanotubes and to establish a relationships between the conditions of synthesis, composition and viscoelastic, thermal-physical, thermal and electrical properties of the nanostructured materials obtained.

Realization of this aim supposed to solve the ***following tasks***:

- to develop the methods of preparing of new polymer nanocomposites from cyclic oligomers of butylene terephthalate or oligomers of dicyanate ester of bisphenol A by in situ synthesis in the presence of MWCNTs;

- to identify the morphological features, dimensional characteristics, structure and properties of MWCNTs used, to optimize the methods of their dispersing in the oligomers of heterocyclic esters, and to determine the optimal methods of forming the samples of nanomaterials;

- to study the influence of MWCNTs and their content on kinetics of reactions of Ring-Opening Polymerization (ROP) of cyclic butylene terephthalate oligomers with formation of linear Poly(butylene terephthalate) and polycyclotrimerization of oligomers of dicyanate ester of bisphenol A during synthesis of polycyanurate network;

- to study the influence of linear or crosslinked structure of polymer matrix, forming conditions and composition of nanocomposites on morphology and viscoelastic, thermal-physical, thermal, electrical and other physical-chemical properties of the nanostructured polymer materials obtained.

The object of the research. Obtaining of new nanostructured polymeric composites by *in situ* synthesis of polymers with oligomeric heterocyclic esters containing a filler.

The subject of the research. Synthesis of new nanostructured polymeric composites based on linear Poly(butylene terephthalate) from cyclic oligomers of butylene terephthalate or crosslinked polycyanurates from oligomers of dicyanate ester of bisphenol A and MWCNTs and establishment of the impact of the nanofiller on specific properties of polymer matrix formation and the main characteristics of the nanocomposites obtained.

Methods: kinetics of chemical reactions and chemical structure - Fourier Transform Infra-Red spectroscopy (FTIR), melt rheometry, Raman spectroscopy; phase structure and morphology of composites were investigated using Scanning Electron Microscopy (SEM), Transmission Electron Microscopy (TEM) and Differential Scanning Calorimetry (DSC); to determine the relaxation characteristics - Dynamic Mechanical Thermal Analysis (DMTA), thermal stability was determined by the method of Thermogravimetric Analysis (TGA). The methods of determination of thermal

conductivity and electrical conductivity under an alternative or direct current were also used.

Scientific novelty of the results: in the study for the first time the nanocomposites from cyclic oligomers of butylene terephthalate or oligomers of dicyanate ester of bisphenol A and MWCNTs were obtained using *in situ* method. For the first time the kinetic regularities of both the reaction of Ring-Opening Polymerization (ROP) of cyclic butylene terephthalate as well as polycyclotrimerization of dicyanate ester of bisphenol A in the presence of CNTs were studied. For the first time the influence of the forming method of samples of the nanocomposites synthesized from the cyclic butylene terephthalate in the presence of CNTs on the morphology, thermal, mechanical, and electrical properties of the materials obtained was found. Percolation thresholds of electrical conductivity for both the types of nanocomposites have been determined. For the first time it has ben established that at PCN synthesis the presence of MWCNTs in the reaction mixture hinders reaching higher conversion of cyanate groups leading to formation of polycyanurate network of lower crosslink density that is confirmed by reducing glass transition temperature of PCN. However, the nanocomposites obtained have high thermal stability and improved strength properties.

The practical significance of the results. The regularities found are the basis for creation of new efficient nanostructured polymer composites. The possibility to regulate the physical-chemical properties of the latter over a wide range by varying CNTs content has been found. The practical significance of the work is the possibility to expand the functionality and the areas of practical application of high performance CNTs-containing polymer nanocomposites based on poly(butylene terephthalate) or polycyanurate network, creation of nanomaterials of improved mechanical and thermal characteristics, conductors or insulators (depending on CNTs content), applicable as adhesives, coatings, compounds, etc. in airspace industry, microelectronics and others.

Applicant's personal contribution in the presented thesis was the search and analysis of corresponding literary data, carrying out experimental and theoretical research work, analysis and interpretation of the results obtained as well as formulating the conclusions of the fulfilled scientific investigatons. Problem definition and determination of the research objectives, a part of theoretical and experimental studies were performed in conjunction with the research supervisor, Prof., Doctor. Sci. Fainleib A.M. in collaboration with

Doctors Korskanov V.V., Grigoryeva O.P., Starostenko O.N. and Gysakova K.G. in the IMC NASU (Kyiv, Ukraine). Planning and execution of theoretical and experimental studies were also performed in conjunction with scientific supervisor, Head of research CNRS, Doctor Boiteux G., involving Director of Laboratory of polymer materials and biomaterials of University Claude Bernard Lyon 1, CNRS, France, Doctor Seytre G., Professor Cassagnau Ph., Doctor Rybak A., and Doctor Gain O. in the IMP@LYON1 (CNRS, France), as well as in conjunction with Professor Ulanski J, head of Department of Molecular Physics, Technical University of Lodz, Poland. Applicant took a part in preparation of publications and presentation the results on international conferences and symposia.

Approbation of the results. Results of the research were presented at scientific conferences: XI Ukrainian Conference on Macromolecular Compounds (October 1-5, 2007, Dnipropetrovsk, Ukraine), VI Open Ukrainian conference of young scientists from Macromolecular Chemostry "IMC-2008", Kiev, Ukraine, September 30 - October 3, 2008, 4th International Symposium on Nanostructured and Functional Polymer-Based Materials and Nanocomposites (April, 16-18, 2008, Rome, Italy), 5th International Conference on Broadband Dielectric Spectroscopy and Its Applications (BDS2008 (August, 25-29, 2008, Lyon, France), International conference "Nanostructured Systems: Technology - Structure - Properties - Applications" (NSS-in 2008) (Uzhgorod "Vodogray", Ukraine, October, 13-16, 2008), 5th International ECNP conference on nanostructured polymers and nanocomposites (Paris, France, April 15-17, 2009) World Forum on Advanced Materials "POLYCHAR 17" (Rouen, France, April, 20-24, 2009), Polymer Reaction Engineering 7 (Niagara Falls, Canada, May, 3-8, 2009), Eurofiller 2009 (Alessandria, Italy, June 21-25, 2009), XII Ukrainian Conference on Macromolecular Compounds,18-20 October 2010, Kyiv, Ukraine), and *etc*.

Publications. The applicant is the author of 23 scientific applications, including 6 articles in scientific journals, 2 patents and 15 abstracts and materials of the conferences.

Chapter 1

Modern conceptions of synthesis and characterization of polymer nanostructured composites based on heterocyclic esters filled by carbon nanotubes

(LITERATURE REVIEW)

1.1. Synthesis, structures and properties of carbon nanotubes

1.2. Nanocomposites based on thermoplastic poly(butylene terephthalate) from cyclic butylene terephthalate and carbon nanotubes

1.3. Nanocomposites based on thermosetting heterocyclic polycyanurates and single-walled carbon nanotubes (SWCNTs)

1.4. Structure-property relationships for nanocomposites based on polycyanurates and multi-walled carbon nanotubes (MWCNTs)

1.1. Synthesis, structures and properties of carbon nanotubes

In this chapter the recently published works on development and characterization of structure-properties relationships for polymer nanocomposites containing different types of carbon nanotubes (SWCNTs, MWCNTs, and functionalized CNTs) have been analyzed. Note that due to rapid development of the nanoscience during last 15-20 years large number of reviews, book chapters and books related to advantages in the field of nanomaterials and nanotechnologies have been published [2-44]. According to the topic of the thesis the main attention in this chapter is attended to analysis of scientific pudlications on synthesis, structure and properties of CNTs-filled nanostructured polymer composites obtained from heterocyclic esters of different chemical architecture.

It is known that CNTs were discovered accidentally. In 1991 Japanese scientist Iijima evaporated graphite in electrical arc and obtained on cathode the precipitate consisting of very thin threads and fibers [45]. The study of the precipitate with an electron microscope revealed that the diameter of these filaments was only a few nanometers, and the length reached several micrometers (Fig. 1.1). They were the first multiwall CNTs investigated; it was found that they consisted of different numbers of graphene layers. There are also references to earlier discovery of carbon nanotubes. So in 1976 Oberlin et al. [46] have published work describing the thin carbon tubes with diameters less than 100 Å, which were obtained by chemical vapor deposition, but more detailed investigation of the structure of these tubes was not carried out. Group of Russian scientists in 1977 recorded the formation of "hollow carbon dendrites" [47], the mechanism of their formation was proposed and structure of the walls was describe. "Nature" [48] has informed in 1992 that CNTs were observed even in 1953. In 1952 Radushkevich and Lukyanovich [49] reported of electron microscopic detection of fibers with a diameter of about 100 nm obtained by thermal decomposition of carbon monooxide on an iron catalyst. Unfortunately, all these studies were not extended.

Nanocomposites containing carbon nanotubes are of a great interest nowadays because they have outstanding complex of properties. There are some recently published books and fundamental reviews on CNTs [10 – 15], several scientific journals dedicated to

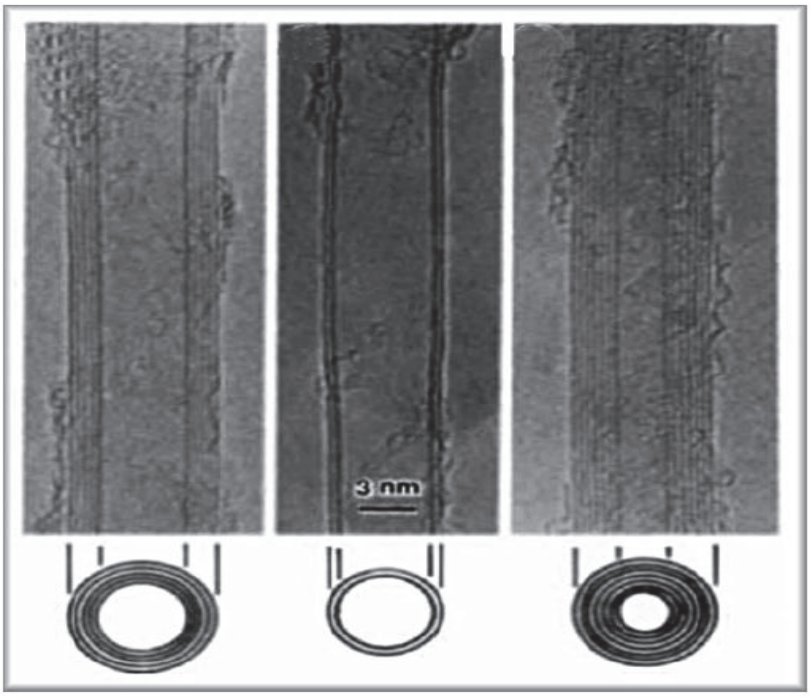

Fig. 1.1. First electronic micrographs of multiwall carbon nanotubes, MCBHTs [45].

nanoscience and nanotechnology and specialized journals: *Fulleernes, Nanotubes and Carbon nanostructures; Carbon Nanotechnology; The Science and Technology of Carbon Nanotubes; Science of Fullerenes and Carbon Nanotubes*, and ect.

Typically, CNTs are long tiny cylinders of graphite structure with cap at each end (Figs. 1.1-1.3). The length of these nanotubes ranges from few tens of nanometers to several micrometers, and the wall thickness 0.07 nm. CNTs are classified as either single-, double- or multi-walled nanotubes (SWCNTs, DWCNTs MWCNTs respectively) [4, 6, 18]. SWCNTs consist of only a single cylinder, DWCNTs – from two and MWCNTs consists of 3 to ≤ 30 concentric tubes. SWCNTs have an average diameter of 1.2 – 1.4 nm, DWCNTs outer diameter is in the range of 1.3 – 5 nm and 10 – 50 nm for MWCNTs. The aspect ratio for CNTs is on average 100 – 3000 [4, 7-9, 10, 12-16]. CNTs can be considered as a graphene sheet (graphene is a monolayer of sp^2-bonded carbon atoms) rolled into a seamless cylinder. The carbon atoms in the cylinder have partial sp^3 character that increases as the radius of curvature of the cylinder decreases. MWCNTs consist of nested graphene cylinders coaxially arranged around a central hollow core with interlayer separations of 0.34 nm, indicative of the interplane spacing of graphite.

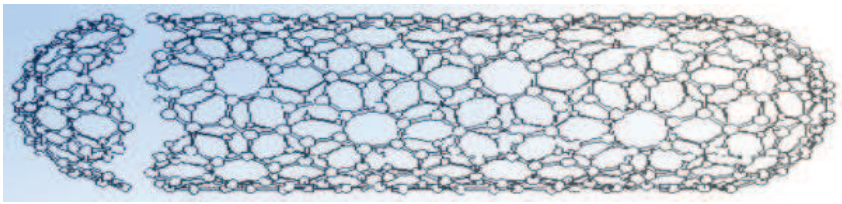

Fig. 1.2. Schematic view of Carbon Nanotube [28].

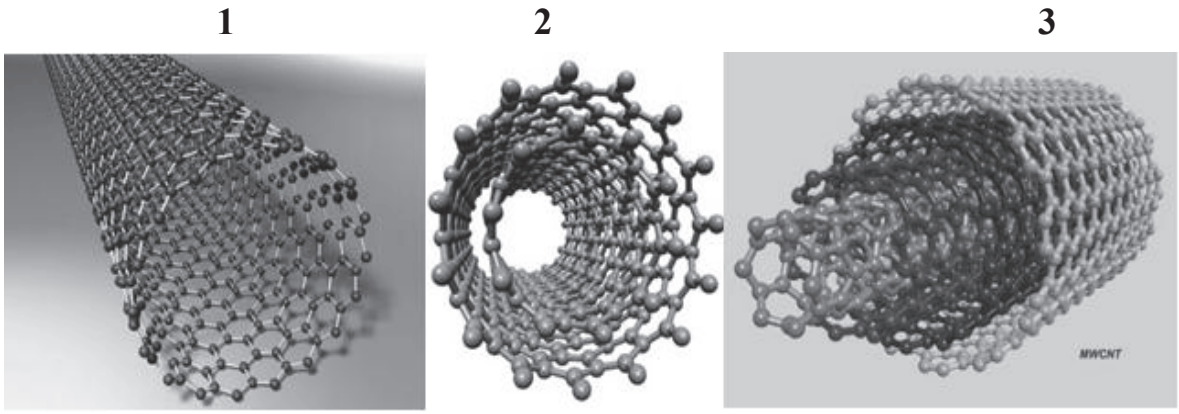

Fig. 1.3. Schematic drawing of: 1 – Single-walled carbon nanotubes (SWCNTs), 2 – Double-walled carbon nanotubes (DWCNTs), 3 – Multi-walled carbon nanotubes (MWCNTs) [42].

The C–C bond length is a_{cc} = 0.14 nm, hence shorter than that in diamond, indicating greater strength [16]. The unique structure provides exceptional properties of CNTs. The range of values of SWNT tensile modulus is E = 1 to 1.5 TPa (that of diamond 1.2 TPa), tensile strength is 11 to 63 GPa (10-100 times higher than the strongest steel at a fraction of the weight) [4-6, 9, 16]. Electrical resistivity is about 10^{-4} W-cm, thermal conductivity 2 kW/(m·K), thermal stability in vacuum up to 2800°C [16-18]. In addition hollow structure of CNTs makes them very light: specific weight varies from 0.8 g/cm^3 to 1.8 g/cm^3.

Nanotubes form different types which can be described by chiral vectors (n, m) [4, 16]. Basically, one can roll up the graphene sheet along one of the symmetry axis: this gives armchair, chiral or zig-zag nanotube (Fig. 1.4). Chirality of CNTs, affects the conductance of the nanotube. CNTs can be metallic (armchair type) or semi-conductung (chiral and zig-zag).

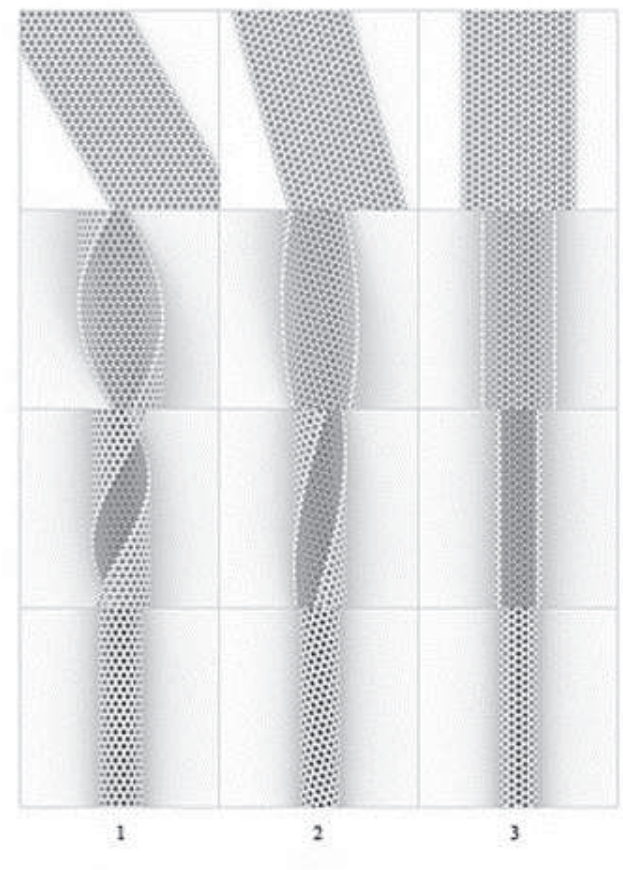

Fig. 1.4. Formation of Carbon Nanotube of different chirality: 1 – Zig-Zag (n, 0), 2 – Chiral (n, m) and 3 – Armchair (n, n) [28] .

Recent studies have shown that the CNTs belong to one of the most strong and hard materials in the world [29-32]. This is due to two reasons: first, it is a carbon-carbon bond - one of the strongest in a nature (Table 1.1). Secondly, the carbon-carbon bond in nanotubes is oriented along the axis that increases their strength more. Because of the specific unique structure the CNTs have very high values of Young's modulus (> 1 Tera Pa) and strength (> 30 Giga Pa) [42-44].

Table 1.1. Energy of homonuclear bonds [29]

Chemical bonding	**C–C**	**N–N**	**O–O**	**Si–Si**	**P–P**	**S–S**
Bonding energy (kJ/mol)	348	163	146	226	201	264

However, the hollow structure of the CNTs makes them extremely light: specific weight ranges from 0.8 (for single-wall CNTs) to 1.8 g/cm^3 (for multi-walled CNTs), for comparison, the specific weight of graphite is ~ 2.26 g/cm^3 [43, 44, 49]. From a theoretical point of view in CNTs-containing nanocomposites Young's modulus can be as high as in the individual CNTs if between nanotubes and polymer matrix will be close (on a nanoscale) bonding and, therefore, even at very low concentrations of CNTs in the polymer matrix, loading can effectively be transmitted to each individual carbon nanotube [41]. One can say that to achieve high physical-mechanical properties of the nanocomposite the problem of efficient dispersing of CNTs in polymer matrix has to be solved. It is clear that chemical purity of CNTs and their functionalization can significantly affect the properties of polymer nanocomposites obtained on their base [24-27, 41, 50-52].

As it was noted above, the CNTs consist of one or more hexagonal layers of graphene rolled up into a hollow cylinder. Graphene in turn is a flat two-dimensional layer of the regular hexagon of carbon atoms (Fig. 1.5) [29, 30]. If to cut out a rectangle from the graphene layer and to connect its opposite edges, a seamless hollow cylinder is formed, i.e. SWCNTs. Ideal surface SWCNT contains only regular hexagon of carbon atoms [35]. Such nanotube is a cylinder, open at both ends. However, these nanotubes can be closed with one or even both sides, such as semi fulerenovoho type, but these nanotubes are not ideal - besides their regular hexagon surface will contain a pentagon or a triangle (Fig. 1.6).

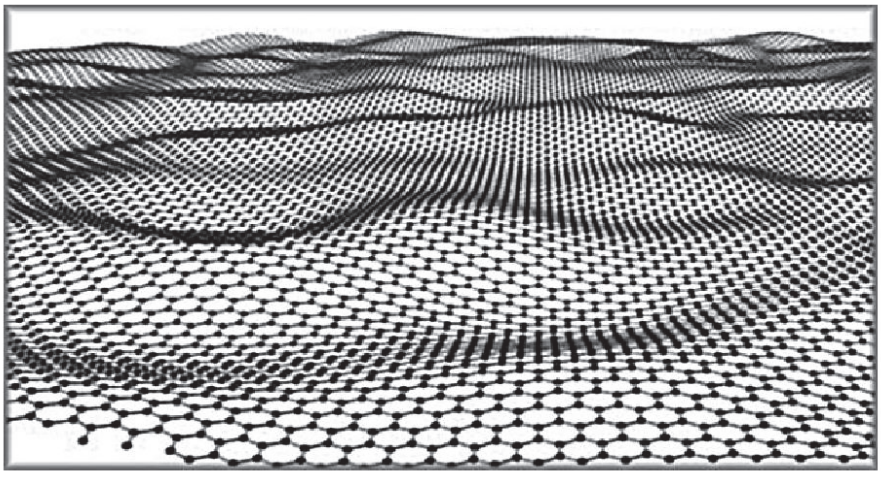

Fig. 1.5. Structure of graphene monolayer [29].

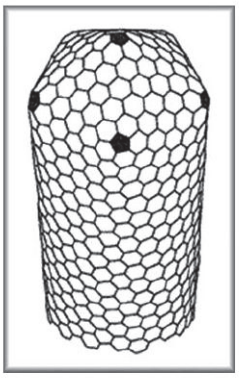

Fig. 1.6. Closed carbon nanotubes, containing five-members cycles [35].

There are a number of methods for producing CNTs that involve high temperatures: the carbon arc (CA) discharge, pulsed-laser vaporization (PLV) of graphite, thermal or plasma-assisted chemical vapor disposition of hydrocarbons (CVD), gas-phase catalytic growth from carbon monoxide [18, 19]. CNTs can also be produced by diffusion flame synthesis, electrolysis, use of solar energy, heat treatment of a polymer, and low-temperature solid pyrolysis, ball milling of graphite powder with subsequent annealing. However the mechanisms of these processes are less studied and it has been unclear how to scale up production to the industrial level using such approaches [17-19].

Chemical vapor deposition of hydrocarbons is a classical method that has been used to produce various carbon materials such as carbon fibers and filaments for over twenty years. The CVD method gives great purity MWCNTs with high aspect ratio. CNTs can be produced in large quantity and low cost by this method. These high-temperature processes are rather efficient and robust, but yield a mixture of metallic and semiconducting tubes, and a mixture of (n, m) nanotube chiral indices.

What the properties make nanotubes to be a promising object for future nanotechnologies? First, as shown above, they have very high mechanical strength – SWCNTs are much stronger than steel. Nanotubes - is not the first carbon material based on graphite, carbon fibers are widely known, they are formed from long and thin layers of graphite [2, 17, 23]. However, the nanotubes - is the strongest carbon fiber. Introduction of CNTs can increase thermal and electrical conductivity of the polymer material, significantly improve its mechanical characteristics and add to composite the new

functional properties (the ability to remove static charges, dissipate and absorb radio waves, laser radiation, enhance electroluminescence), etc. [24 - 27, 41, 50-52].

Recently, much attention has been given to the use of CNTs in composite materials to improve their exceptional mechanical and electronic properties. Basically, for obtaining conductive CNTs-polymer composites, the highly electrical conductive CNTs filler is dispersed into the polymer matrix. Hence, a three-dimensional conductive network of the CNTs in the polymer matrix is obtained.

There are some important issues in integration of CNTs to polymer matrix. To maximize the advantage of CNTs as effective reinforcements in high performance composites, they should not form aggregates and must be well dispersed to prevent slippage. So, the first issue is using exfoliated CNTs (or slightly bundled CNTs). There are several techniques to improve the dispersion of CNTs in polymer matrices, such as by optimum physical blending, in-situ polymerization and chemical functionalization [16, 20-22].

Like in fullerenes, the surface of nanotubes can be modified by chemical means that enables even to transform them to a soluble state [43]. Due to the high specific surface the nanotubes can be used as a substrate for heterogeneous catalysts. Unique electronic properties of nanotubes make possible to use them in constructions of diodes, transistors, electronic guns and probe microscopes [26]. Mechanical strength of nanotubes is used in composite materials for producing super light weight and super strong tissues for clothing of fire fighters, astronauts and others. CNTs - is one of the important components of electromechanical nanodevices. So there are many fields of application of nanotubes. Now the main task for the researchers is to create a technology, which will enable to obtain homogeneous nanotube of terged size, shape and properties.

1.2. Nanocomposites based on thermoplastic poly(butylene terephthalate) from cyclic butylene terephthalate and carbon nanotubes

Beside conventional polymer composites (fiber reinforced with carbon fiber, glass fiber, nylon etc.) CNTs-containing polymer nanocomposites became the most versatile industrial advanced materials [20-22, 53-86]. Polymer nanocomposites based on commercially available Thermoplastics (TP) filled with CNTs have a high potential for

production of different devices for electronic equipment. In the past decade a variety of CNTs-filled TP polymer nanocomposites were developed and their properties were investigated [26, 41, 42, 53-55].

For preparation of high performance polymer/CNTs nanocomposites the decisive factor is effective dispersing of CNTs in polymer matrix. The main routes to formation of TP/CNTs nanocomposites are: (1) by dispersing CNTs in solution of polymer followed by solvent evaporation; (2) by dispersing CNTs in solution of monomers followed by polymerization of the latter and then solvent evaporation. Both the methods usually require high-cost and toxic solvents, complicated technological equipment. However, for thermoplastics a third method, melt compounding of polymer with CNTs, is also used [26, 42]. Evidently, the melt compounding is preferred in an industrial scale, but dispersing is less effective.

The alternative approach to produce TP/CNTs nanocomposites is using of recently developed alkylene phthalate cyclic oligomers like cyclic ethylene terephthalate (CET) oligomers, cyclic buthylene terephthalate (CBT) oligomers of low viscosity [87-91] that convert to high-molecular-weight linear polymers – Poly(etylene terephthalate) (cPET), Poly(butylene terephthalate) (cPBT), correspondingly. These macrocyclic oligomers have some important advantages: low viscosity (water-like), the capability of rapid polymerization into high molecular weight polymers (Fig. 1.7) and the ability to be processed like thermosetting resins.

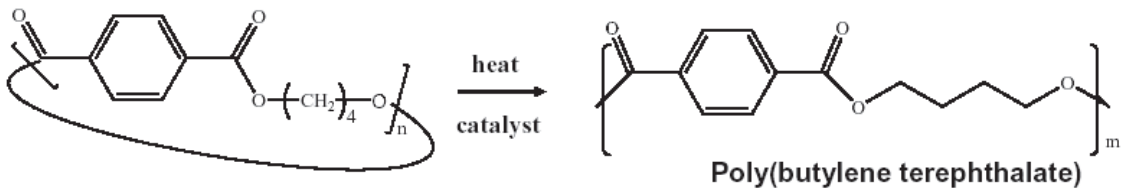

Fig. 1.7. Scheme of CBT polymerization [91].

Particular interest is devoted to PBT, typical engineering thermoplastic polyester, that is extensively used as a raw material for injection-molded articles such as elements for automobiles, electric and electronic equipment, because of easiness of molding as well as excellent mechanical properties, heat resistance, chemical resistance, and other physical-

chemical properties [92].

Method of cPBT synthesis from CBT as well as cBPT-filled composites resin becomes very promising. Basically, CBT resin polymerizes via Ring-Opening Polymerization (ROP) in the presence of tin or titanium-based catalysts that work by a coordination-ligand exchange mechanism [89]. Since CBT oligomers became commercially available, a number of scientific papers on investigation of their polymerization and properties have been published [93-101]. It was reported that CBT oligomers melt and polymerize at temperatures well below the melting point (T_m) of the resulting polymer (T_m of CBT oligomers observed by DSC is around 140 ºC while the T_m of cPBT is around 226 ºC). Thus, polymerization and crystallization can occur isothermally in a narrow temperature interval and, therefore, the time and expenses required for full thermal cycle are favorably reduced. However, the crystallization of the polymer formed occurs simultaneously with polymerization of CBT, therefore, the processing temperature of polymer nanocomposite should exceed the melting temperature (T_m) of the polymer formed. Obviously the properties of cPBT synthesized from CBT should be similar to that of PBT obtained by conventional copolycondensation of 1,4-butanediol and dimethyl terephthalate.

Several works on PBT/CNTs nanocomposites prepared by melt mixing of PBT with CNTs [71, 102, 103] or *in-situ* polymerization of 1,4-butanediol and dimethyl terephthalate in the presence of CNTs [72, 104-106] as well as via dispersion of CNTs in the solution of PBT [107] are published. Electrical, thermal and physical-chemical properties were discussed in details.

A few works on cPBT/CNTs have appeared in recent years [108-111]. Baets et al. in [108] produced nanocomposites based on CBT oligomers and ground MWCNTs with or without glass fiber by vacuum-assisted resin transfer molding (VAPTM). First the oligomers were heated above their melting point (190 ºC) and then, before adding the catalyst, the molten CBT was blended with MWCNTs, using a simple rotational mixer. The catalyst was then added and the resulting mixture was stirred for 20 s. The low viscosity mixture was vacuum infused into a closed mould (at 190 ºC) with or without fibers. The authors noted that significant increase in viscosity was observed when 0.05 wt. % of CNTs was added. Therefore, a lower amount of catalyst was used for the samples

with higher filler loadings [108]. We suppose that such drastic increase of viscosity possibly is explained by the catalytic effect of CNTs on CBT polymerization.

The dispersing efficiency of CNTs in cPBT matrix was investigated by TEM analysis. It is reported [108] that mixing the CNTs with molten low viscosity CBT oligomers using high shearing forces for 5 min only provides a fine dispersion. However, it was observed that some small agglomerates of size up to 2 μm are inhomogeneously distributed in the mixture that authors related to the existence of very strong van der Waals interactions between individual nanotubes preventing a complete exfoliation. Authors reported that addition of CNTs decreased the degree of crystallinity of cPBT/CNTs composite (from 42.5 % for pure cPBT to 39.8 % for cPBT filled with 0.1 wt. % of CNTs). From DSC thermograms (cf. Fig. 1.8) it was observed no significant changes in the shape of melting peak and T_m value and concluded that there was no significant influence of CNTs on the perfection of the crystals. From the observation of crystallization peaks authors reported that CNTs did not act as nucleation agent. We should note that at high loadings the influence of CNTs on cPBT thermal physical behaviour should be much stronger. This was found for nanocomposites based on commercial PBT with CNTs content from 0.2 to 7.0 wt. % [71, 72, 102-105].

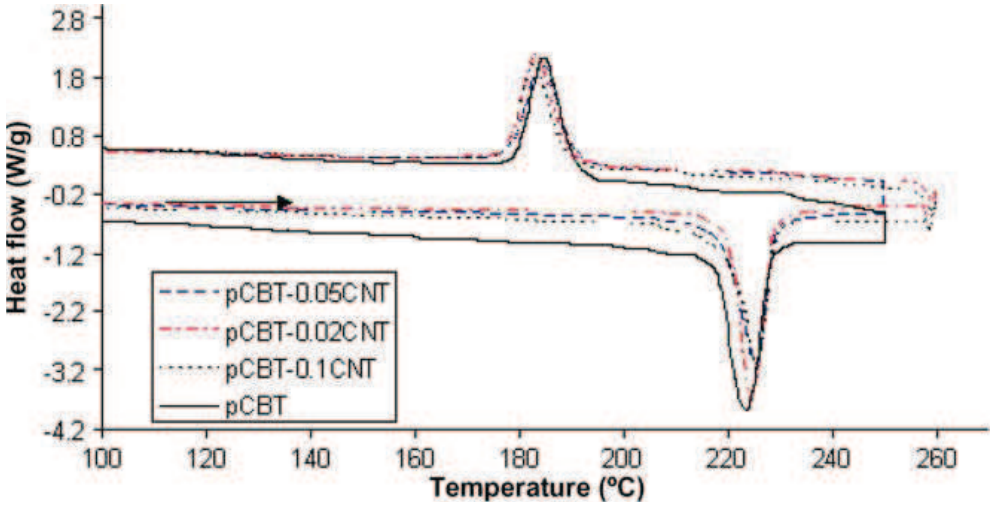

Fig. 1.8. Typical dynamic DSC thermograms (heating - cooling) for individual cPBT and for cPBT with different content of CNTs (indicated on the plot) [108].

Authors [108] observed a significant enhancement of mechanical properties of nanocomposites compared to pure cPBT: stiffness increased by 30 % and strength by 80 %

with adding of 0.05 wt. % of MWCNTs. It was noted that increase of these two properties in turn increased the energy of nanocomposite failure, which is linked to the toughness. These enhanced mechanical properties are a result of direct influence of the CNTs, but not of the changes in polymer matrix: in crystallinity degree or crystal perfection. This shows CNTs efficiency in transferring the applied load and bridging and deflecting cracks. However, to get these benefits, a fine dispersion is required. The addition of CNTs to CBT was also combined with reinforcing fibers. Authors emphasize that with the technique used in their work, it was impossible to produce fine sheets with well dispersed CNTs (cf. Fig. 1.9), because the fiber densely packed in a fabric in the mould filtered out the CNTs from the matrix. Therefore, the CNTs were not homogeneously distributed in the produced sheet, but were concentrated and agglomerated in the resin rich areas between the fiber yarns. Therefore, even after fixing a positive influence of the addition of CNTs to CBT, it was not possible to observe similar effects in a produced composite. It was reported that the production technology had to be modified before making any further conclusions.

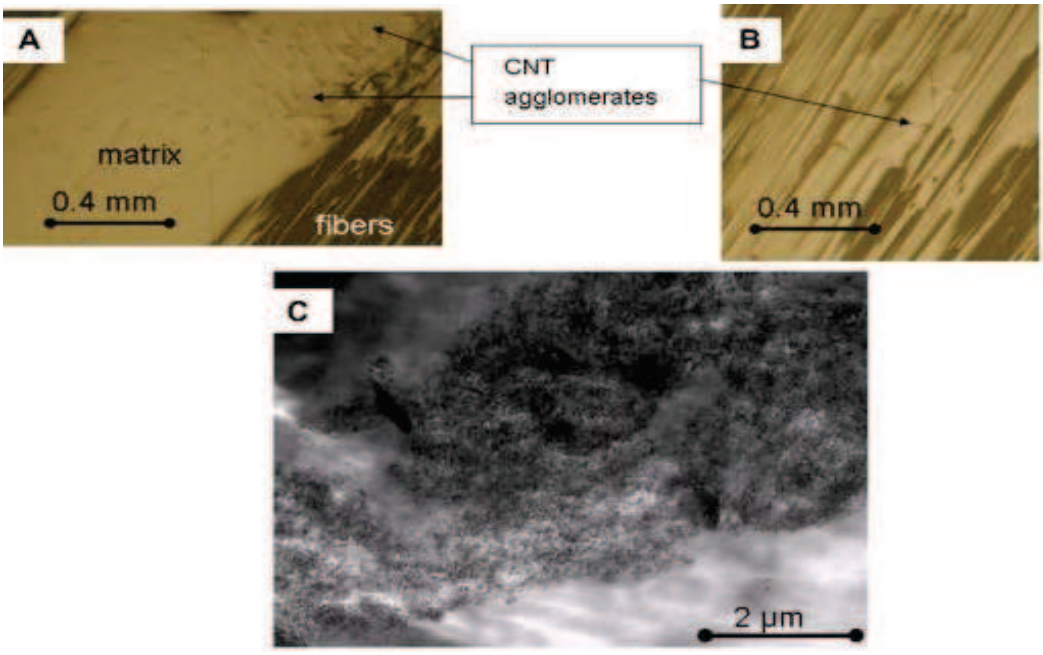

Fig. 1.9. Microphotographs of nanocomposites of fiberglass/cPBT/CNTs (0.02 wt.%): A, B - optical microscopy; C - TEM-microphotographs of CNTs agglomerates [108].

In [109] Baets et al. reported the results of toughening of isothermally polymerized CBT by chemical and physical modification. The in-situ polymerization in the presence of 0.02 wt. % of ground MWCNTs as a physical modifier was reported. cPBT/CNTs nanocomposite was prepared using the thechnique described in [108]. Authors [109] reported a

slight decrease of CBT conversion (96 %) in cPBT/CNTs measured by GPC (cf. Fig. 1.10) that they explained by hindering diffusion of oligomers, leading to slower polymerization. However, authors note that with a longer processing time this would not occur.

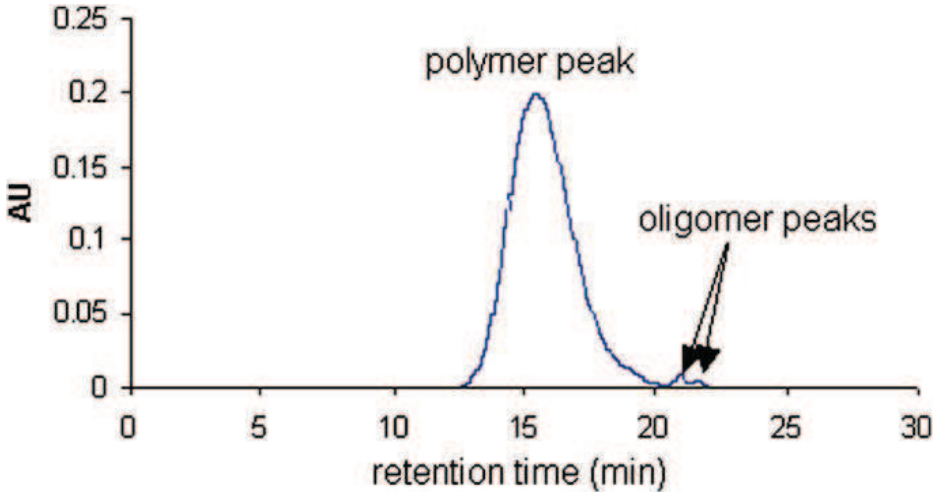

Fig. 1.10. Retention time for the polymer cPBT and oligomer CBT (GPC data) [109].

Nanocomposites based on cPBT and MWCNTs were prepared through the *in-situ* polymerization and *in-situ* compatibilization approach by Wu and Yang in [110, 111]. In both works authors obtained cPBT covalently attached onto the MWCNTs surface via *in-situ* ring-opening polymerization of CBT oligomers using MWCNTs-supported initiator (MWCNTs-g-Sn). Briefly, hydroxyl-functionalized MWCNTs (MWCNTs–OH) were obtained by reaction of carboxyl-functionalized MWCNTs (MWCNTs–COOH) with excess of $SOCl_2$. Then the MWCNTs–OH reacted with excess of glycol and was dried. Then the dried MWCNTs–OH and dibutyl tin (IV) oxide were mixed in dry toluene. The solid was filtrated and dried and MWCNTs-g-Sn was obtained. The needful amount of MWCNTs-g-Sn was added to a solution of CBT in tetrahydrofuran (THF) and was sonicated for 1 h at room temperature. Most of the THF was evaporated in vacuo, and then, the black mixture was heated to 200 ºC in vacuo for another 30 min to remove the residual traces of THF. Afterward, appropriate amount of butyl tin chloride dihydroxide was added to ensure that the content of the initiator in all the samples was identical. The whole procedure was completed within 30 min under mechanical stirring at a speed of 500 rpm. According to the content of the MWCNTs-g-Sn (weight percentage), the nanocomposites were identified as PBT/ MWCNTs-g-Sn-0.5, PBT/MWCNTs-g-Sn-0.75, PBT/MWCNTs-

g-Sn-1.0, and PBT/MWCNTs-g-Sn-1.5. For comparison, a PBT/MWCNTs–COOH composite with 0.75 wt % of MWCNTs–COOH was also prepared by the aforementioned method. Authors [110, 111] reported that the polymerization proceeded via breakage of acyl–oxygen bond in the CBT cycle with insertion of the monomer into the metal–oxygen bond of the initiator. First, the monomer formed a complex with the initiator through interaction between the carbonyl group of CBT and the metal atom of initiator, followed by the ring opening of the CBT via the acyl– oxygen bond breakage. Then, the hydroxyl groups of butyl tin chloride dihydroxide blocked the active macrorings and remained in a linear polymer.

Chemical structure of the MWCNTs–cPBT copolymer formed was confirmed using NMR and FTIR techniques [110]. The efficiency of MWCNTs dispersing in the cPBT matrix was characterized by FESEM and TEM. The results reveal that the MWCNTs were homogeneously dispersed in the cPBT matrix when the content of MWCNTs was lower than 0.75 wt. %. FESEM images indicated a core-shell structure of MWCNTs–cPBT and the thickness of the polymer shell of about 6 nm was observed. Additionally, the presence of MWCNTs significantly promoted the crystallization rate of cPBT because of heterogeneous nucleation. Meanwhile, the lower T_m shifted to a high temperature, and the area of the lower T_m became larger. The effectiveness of crystallization promotion was less seen as the content of MWCNTs was increased. This may have resulted from the balance between the heterogeneous nucleation effect and the confined crystallization effect at high MWCNTs contents.

Wu and Yang reported the improvement of thermal stability of cPBT by the addition of MWCNTs. In [111] authors using TGA method observed that MWCNTs–COOH degraded faster than MWCNTs-g-Sn due to fast decomposition of carboxyl groups. Using the TGA data the authors performed calculations of grafting degree of cPBT to MWCNTs-g-Sn (about 59.3 %) taking as the reference the weight loss of MWCNTs–COOH at 500 ºC.

In conclusion, the literature review on CBT/CNTs nanocomposites have shown that the *in-situ* synthesis of PBT/CNTs composites using CBT oligomers have many technological advantages over melt blending of PBT with CNTs or synthesis of PBT/CNTs via conventional polycondensation. Moreover, the development of cPBT/CNTs

nanocomposites and investigation of their properties have just recently started. For the present only a few works [108-111] on cPBT/CNTs synthesis and investigation have been published. The knowledge related to the technology of cPBT/CNTs preparation is insufficient and properties of such nanocomposites are not completely investigated. Thus, it is necessary to extend existing knowledge on the methods of cPBT/CNTs preparation, to study kinetic peculiarities of CBT polymerization in the presence of CNTs, to study the effect of CNTs on basic physical-chemical properties, especially on electrical behavior of cPBT-based nanocomposites and materials formed from them using different methods, to establish synthesis-structure-properties relationships that is very important in terms of their industrial application.

1.3. Nanocomposites based on thermosetting heterocyclic polycyanurates and single-wall carbon nanotubes (SWCNTs)

In this section, the first scientific articles that recently appeared on synthesis and investigation of structure-properties relationships for composites based on thermostable polycyanurate networks, PCN, and different types carbon nanotubes (single-walled, multi-walled, non-functionalized, functionalized) [112-116] have been analyzed.

Thermosetting PCN prepared by polycyclotrimerization of dicyanate esters of bisphenol A (DCBA), E (DCBE), M (DCBM) etc. attract scientific and practical interest due to their unique complex of physical and chemical properties: high thermal stability (temperature of the beginning of destruction T_d>670 K); high glass transition temperature (T_g>520 K), fire resistance, high adhesion to metals (titanium, aluminum, etc.), to carbon and glass fiber, to composite materials; low dielectric constant (ε '~ 2,5 ÷ 3,2); minor moisture and water absorption (<2.5%); resistance to aggressive environments (acids, alkalis and petroleum products), etc. [117]. As it was mentioned above, polycyanurates owing such complex of properties are used in electronic, aerospace and other high-tech industries as an effective matrixes for composites, adhesives, sealants and more.

So far we know only two works [112, 115] where nanocomposites based polycyanurate networks filled by SWCNTs were synthesized and investigated.

Recently Latypova and Pozdnyakova [118] have published an interesting and important theoretical work where they calculated the optimal conditions of synthesis of ordered dendrymer polymer networks (PCN-based films) containing an ordered structure of SWCNTs. Authors supposed that as CNTs are highly polarized particles, using electrostatic field, one can determine the conditions of preparing a stable homogeneous suspension of the oriented SWCNTs in the melt (at $T \sim 100$ °C) of cyanate ester (CE), and also control the movement of SWCNTs in CE, and even growing up the SWCNTs during the synthesis of PCN matrix.

Hopkins and Lipeles in 2005 [112] obtained the nanocomposites based on PCN and SWCNTs for the first time. Incorporation of SWCNTs (0.5 wt. %)/acetone suspension into the dicianate ester of bisphenol A (DCBA) with subsequent sonication for 40 minutes yielded the mixture stable for 2 months without any signs of phase separation, unsheathing layers and overall inhomogeneity. Furthermore, the resulting composite exhibited a marked improvement in homogeneity without decreasing elasticitu modulus (E) or glass transition temperature (T_g) of the PCN matrix. Optimum sonication time (defined here as the shortest time to disperse SWCNTs into the cyanate monomer) was experimentally found to be 40 minutes. According to Hopkins et al. [112] excessive mixing time did not improve physical-mechanical properties of PCN/SWCNTs nanocomposites, obtained by thermal curing of DCBA in the presence of SWCNTs, and even had a potential both to introduce defects into the carbon nanotubes and degrade the polycyanurate matrix. We should note here that the authors called “polycyanurate” correctly for PCN network and incorrectly for cyanate monomer (for example DCBA). The monomer one can only call cyanate, dicyanate, or dicyanate ester (dicyanate ester of bisphenol), or, generally, Cyanate Ester Resins. The latter can be also used for PCN network, but with a note that it is crosslinked (cured) product.

It is worth to describe here in more details the specificity of preparing method used by the authors. Using the SWCNTs/acetone stock solutions, a series of DCBA/acetone mixtures were prepared under sonication with SWCNTs concentration ranging from 0.01 to 2.00 wt. %. Control samples were prepared in a similar way. Since nanotube additions caused the monomer solution to become optically opaque, the dispersion homogeneity was evaluated in dilute solutions visually. All the compositions were cast onto a metal tin pan and cured using step-by-step temperature schedule up to 300 °C. It should be noted that

SWCNTs/acetone solutions were allowed to sit idle for a period of 2-3 months to allow for heavy rope/bundle sedimentation to occur and tubes to become solubilized. The upper 75-80 % of supernatant (upper layer) was carefully decanted, leaving suspended nanotube solutions at a typical mass concentration of 0.56 wt. %.

The elastic modulus *E* calculated from a linear correlation for neat PCN and PCN/ SWCNTs composite thin film with 0.54 vol. % of SWCNTs were 303,400 Psi and 690,000 Psi, respectively (cf. Table 1.2). This represents a 127 % increase in stiffness for a 0.54 vol.% loading of SWCNTs compared to that for neat PCN. Using rule of mixtures, the predicted value for this PCN/SWCNTs nanocomposite was obtained higher. This indicates that dispersing procedure was not optimized [112]. Decreasing the SWCNTs loading to 0.01 % gives the lower value of modulus (313,000 psi) which is close to the 317.800 psi predicted value. As nanotubes concentration increases, they are bundling, that yield *E* values markedly lower compared to the predicted values.

Table 1.2. Theoretical and experimental value of elasticity modulus (*E*) for individual PCN and PCN/SWCNTs nanocomposites [112]

SWCNTs content, vol.%	E_{theor}, Psi	E_{exp}, Psi
0	-	303 400
0,01	317 800	313 000
0,54	718 000	690 000
0,79	145 200	383 000
1,00	174 900	340 000
2,00	204 000	312 000

PCN/SWCNTs nanocomposites and PCN/graphite and PCN/(carbon black) composites (with the same filler content of 0.5 wt. %) were compared (cf. Fig. 1.11). It was determined that such fillers as carbon black (particle size 0,5÷5 μm) and graphite (particle size 2÷15 μm) increased the modulus *E* of composites (in comparison with individual PCN), but less efficiently than SWCNTs that the authors explained by specific properties of the structure of CNTs. In our opinion, the authors of this paper have achieved their goal,

since by reinforcing of polycyanurate matrix with SWCNTs they managed to improve significantly its adhesive strength to metal (probably aluminum or titanium) used in aircraft and airspace industries [117].

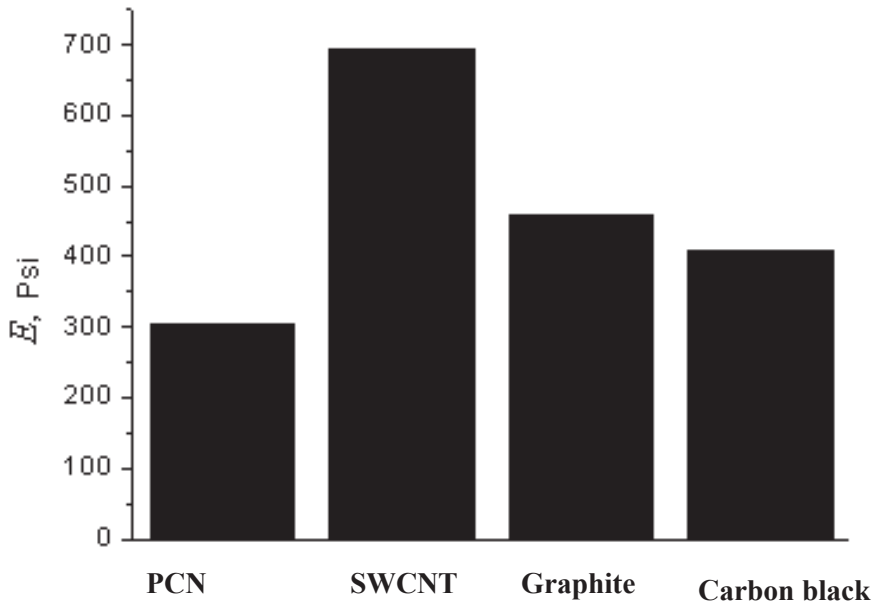

Fig. 1.11. Modulus of elasticity *E* for individual polycyanurate and various PCN-based composites with filler content equal 0.5 wt. % [119].

Reactive spinning of cyanate ester fibers reinforced with aligned amino-functionalized SWCNTs. The tensile modulus and strength of one-dimensional SWCNTs have been estimated experimentally and theoretically to be of the order of 1 TPa and 30 GPa, respectively, making them excellent candidates as fillers in high performance polymer nanocomposites [19-24]. However, present approaches to bulk production of carbon nanotubes (CNTs) based composites often result in a dense entangled network of nanotube bundles with rather unimpressive increase in mechanical properties. Alignment of CNTs in micro-sized fibers has been confirmed to be a highly effective way of exploiting the anisotropic superior mechanical properties of CNTs [25, 26]. As it is reviewed by Che and Chan-Parc [115] polymer matrix composite fibers can be produced by solution-based methods [120], traditional melt-spinning [119], or electrospinning [121].

High viscosity makes it difficult to disperse CNTs in the polymer matrix and/or to remove the solvent. The alternative approach of processing CNTs reinforced fibers using

thermosetting oligomers would promote the dispersion of CNTs and removal of solvent from the blend after fiber spinning due to their lower molecular weight and thus viscosity. Also, reactive groups in thermosets would enable their covalent bonds with functional groups on the CNTs surfaces to improve interfacial adhesion [122].

First the thermoset composite fibers with aligned CNTs have been reported by Che and Chan-Parc [115]. They have noted that since thermosets have low viscosity, control of reactivity and hence viscosity during spinning is necessary. During curing, thermosets transform from a liquid state to a gel state, before reaching a solid state. During the liquid stage, it is relatively easy to get a uniform dispersion of CNTs. The polymer builds up its viscosity before it begins to gel. For condensation curing, the rate can be controlled to obtain an appropriate viscosity over a period of time sufficient for spinning. Then the spun fibers can be further cured to obtain improved properties. In their study polycyanurate composite micro-sized fibers reinforced with aligned SWCNTs were fabricated by reactive spinning. Two types of fibers were produced from neat cyanate CE resin: pristine SWCNTs (p-SWNTs)/CE composite, and amino-functionalized SWCNTs (f-SWNTs)/CE composite. Dicyclopentadienyl bisphenol CE (Fig. 1.12a) and 2,2-Diallyl bisphenol A hardener (DBA) (Fig. 1.12b) were used for PCN synthesis (Fig. 1.12c). f-SWNTs were amine-functionalized using ethylenediamine (EDA) (Fig. 1.12d) via bridging isocyanate to improve nanotube dispersion and enable covalent bonding with the CE matrix [115]. The resin, together with or without the SWCNTs, was prepolymerized to increase viscosity, and then spun to produce fibers. The mixture was forced to flow through a spinneret and then drawn into a much finer fiber at an elevated temperature. The high drawing of the spun strand is expected to align the nanotubes along the draw direction. The spun fibers were then cured in stages to achieve good mechanical and thermal properties. The viscosity and degree of cure of the composite during reactive spinning were characterized by rheometry, FTIR spectroscopy, and softening point measurements. The SWCNTs and composite fibers were characterized by SEM, optical microscopy, tensile measurement, Raman spectroscopy and TGA. Unless otherwise stated, the SWCNTs contents were 1 wt. %.

For the purpose of reinforcement, a mild acid treatment was employed in order to avoid severe damage but obtain micrometer lengths of disentangled small nanotube bundles [115]. As far as the viscosities of neat CE resin and 1 wt. % f-SWNTs/CE mixtures are too low for fiber spinning the SWCNTs/PCN composite fibers were made by

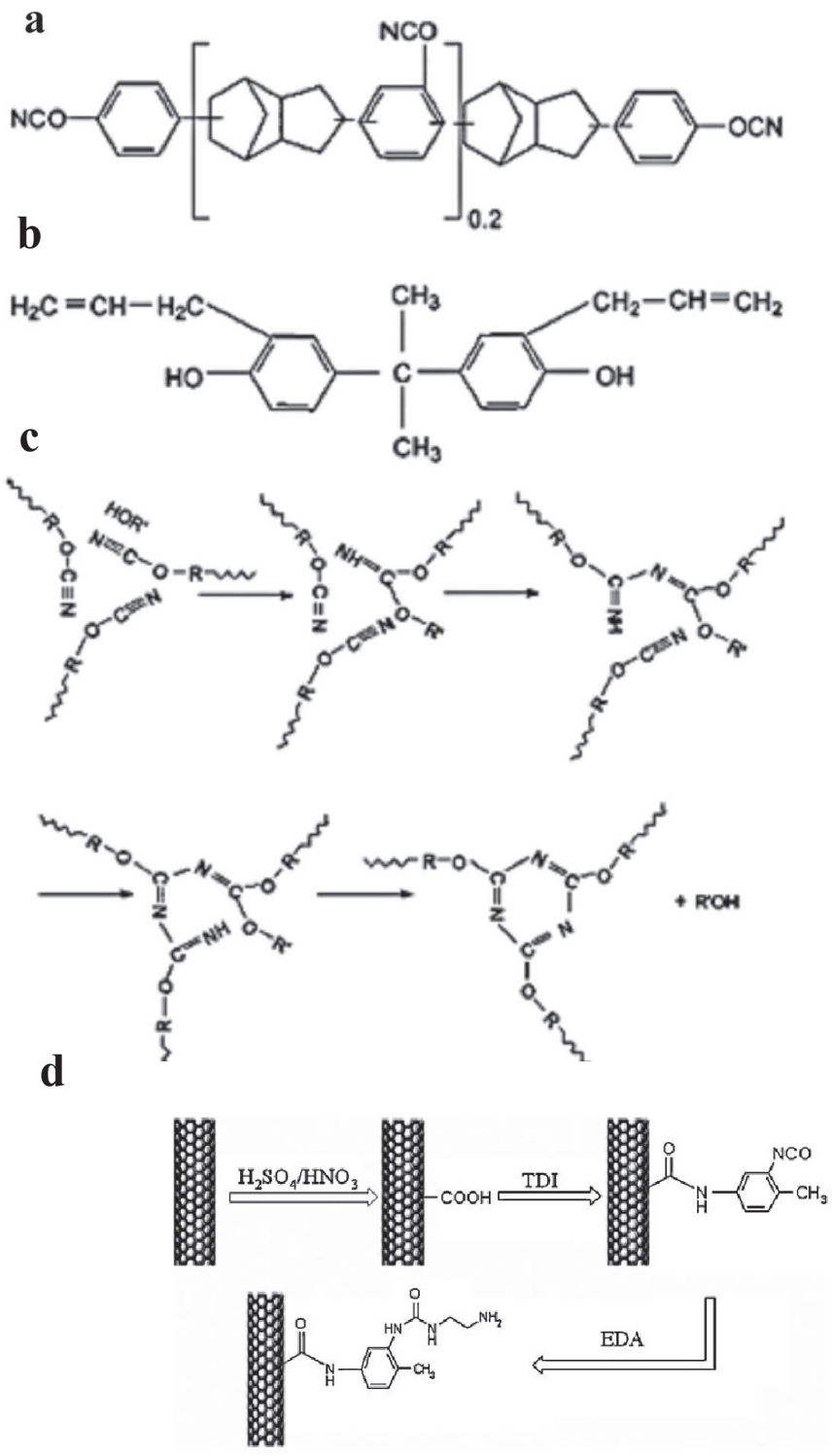

Fig. 1.12. Chemical structure: a - cyanate ester of dicyclopentadienyl of bisphenol; b - 2,2-dialilbisphenol A (DBA, coupling agent); c - the reaction of polycyanurate synthesis (R - a fragment of cyanate ester between cyanate groups; R '- fragment of coupling agent between the OH-groups); d – the scheme of process of amino-functionalization of SWCNTs [115].

a three-stage curing: (I) pre-polymerization before spinning to raise the viscosity for improving spinnability; (II) pre-curing of spun fibers at a temperature below the softening point to increase curing degree and softening point without fiber conglutination; and (III) curing and post-curing at higher temperatures to achieve good thermal and mechanical properties.

During prepolymerization at 120 ^{o}C the viscosity initially remained low for about an hour. The viscosity increases only marginally from 0.8 Pa·s to 1.3 Pa·s, 1.9 Pa·s, and 2.3 Pa·s (at 120 ^{o}C) as SWCNTs content increases from 0 to 0.5, 1.0 and 2.0 wt. %, respectively. However, at around the gel point, the viscosity increased dramatically. All the mixtures attain a high enough viscosity (about 30 Pa·s) to achieve spinnability with extended pre-polymerization time. Hence, the pre-polymerization time can be controlled to achieve almost the same starting viscosity before fiber spinning. Authors [115] have observed that the gelation of f-SWCNTs/CE blend was retarded with higher f-SWCNTs content even though the catalytic amine content was increased. They noted that the π-stacking interaction between the aryl group of DBA and f-SWCNTs can cause the DBA molecules to easily immobilize onto f-SWCNTs sidewalls making them difficult to diffuse into the blend. If the curing is catalyst diffusion controlled or impeded by lower catalyst content in the bulk, then the lower polymerization rate of cyanate ester resin with increased SWCNTs is reasonable.

The degree of polymerization during the pre-polymerization of the f-SWCNTs/CE composition at 120 ^{o}C was also monitored by FTIR [115]. FTIR spectra showed that the cyanate ester group absorption peak at 2260 cm^{-1} decreased, and two peaks at 1560 and 1370 cm^{-1}, characteristic for cyanurate cycle appeared. The ratio of the normalized area of the cyanate ester absorption peak at 2260 cm^{-1} to its original peak area was used to calculate the degree of polymerization at various stages of polymerization. Authors used the unusually low temperature for polymerization of cyanate monomer, it is usually >150 ^{o}C. However at this temperature the pre-polymerization cannot sequentially be precisely controlled to obtain suitable spinnability. After 100 min of the pre-polymerization at 120 ^{o}C the viscosity and the softening point had increased sufficiently but the polymerization degree of CE was still low (about 17.7 %) so that the mixture was still spinnable. It was found experimentally that the optimum condition for spinning was when the melt viscosity

was 50-80 Pa·s. The temperature of the spinning process should be adjusted so that the polymer has sufficiently high fluidity at the spinneret and almost-constant viscosity.

The optimum fixed temperature for the spinning is about 100 ^{o}C since the pot life is long at this temperature and the viscosity is mostly in the suitable range; the lower reaction speed at this temperature makes viscosity stable for an extended time period to improve spinning control. After spinning, the fibers were further pre-cured in order to achieve shape stability during subsequent higher temperature curing. To avoid the fiber melting after spinning, with attendant loss of SWCNTs alignment and fiber shape, the spun fibers must be cured at sufficiently low temperature: 80 ^{o}C was chosen as it was lower than the achieved softening temperature of the spun fibers (90 ^{o}C). The polymerization progress of CE in f-SWCNTs/CE during pre-curing at 80 ^{o}C was monitored by FTIR (data not shown). At this stage (pre-curing) the polymerization degree reached 33.9 %.

The fibers were then post-cured at 120, 140, and 160 ^{o}C consecutively each for 2 h in an air-circulating oven. After these curing steps, the polymerization level of CE in f-SWCNTs/CE, measured by FTIR, increased to 70 %. Authors [115] noted that it was difficult to further increase the polymerization degree at 160 ^{o}C, even with prolonged curing time. Post-curing was completed at a higher temperature of 250 ^{o}C for 4 h to achieve maximum conversion of cyanate groups into crosslinked triazine structures. The synthesis of carbon nanotube composites with enhanced mechanical properties requires strong interfacial bonding for load transfer between matrix and filler. Authors have confirmed chemical grafting of the polycyanurate formed onto the f-SWCNTs surface using FTIR technique. The amount of the polymer grafted onto the nanotube surface was estimated as ~100 % based on f-SWCNTs. Using SEM analysis it was observed a good dispersion of nanotubes, they also found that the nanotubes are oriented in the longitudinal direction of the fibers. The alignment of SWCNTs in the composite fibers was also confirmed by Raman spectroscopy. It was found that the reinforcement of PCN-fibers by SWCNTs and especially f-SWCNTs increased the values of tensile strength by 85÷140% (depending on CNTs content); impact strength of PCN-fibers micro-reinforced with f-SWCNTs increased by 420%; elongation at break increased by ~36÷144%.

Similar results have been obtained in CNTs/epoxy composites by Tseng [123]. This result contradicts the general phenomena of micro-sized fiber-reinforced composites, i.e.,

the elongation at failure typically drops drastically when short fibers are added to the matrix [41]. However, carbon nanotubes present a peculiar form of reinforcement with high aspect ratio and highly flexible elastic behavior during loading.

1.4. Structure-property relationships for nanocomposites based on polycyanurates and multi-walled carbon nanotubes (MWCNTs)

Search in electronic databases of scientific libraries (Science Direct-www.sciencedirect.com, Wiley - www3.interscience.wiley.com, Springer Link - www.springer link.com, SciFinder - www.scifinder.com and Scopus - www.scopus .com), has shown that up to now there are only a few works [113, 114, 116], where the synthesis and study of new nanocomposites based on PCN and MSWCNTs are described.

Fang et al. [113] presents mechanical and thermal properties as well as microstructure characterization of PCN/MWCNTs nanocomposites containing MWCNTs (or their functionalized analogue, f-MWCNTs) of different structure: single MWCNTs or grouped in bundles. Okotrub et al. [114] described in detail synthesis of MWCNTs (L=40÷400 nm and $D_{external}$=10÷15 nm) using the method of electroarc evaporation of graphite and method of MWCNTs oxidation (for their purification out of graphite particles and amorphous carbon) and presented the results of thermal and mechanical properties of PCN/MWCNTs nanocomposites (unfortunately the chemical composition of the cyanate ester is not given) depending on the content of the oxidized MWCNTs. Tang et al. [116] described a method of synthesis of nanocomposites based on blends of DCBA and diglycidyl ether of bisphenol A (DGEBA) in the presence of functionalized MWCNTs. The influence of nanotubes content on the reaction kinetics of polycyclotrimerization of cyanate ester and on physical and mechanical properties of the nanocomposites obtained was investigated. The above work will be reviewed in detail below.

In situ reactive formation and dispersion of MWCNTs. Since polycyanurates are high crosslink density polymer networks the only high-tech way to prepare CNTs-containing nanocomposites is the reaction of polycyclotrimerization of cyanate esters in the presence of nanofiller (CNTs) i.e. under the conditions of the *in situ* reactive formation

at high temperature (T~390÷570 K) [112-117].

Physical and chemical properties of CNTs-containing nanocomposites are controlled, primarily, by the level of dispersion of CNTs in a matrix. Thus the best mechanical properties are measured for the nanocomposites, where CNTs are dispersed to individual nanotubes. The presence of CNTs aggregates leads to less effective influence of nanofiller on final properties of nanomaterials based on them [41-50]. The most effective way of CNTs introduction to oligomeric or polymer matrixes known is their dispersing using ultrasonic equipment of different capacity (from 12 to 500 W) and frequency (20÷55 kHz) [42, 43]. In a number of works for the dispersing CNTs a high-speed mechanical mixers (500÷3000 rpm [3, 113]) or calenders (rolls speed 20 - 180 rpm [43, 119]) were used.

It is interesting to note that Okotrub et al. [114] prepared a filled thermosetting composition by simple grinding in a mortar of initial or oxidated (by a specially developed technique) MWCNTs with cyanate resin (cyanate monomer) at ambient temperature to obtain a homogeneous mixture (content of nanotubes was 20.0; 33.3 or 50.0%). The authors believe that the degree of dispersing of nanotubes was good, but the experimental confirmation of this fact is absence in the work. Note that only for one sample, obtained with oxidated and annealed (in argon atmosphere at T=400 °C) MWCNTs (the content is not specified), the structure of surface cracking was investigated by atomic force microscopy (AFM). It was found that anisotropic grooves of a height less than 20 nm only are present on the surface (authors believe that they are the CNTs embedded into the PCN-matrix). So, it was concluded that aggregates of CNTs are absent in this sample. Note that in order to improve dispersing of MWCNTs authors used their original developed method of oxidation and purification of nanotubes, based on a different ability to interact of individual carbon phases with solution of potassium permanganate in concentrated sulfuric acid [114]. The structure of purified MWCNTs was studied by transmittance electron microscope (JEM-100CX) and it was found that the material has only pipe and polyhedral multilayer structures. By means of X-ray analysis it was found that two or three surface layers of MWCNTs only undergone oxidation while the inner layers of nanotubes were not chemically modified.

It is known that chemical functionalization of CNTs promotes the chemical interaction

between CNTs and polymer matrix that enhances the interfacial adhesion between components and prevents phase separation [113, 124-127]. So Fang et al. [113] described a preparing method of nanocomposites based on cyanate ester (the concrete name was not given, but one can assume it was DCBA) and two types of functionalized (using triethylene tetraamine) MWCNTs of different morphological structure: single nanotubes (f-$MWCNTs_1$) and grouped in bundles nanotubes (f-$MWCNTs_2$) (Fig. 1.13) Authors found that after functionalization nanotubes became of shorter size and were better dispersed than their non-functionalized analogues. Also, it was shown that the chemical functionalization of $MWCNTs_2$ led to unbundling and their better dispersing in comparison with f-$MWCNTs_1$. In this paper, dispersing of CNTs was carried out for 15 minutes at a temperature higher than the melting temperature of the cyanate monomer ($T \geq 363$ K) using high-speed mixer (rotation speed of ~ 500 rpm). Then the PCN/MWCNTs mixture was dried in vacuum and after this was cured.

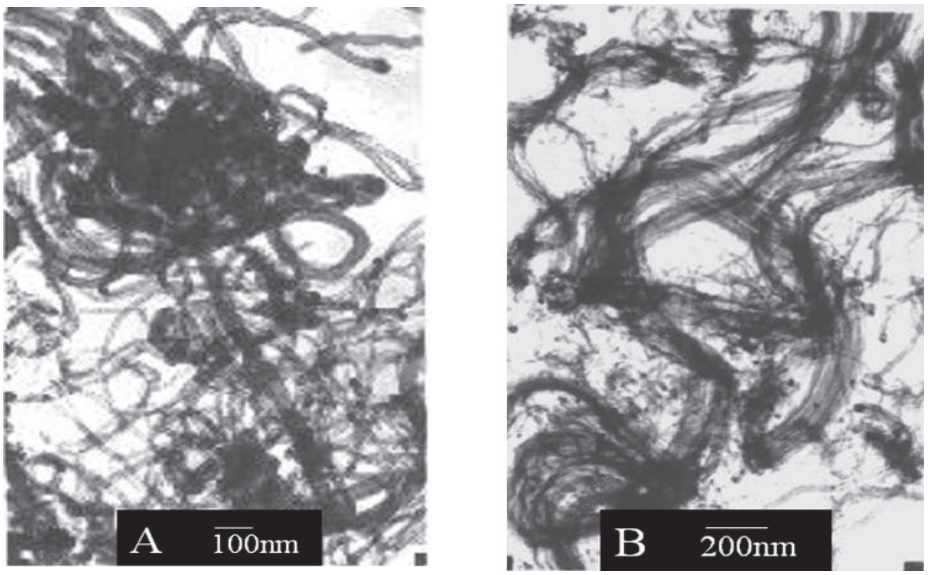

Fig. 1.13. Photomicrographies (TEM data) of the functionalized MWCNTs: A - single MWCNTs and their agglomerates; B - grouped in bundles MWCNTs [113].

Influence of MWCNTs on mechanical and thermal properties of nanocomposites. Fang et al. [113] basic on the results of mechanical tests of PCN/$MWCNTs_1$ and PCN/f-$MWCNTs_1$ as well as PCN/$MWCNTs_2$ and PCN/f-$MWCNTs_2$ nanocomposites ($MWCNTs_1$ - single nanotubes with $D \approx 20 \div 50$ nm; $MWCNTs_2$ - grouped in bundles nanotubes, D of one CNT was ≈ 10 nm) concluded that the morphology of MWCNTs (isolated or grouped in bundles) and the presence of functional groups on a surface of the

nanotubes affected the final mechanical properties of nanocomposites obtained. It was shown that the nanocomposites filled with the non-functionalized and functionalized nanotubes grouped in bundles ($MWCNTs_2$ and $f\text{-}MWCNTs_2$) have a higher value of flexibility modulus and impact strength (Table 1.3) than nanocomposites of $PCN/MWCNTs_1$ and $PCN/f\text{-}MWCNTs_1$ (non-functionalized and functionalized isolated nanotubes). Authors explained that fact by lower entanglement of $MWCNTs_2$ and $f\text{-}MWCNTs_2$ and lower content of agglomerates (in comparison with isolated $MWCNTs_1$ and $f\text{-}MWCNTs_1$) according to SEM data.

Table 1.3. Mechanical properties of PCN and PCN-based nanocomposites with 0,5 wt. % of different type MWCNTs [113].

Composition	Flexibility modulus, GPa	Impact strength, kJ/m^2
PCN	3.04	3.24
$PCN/MWCNTs_1$	2.95	3.08
$PCN/MWCNTs_2$	3.13	3.49
$PCN/f\text{-}MWCNTs_1$	3.38	3.20
$PCN/f\text{-}MWCNTs_2$	3.47	3.66

It was also found that the nanocomposites, obtained from functionalized f-MWCNTs, had better physical-mechanical parameters (Table 3) than analogous samples obtained with non-functionalized $MWCNTs_1$ and $MWCNTs_2$. Enhancement of physical-mechanical properties of nanocomposites obtained from functionalized $f\text{-}MWCNTs_1$ or $f\text{-}MWCNTs_2$ authors associated with increasing interfacial adhesion between the components through the chemical reaction of amine-groups grafted onto a surface of nanotubes with cyanate groups of the forming PCN (this chemical reaction was studied and described before [117, 128]). This conclusion was based on FTIR data (Fig. 1.14) shown that the intensity of the band of stretching vibration of NH-groups (with a maximum at $\nu \approx 610\ cm^{-1}$) significantly reduced during the synthesis of PCN-matrix in the presence of carbon nanotubes.

It was also shown [113] that the introduction of nanotubes slightly improves the thermal stability of the obtained nanocomposites, especially with $f\text{-}MWCNTs_2$ (Table 1.4). It is concluded that better dispersing of $f\text{-}MWCNTs_2$ and its covalent (chemical) bonding

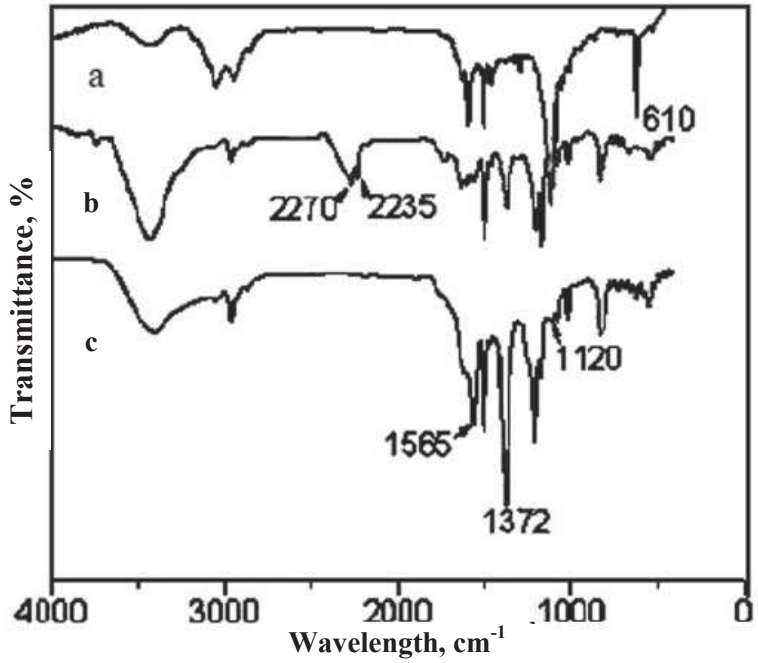

Fig. 1.14. FTIR spectra: a - f-MWCNT$_1$; b – monomer of cyanate ester; c - PCN/f-MWCNT$_1$ nanocomposite (10 wt. %) after curing at 160 °C for 2 h [113].

Table 1.4. Thermal stability (TGA data in N_2) of individual PCN and nanocomposites containing 0.5 wt. % of different type MWCNTs [113]

Composition	Temperature of destruction onset (T_d), K (2 % of mass loss)
PCN	540,3
PCN / MWCNTs$_1$	540,6
PCN / MWCNTs$_2$	547,0
PCN / f-MWCNTs$_1$	544,9
PCN / f-MWCNTs$_2$	550,0

to the PCN-matrix slow down the decomposition of the nanocomposites obtained. However, it was found that in all the nanocomposites obtained the glass transition temperature (T_g) of PCN matrix was lower by ~ 9÷11 °C than the T_g for non-filled PCN. Authors explained this fact by decreasing crosslink density of PCN-network caused by introduction of CNTs. It is noteworthy that in general the authors of this paper failed to

improve significantly physical-mechanical properties of PCN/CNTs nanocomposites prepared.

Tang et al. [116] investigated the mechanical and thermal properties of nanocomposites prepared by *in situ* synthesis of PCN from the mixture of DCBA and diglycidyl ether of bisphenol A, DGEBA, with the functionalized MWCNTs (MWCNTs content was 1.0, 1.5 and 2.0 wt.%). MWCNTs of $D_{intern} \approx 10 \div 30$ nm, $D_{extern} \approx 40 \div 60$ nm and L/D ratio ≈ 1000 were used. Functionalization of MWCNTs was carried out by pyrolysis (at $T = 580$ °C for 1 h) followed by treatment (during 40 min) with acids HCl, HNO_3 (65%) or with mixture of acids HNO_3/H_2SO_4 (1/2 or 1/3). Using FTIR it was found that after treating by acid carboxyl, carbonyl and hydroxyl groups appeared on the surface of MWCNTs. It has been determined that the introduction of 1 wt. % of the functionalized MWCNTs obtained increases flexural strength from 132 to 147 MPa and impact strength from 14.0 to 16.5 kJ/m^2 (compared with initial PCN). However, further increasing of nanotubes content in the composite caused the lowering the above mentioned parameters (almost to the level of initial PCN). It was found that loading of 1 % of nanotubes decreased by ≈ 30% water absorption of nanocomposites. Increasing storage modulus (E') in the temperature range of 50÷300 ºC at introduction of up to 1.5 wt. % of nanotubes was detected by DMA, however at the concentration of nanotubes ≥ 2 wt % some drop in value of E' was observed. Unfortunately the authors did not give any explanations of these non-monotonic dependencies. In our opinion, such non-monotonic mechanism can be explained by the fact that at increasing of nanotubes content agglomerates are formed and hinder stress transfer between MWCNTs and matrix, so nanotubes become the centers of crack formation that leads to reducing physical-mechanical properties of nanocomposite.

Okotrub et al. have been studied [114] the effect of oxidated MWCNTs content on mechanical properties of new carbon fiber reinforced plastic materials based on Cyanate Ester Resins and carbon fibers "ELUR" (fiber content is not mentioned). These polymer composites were obtained by multiple impregnations of carbon fibers with a diluted solution of oxidized MWCNTs/CE/acetone achieving the content of CNTs on the fibers surface of 0.25÷1.00 %. The sample was then formed by direct pressing at a special temperature conditions (the details are not specified) to achieve the highest curing degree of the polymer matrix. Mechanical properties of carbon fiber reinforced composites obtained were studied at temperatures T = 20 and 180 °C: flexural strength (σ_{flex}),

compression strength (σ_{compr}), and flexural modulus (E_{flex}) were measured. It was found that at above mentioned temperatures the original carbon fiber reinforced composites (without nanotubes) had the following parameters: σ_{flex} = 1.12 (1.10) GPa, σ_{compr} = 8.95 (7.90), E_{flex} = 102.64 (96.66) GPa (the values at T = 180 °C are indicated in brackets). It was found that treatment of fibers by nanotubes enhanced physical-mechanical properties of carbon fiber reinforced composites, especially at elevated temperatures; the greatest effect was observed at MWCNTs content of 0.25%: σ_{flex} = 1.42 GPa, E_{flex} = 134.43 (125.3) GPa and for composite, containing 0.5 % of MWCNTs: σ_{compr} = 9.97 (8.99) GPa (the values at T = 180 °C are indicated in the brackets).

As in the previous work the authors [114] do not give explanations of the non-monotonic effect of MWCNTs content on the basic properties of the investigated nanocomposites. However, from DMTA data, namely temperature dependence of storage modulus (E') and loss tangent ($tan\ \delta$), one can conclude that already at 1 % of nanotubes content in the investigated samples a significant decline (compared with the original carbon fiber) of material stiffness (modulus E' decreases from ~95 to ~70 GPa at $T \approx 50 \div 200$ °C, and from ~75 to ~35 GPa for $T \geq 250$ °C) and increasing intensity of α-relaxation transition (at $T_g \approx 250$ °C) of PCN-matrix occurs. These facts can be associated with decreasing crosslink density and appearance of defects in the structure of PCN-network, i.e. increasing content of oxidized MWCNTs hinders the polycyclotrimerization of cyanate monomer. This conclusion is in a good agreement with the one reported by dynamic DSC, since it was found that with increasing concentration of the oxidized MWCNTs (from 20 to 50%) enthalpy of PCN formation decreased non-additively and exothermal peak at 70÷130 °C simultaneously appeared that the authors attributed to chemical interaction of cyanate groups of the monomer and oxygen-containing functional groups on the surface of oxidized MWCNTs (no doubt that this assumption requires further experimental confirmation). It is shown that at content of 50 % of the oxidized MWCNTs the first peak becomes dominant and curing of polycyanurate matrix almost not occurs. However, after annealing of oxidized MWCNTs in an inert atmosphere authors managed to obtain nanocomposites (nanotubes content is not specified) with a uniformly glossy black surface.

* * * *

Thus, the literature review shows that to date investigations on the synthesis and

structure-property relationships of nanostructured polymer composites based on heterocyclic esters and carbon nanotubes are just at the beginning. So far the investigation of effect of CNTs on the kinetics of polymerization of cyclic oligomers of butylene terephthalate and polycyclotrimerization of cyanate esters of bisphenols was not carried out. There is no information in the literature about the effect of CNTs on thermal, viscoelastic and electrical properties of nanostructured polymer composites synthesized by *in situ* polymerization of cyclic oligomers of butylene terephthalate in the presence of MWCNTs. The influence of CNTs on stability to thermooxidative destruction of nanocomposites based on cPBT/MWCNTs has not been investigated yet. There are no publications on research of impact of CNTs on heat and electric conductivity and other basic physical-chemical properties of nanocomposites obtained by *in situ* polycyclotrimerisation of cyanate esters of bisphenols in the presence of MWCNTs. Thus one can say that today there is an absolute need for comprehensive investigation to identify regularity of *in situ* synthesis of polymer nanocomposites based on heterocyclic esters of different chemical structure in the presence of carbon nanotubes and to establish the regularities of the influence of nanofiller on basic physical-chemical properties of nanocomposites synthesized.

Chapter 2

Methods of synthesis of polymer nanocomposites from heterocyclic esters and carbon nanotubes

2.1. Introduction

In this chapter the basic characteristics of the initial components used for synthesis of polymer nanostructured composites (nanocomposites) from heterocyclic esters of different structure in the presence of CNTs and the methods of synthesis and forming samples for measurements have been described.

In this work two serieses of the nanocomposites with varying content of CNTs were synthesized and studied : first series based on linear thermoplastic Poly(butylenes terephthalate), cPBT synthesized from oligomers of cyclic butyleneterephthalate, CBT, in the presence of $MWCNTs_1$ (made in France) and second series based on polycyanurate network, PCN (thermoset), synthesized from oligomers of dicyanate ester of bisphenol A, DCBA, in the presence of $MWCNTs_2$ (made in Ukraine).

Note that the oligomers selected for synthesis of both the serieses of the nanocomposites are from the class of heterocyclic esters and the polymers synthesized from them are thermostable polymers. For both the series the nanocomposites were synthesized by *in situ* method using the initial oligomers of low viscosity that allowed easy effective dispersing of CNTs without any damage of latter. Importantly, the initial componets are industrially available, so the new nanocomposites can easy be applied in some devices and processes.

2.2. Characterization of the initial components for synthesis and other chemical compounds used

Macrocyclic oligo(1,4-butylene terephthalate), the mixture of cyclic oligomers of butylene terephthalate with polymerization degree $n = 2 \div 5$ (Fig. 2.1) was supplied by "Cyclics Corp." (trademark "CBT 160", USA). CBT – white crystalline pellets with $T_m \sim$ 413 K, viscosity (η) ~ 20 мPa·s (at T_m). According to the information from the producer the granules of CBT-160 contain 0.5 wt. % of the catalyst butyltin dihydroxy chloride (trade mark - "Fascat 4101"):

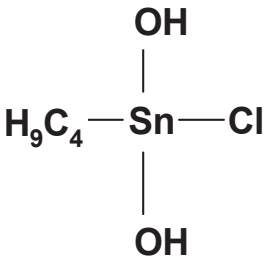

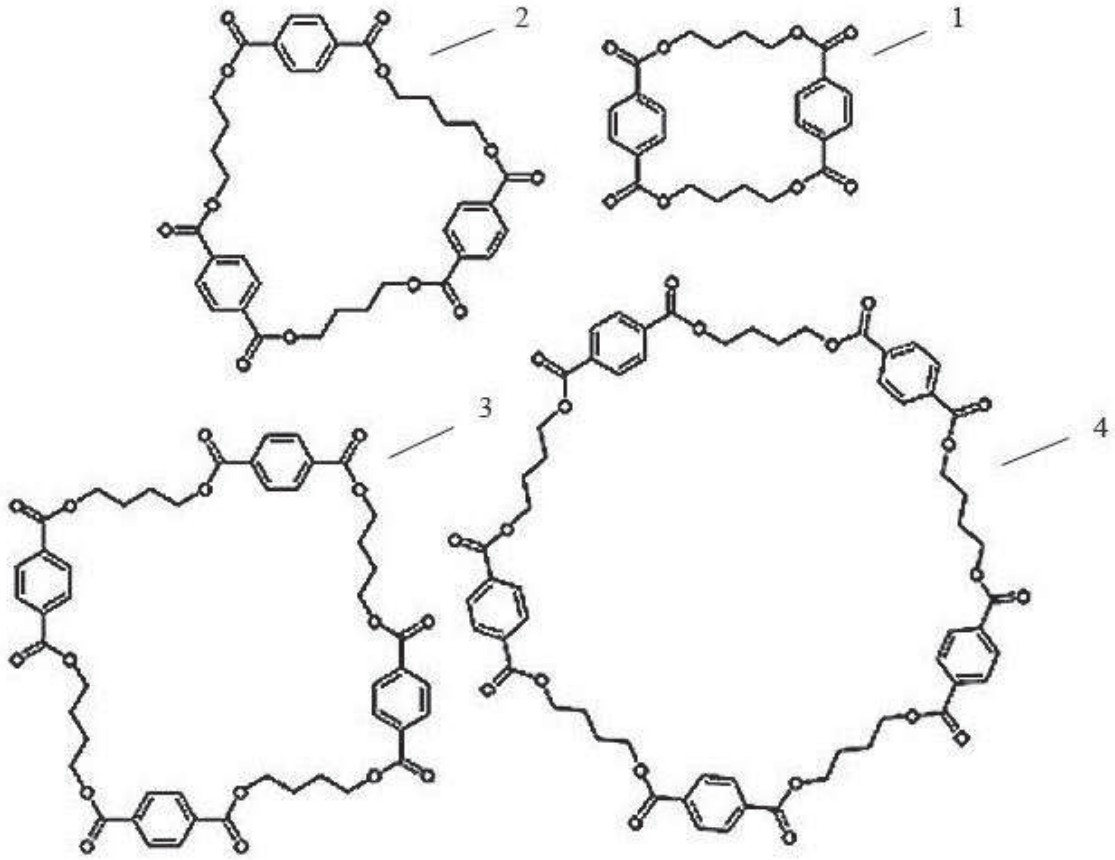

Fig. 2.1. Cyclic oligomers of butylene terephthalate: 1 – $C_{24}H_{24}O_8$; 2 – $C_{36}H_{36}O_{12}$; 3 – $C_{48}H_{48}O_{16}$ and 4 – $C_{60}H_{60}O_{20}$.

2, 2'–bis(4-cyanatophenyl)isopropylidene (dicyanate ester of bisphenol A), DCBA, trade mark - "Primaset BADCy" (purity > 99.00 %) was kindly supplied by "Lonza Ltd" (Switzerland). DCBA – white crystalline powder with $T_m \approx 352$ K.

In some synthesis the industrial oligomer of DCBA (with conversion of cyanate groups ~ 52 %) as a solution in methyl ethylketone (~ 75 %), trade mark "Primaset BA-

230S 75", supplied by "Lonza Ltd" (Switzerland), was also used.

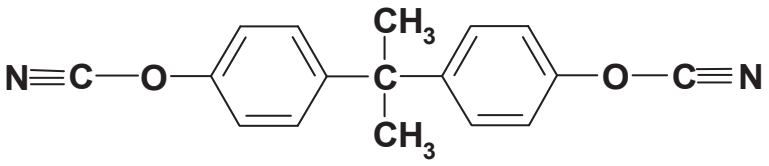

Multiwalled carbon nanotubes (MWCNTs)**,** synthesized by the method of chemical vapor deposition (CVD), were used as nanofiller. MWCNTs – friable powder of a black colour. Two types of MWCNTs were used: 1) $MWCNT_1$ – carbon nanotubes of the trade mark "C100" supplied by "Arkema" (France); 2) $MWCNT_2$ - carbon nanotubes supplied by "TMSpetsmash Ltd" (Kyiv, Ukraine).

$MWCNT_1$ had the following characteristics (from the producer): density 50 ÷ 150 κg/m^3; outer diameter of the nanotubes 10 ÷ 15 nm; length of the nanotubes 0,1 ÷ 10,0 μm.

$MWCNT_2$ had the following characteristics (from the producer): density – 29 g/dm^3; specific surface – 286 m^2/g; outer diameter of the nanotubes 10 ÷ 20 nm.

Carbon fibers (CF) were also used in the work for comparison as filler. CF were supplied by "Europe Toho Tenax" (Germany). CF had a diameter ~7 μm, and L/D ≈ 900.

All the components were used without any additional purification. CBT before use was dried in vacuum for 12 h at $T \approx 353$ K.

2.3. *In situ* synthesis of cPBT/$MWCNT_1$ and $cPBT_{in}$/$MWCNT_2$ nanocomposites by polymerization of cyclic oligomers of butylene terephthalate

The nanocomposites were obtained using reactive extrusion method by *in-situ* synthesis of poly(butylene terephthalate), cPBT, from the oligomers of cyclic butylene terephthalate, CBT, in the presence of $MWCNTs_1$. The series of the nanocomposite samples cPBT/$MWCNTs_1$ was synthesized with the $MWCNTs_1$ content, wt. %: 0.01; 0.05; 0.1; 0.3; 0.5; 1.00; and 2.00.

CBT160 and $MWCNTs_1$ were first dry mixed in a flask and then blended in a

"DSM 15" twin-screw compounder (DSM Research Netherlands) at 503 K and screw speed 100 rpm during 15 min. The extruded material was then used for measurements as obtained (strand), or as films prepared by pressing of strands: the strands were cut in small grains, placed into the mold with a thickness of 0.5 mm and diameter of 25 mm and pressed during 8 min at 513 K with a pressure of 6 MPa, using hot press machine "Carver" (USA), then cooled with the rate of 9 K/min during 30 min. The third type of samples for measurements was obtained by injection molding: the melt of the product from extruder was collected to the heated transportable box, where the temperature was kept as 503 K, then the box was fixed onto the laboratory injection molding machine "BabyPlast" (UK) and next the melt was injected to the mold ($T \approx 473$ K, injection pressure $p \approx 265$ MPa). After cooling to room temperature with speed of 9 K/min for ~40 min the samples of the nanocomposites with diameter of 25 mm and thickness ~ 1 mm were obtained.

For some measurements the nanocomposites of $cPBT_{in}$/$MWCNTs_2$ were obtained using the same method, but CBT was used without any preliminary drying. The nanocomposites with $MWCNTs_2$ content, wt. %: 0.01; 0.05; 0.1; 0,3; 0.5; 1.00 and 2,00 were prepared.

2.4. *In situ* synthesis of PCN_1/$MWCNT_2$ nanocomposites from oligomer of dicyanate ester of bisphenol A

The film samples of PCN_1/$MWCNTs_2$ nanocomposites were prepared by the following step by step method. In a first stage the oligomer of dicyanate ester of bisphenol A was synthesized: the initial crystalline DCBA was heated in isothermic conditions in programmable thermal oven "Memmert UNP" (Germany) at $T \approx 423$ K during ~ 40 h. The oligomer synthesized was a viscous liquid at room temperature. According to the calculations on the results of FTIR spectroscopy the conversion of cyanate groups of the DCBA in the oligomer obtained was estimated as $\alpha \approx 28$ %.

In a second stage the $MWCNTs_2$ were sonicated in liquid DCBA prepolymer at room temperature and frequency of 44 Hz during 45 min using the ultrasound equipment UZDN-2E (Russia). In order to avoid self-heating the vessel with the composition was continually cooled using water with ice. The optimal conditions of $MWCNTs_2$ dispersing

were selected by empirical way. It was impossible to disperse the $MWCNTs_2$ directly in the melt of DCBA monomer, because the latter crystallized during mixing procedure. The content of $MWCNTs_2$ in the compositions was 0.01; 0.1 and 0.5 wt. %. For the composition with 0.5 wt. % of $MWCNTs_2$, the critical self-heating was observed shortly, leading to gel formation, so the uncontrollable polycyclotrimerization of DCBA to PCN network in the presence of 0.5 wt. % of $MWCNTs_2$ occurred.

In a third stage the high temperature *in situ* synthesis of PCN_1 was carried out in the presence of $MWCNTs_2$. The mixture was poured between two glass plates covered by antiadhesive film and heated using step by step curing schedule: 3h at 353 K, 1h at 483 K, 1h at 503 K, 1h at 523 K. There were no any traces of unreacted cyanate gropus observed in FTIR spectra of the cured compositions.

2.5. *In situ* synthesis of $PCN_2/MWCNT_2$ nanocomposites from the industrial oligomer of dicyanate ester of bisphenol A

Prepolymer of dicyanate ester of bisphenol A (DCBA) supplied as a 75 % solution in methyl ethyl ketone (BA-230S 75) was used as the initial component for preparation of polycyanurate-based $PCN_2/MWCNTs_2$ nanocomposites. $MWCNTs_2$ were sonicated in a solution of the DCBA prepolymer at room temperature and frequency of 44 Hz during 45 min using the ultrasound equipment UZDN-2E (Russia). Before synthesis procedure the mixture was poured on the glass plate covered by antiadhesive film and vacuumized at $T \sim$ 423 K, p ~ 0.13 кPa during ~ 4 h to remove the solvent, and then heated using step by step curing schedule: 3h at 453 K, 1h at 483 K, 1h at 503 K, 1h at 523 K, and 30 min at 543 K. The nanocomposites with $MWCNTs_2$ content, wt. %: 0.02; 0.03; 0.04; 0.05; 0.06; 0.08; 0.50; 1.00; and 1.20 were prepared.

2.6. *In situ* synthesis of composites cPBT/CF by polymerization of cyclic oligomers of butylene terephthalate

In order to compare some properties of the nanocomposites of cPBT filled by

CNTs with that filled by carbon fiber, some cPBT/CF composites were synthesized. The *in situ* synthesis of cPBT from CBT in the presence of different amount of CF using reactive extrusion was carried out in "Rheomix 600 Haake" batch mixer at $T \sim 513$ K during 13 ÷ 15 min. The series of the cPBT/CF samples was synthesized with the CF content, wt. %: 0.5; 1.5; 2.5; 5.0 and 10.0. The samples were then pressed at 523 K in sample mould with thickness of ~0.5 mm between two steel plates covered by antiadhesive film, and next cooled to the room temperature with the rate of 9 K/min during ~25 min.

Chapter 3

Characterization techniques

3.1. Scanning Electron Microscopy (SEM)

Scanning electron microscopy method (SEM) [129, 130] was used to study the morphology of the nanocomposite samples synthesized. SEM microphotographs were carried out using "SEM HITACHI S800" at the accelerating voltage of 15 kV. The specimens were quenched and fractured in liquid nitrogen and then coated with a thin Au/Pd film (thickness around 10 nm) for investigation. The program "Image SEMICAPS software" was used for size particles calculations.

3.2. Transmission Electron Microscopy (TEM)

Transmission electron microscopy method (TEM) [131] was used to obtain TEM microphotographs of MWCNTs or nanocomposites studied using a microscope "PHILIPS CM 120". The operating voltage was set to 80 kV. MWCNTs were ultrasonically dispersed in acetone and a drop of obtained dispersion was deposited on a copper microscopy grid covered with a thin polymer film "Formvar".

3.3. Fourier –Transmission Infrared spectroscopy (FTIR)

Kinetic peculiarities of the polymerization reaction were studied by using FTIR spectroscopy technique [132]. FTIR measurements were fulfilled using "Bruker TENSOR 27 DTGS" spectrometer in the range of 4000 - 500 cm^{-1}. The mixture of MWCNTs dispersed in pre-polymer was deposited between two NaCl glasses and the measurements were performed after each stage of curing.

3.4. Differential Scanning Calorimetry (DSC)

Differential scanning calorimetry investigations (DSC) were carried out using "TA Instruments 2920 MDSC V2.6A" in helium and air atmosphere in the range of temperature

of $T \approx 286 \div 533$ K for the samples of cPBT the nanocomposites cPBT/MWCNT$_1$ and in the range of temperature of $T \approx 300 \div 625$ K PCN and the nanocomposites PCN/MWCNT$_2$. Data of DSC measurements were analyzed utilizing TA Instruments Universal Analysis 2000 ver. 3.9A.

Degree of crystallinity (X_c) of the samples was determined according to the equation:

$$X_c = \frac{\Delta H_m}{\Delta H_m^0} \cdot 100\%, \tag{3.1}$$

where ΔH_m – melting enthalpy (J/g), ΔH_m^0 = 142 J/g – theoretical value of melting enthalpy for 100% crystalline PBT [133].

3.5. Raman Spectroscopy (CNTs characterization)

The characterization of the samples was performed by Raman spectroscopy method [134-136] using the "Jobin-Yvon Raman Spectrometer T64000" combined with "Olympus confocal microscope BX40" by using green laser light (λ = 514.5 nm) at room temperature, the beam focal length was 640 mm, a pitch dimension was 0.0066 Å.

3.6. Dynamic Mechanical Thermal Analysis (DMTA)

Dynamic mechanical thermal analysis (DMTA) [137] scans were performed with a single-cantilever blending mode by using a dynamic mechanical analyzer "TA Instruments DMA 2980" from 130 to 420 K at a heating rate of 2 K/min. For the cPBT-based samples the range of frequency was taken from 1 to 15 Hz, the amplitude of oscillation was chosen equal to 20 μm. Samples size was 0.5 x 5 x 17.5 mm^3.

For the PCN-based samples the DMTA scans were performed with a single-cantilever blending mode by using a dynamic mechanical analyzer "TA Instruments Universal Analysis 2000 ver. 3.9A" from 300 to 645 K at a heating rate of 2 K/min, the range of frequency was taken from 1 to 5 Hz, the amplitude of oscillation was chosen equal to 20 μm.

The relaxation transition temperature was determined as the maximum of the temperature dependence of the mechanical losses modulus.

The stress-strain dependence was determined for some PCN/MWCNTs$_2$ nanocomposites using an analyzer "TA Instruments DMA 2980" at frequency of 1 Hz and the value of tensile strength at break (σ_b) was determined depending on nanofiller content. Samples size was 50.0 x 5.0 x 0.5 mm^3.

3.7. Thermogravimetry Analysis (TGA)

Study of thermal-oxidative destruction of the samples of the nanocomposites samples was carried out using "TA Instruments Thermogravimetric Analyzer TGA 2950" in air or in inert media (helium or nitrogen) in the temperature interval from 300 up to 1120 K for PCN/MWCNTs$_2$ nanocomposites, and from 300 up to 825 K for cPBT/MWCNTs$_1$ nanocomposites. The heating rate was 10 K/min and the mass of samples studied was 10 ÷ 15 mg.

3.8. Melt Rheology

The frequency dependence of viscosity for CBT and for the CBT/MWCNTs$_1$ dlends in oscillation regime was determined using "Rheometrics RMS 800 Spectrometer". The samples for measurements were placed between two parallel plates of the diameter of 20 mm each. The distance between the plates was ~1 mm. To study the influence of MWCNTs$_1$ on kinetics of CBT polymerization using rheometer the dynamic test with constant slip frequency ω = 10 rad $\cdot$ sec^{-1} at temperature $T \approx$ 503 K was applied.

3.9. Determination of Thermal Conductivity

The measurements of thermal conductivity of PCN$_2$/MWCNTs$_2$ nanocomposites were carried out at their linear heating by using modernized model of industrial controlling

and measuring apparatus for thermal conductivity "IT-λ-400" in the temperature rage from 323 K to 373 K. The circular-shaped samples of diameter of 15 mm and thickness of 0.2 ÷ 0.7 mm were placed between two parallel metallic discks treated by lubricant for the better contact with the sample and to avoid the heat loss.

3.10. Electric properties

3.10.1. Electric conductivity measurements under the alternative current (ac)

The electric conductivity measurements under the alternative current (ac) were performed under the room temperature in the frequency range between 10^{-1} and 10^{6} Hz using a two-contact scheme. The pressed disk of a sample was held between two electrodes made from 1cm thick steel. The ac output voltage was adjusted to 1.5 V. The ac conductivity for ac percolation curve was determined as a value of the conductivity in the region of the low-frequency plateau.

3.10.2. Direct current (dc) electrical conductivity

Measurements of the direct current (dc) electrical conductivity of all the samples were performed at room temperature using two- or four-point techniques. For this purpose a sample holder was prepared using strips of graphite paper fixed on an insulating poly(ethylene terephthalate film). The copper wires were attached to graphite electrodes and junction points were covered by silver paint. In the four-point technique the external wires were connected to current source, and the internal to the voltmeter. The samples were cut into 6 x 12 mm strips, were deposited on a sample holder and were pressed against the graphite strips. The dc current was applied using regulated power supply "Keithly 6517A Electrometer High Resistancemeter". Current flow and voltage were measured using digital multimeter "Keithly 2400 Sourcemeter".

Two-point technique (using the same holder type with two electrodes) was used for determination of electrical conductivity of the samples below the percolation point. Current flowing at fixed value of voltage was recorded until constant value was reached.

The volume resistivity, ρ, of all the samples was calculated using the following equation:

$$\rho = \frac{U}{I} \cdot \frac{\delta \cdot w}{L}, \tag{3.2}$$

where U is a tension, V; I - current flowing through the sample, A; δ - sample thickness, cm; w - width of the sample, cm; L – the distance between two electrodes connected to the multimeter, cm. Electric conductivity was determined as $\sigma = 1/\rho$.

In order to describe the mechanism of charge transport in the nanocomposites the temperature dependence of the dc conductivity was measured in a broad temperature range using helium cryostat.

3.11. Size Exclusion Chromatography (SEC)

Molar masses of cPBT samples synthesized were measured using gel-permeation chromatography method. The following devices were used: “Spectra Physics P100 pump”, two “PLgel 5 μm mixed C-columns” (Polymer Laboratories) and “Shodex RI 71 refractive index detector”. For calibration a standard sample of polystyrene (M_w = 30 000, polydispersity index M_w/M_n = 1.01) was used. As eluent a mixture of chloroform/hexafluoro-2-propanol (98/2) was used, the flow speed was 1 ml/min. The sample weight was 0.001 ÷ 0.02 g.

Chapter 4

Structure and properties of nanocomposites based on linear poly(butylene terephtalate) from CBT and multiwalled carbon nanotubes

4.1. Introduction

4.2. Investigation of structure of multiwalled carbon nanotubes

4.3. Investigation of the effect of carbon nanotubes on polymerization of cyclic oligomers of butylene terephthalate

4.4. Determination of morphology of cPBT/$MWCNTs_1$ nanocomposites using scanning and transmission electron microscopy

4.5. Viscoelastic properties of cPBT/$MWCNTs_1$ nanocomposites

4.6. Effect of carbon nanotubes on thermophysical properties of nanocomposites

4.7. Effect of MWCNTs on stability to thermal-oxidative degradation of the cPBT/$MWCNTs_1$ and $cPBT_{in}$/$MWCNTs_2$ nanocomposites

4.8. Determination of the effect of carbon nanotubes on electrical performance of the nanocomposites synthesized

4.1. Introduction

The present section represents the results on investigation of the structure and main physical and chemical properties of nanostructured polymer composites based on linear poly(butylene terephthalate) synthesized from a mixture of heterocyclic oligomers of butylene terephthalate ("CBT160"), polymerizable by ring-opening polymerization (see sect. 2.1) in the presence of multiwalled carbon nanotubes $MWCNTs_1$ ("Arkema", France) or $MWCNTs_2$ ("TMSpetsmash", Ukraine). Description of the initial components, details of synthesis and molding of the nanocomposite samples are given in sect. 2.1 and 2.2, respectively. As noted above in sect. 2, dispersing of $MWCNTs_1$ and synthesis *in situ* of cPBT in the presence of carbon nanotubes, was carried out directly in the laboratory twin-screw miniextruder. After the synthesis, the nanocomposite samples were formed either as extrudate (strands) from extruder, or as films and plates by hot pressing or injection molding, respectively. The cPBT/$MWCNTs_1$ nanocomposites contained the following amount of $MWCNTs_1$, (wt. %): 0.01, 0.05, 0.10, 0.30, 0.50, 1.00 and 2.00. The content of $MWCNTs_2$ in the nanocomposite samples of $cPBT_{init}$/$MWCNTs_2$ was as follows, (wt.%): 0.01, 0.05, 0.10, 0.20, 0.50 and 1.00.

4.2. Investigation of structure of multiwalled carbon nanotubes

Multiwalled carbon nanotubes $MWCNTs_1$ and $MWCNTs_2$ were studied using transmission electron microscopy (TEM), the corresponding TEM microphotographs are presented in Fig. 4.1 (a, b). It was established that $MWCNTs_1$ had the following dimensional characteristics: outer diameter $D \approx 10 \div 17$ nm, inner diameter $D_{in} \approx 4 \div 7$ nm, length of nanotubes $L \approx 0{,}1 \div 10$ μm, thus was $L/D \sim 6 \div 1000$. At the ends of some nanotubes hemispherical closed tops are clearly visible (1/2 of fullerene molecule), but the rest of the nanotubes have open endings. In $MWCNTs_1$ one can see the aggregates, i.e. some nanotubes are substantially curved in shape, that may indicate the presence of defects in the walls of nanotubes, namely the presence of not only six-

membered, but four-, five- or hepta-membered carbon rings, that provides bendability (see Fig. 4.2) or even twistability of the nanotubes (Fig. 4.1 d). It should be noted that

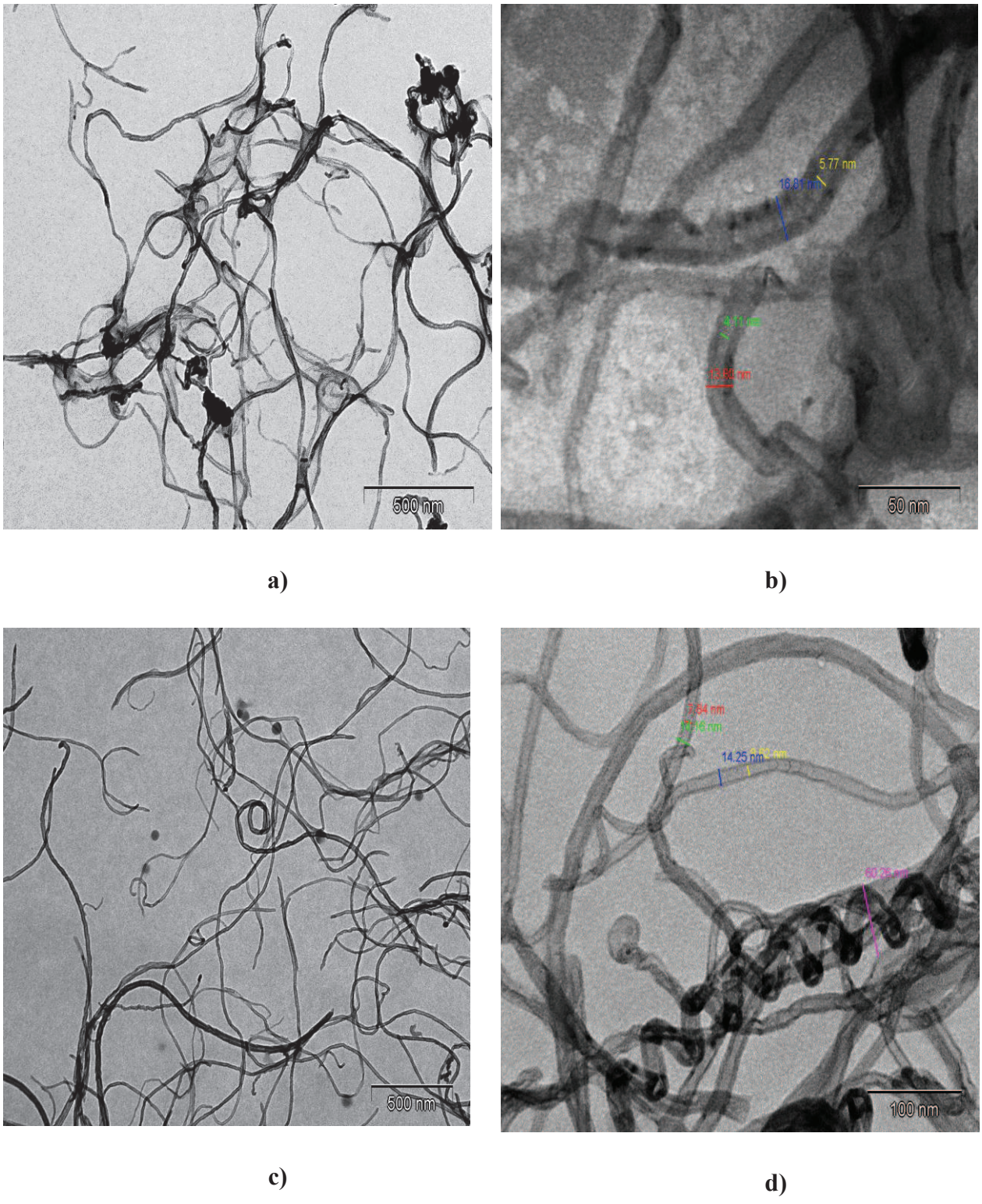

a) **b)**

c) **d)**

Fig. 4.1. TEM microphotographs of multiwalled carbon nanotubes used: a, b – $MWCNTs_1$; c, d – $MWCNTs_2$.

imperfection of nanotubes decreases their strength. Such MWCNTs present also specific properties of electronic conduction as they behave as a tank of electrons.

TEM micrographs of $MWCNTs_2$ are presented in Fig. 4.1 (c, d). It was found that external diameter was nearly $D \approx 10 \div 20$ nm, inner diameter $D_{in} \approx 6 \div 9$ nm and length of nanotubes was $L \approx 0{,}2 \div 11$ μm, i.e. $L/D \sim 10 \div 1100$. Thus, according to TEM data one can conclude that the structural characteristics of $MWCNTs_1$ and $MWCNTs_2$ are very similar, that apparently is caused by the identical methods of synthesis (CNT were obtained by chemical vapor deposition).

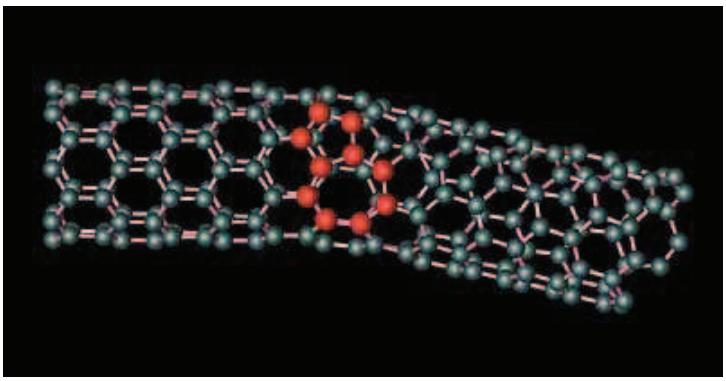

Fig. 4.2. Schematic view of single-walled carbon nanotubes with defects in wall structure [28].

For more detailed characterization of $MWCNTs_1$ and $MWCNTs_2$, their structures were investigated by Raman spectroscopy (Fig. 4.3), which allows determining electronic structure of CNTs using their vibratory characteristics [134, 138-140]. The Raman spectrum of CNTs has several specific and unique features. Firstof all, it is the so-called G-mode (Fig. 4.3, peak at 1573-1575 cm^{-1}) associated with optical vibrations of two adjacent carbon atoms in the nanotube lattice (Fig. 4.4 a). For semiconducting nanotubes, this band has a clear doublet structure, with one of the peaks (G+), caused by vibrations of atoms along the axis of nanotubes (LO-mode) and another one (G–), weaker in intensity and having a lower frequency, represented by fluctuations in the direction perpendicular to the main axis of CNTs directions (TO-mode). In Raman spectra of metallic nanotubes another situation is observed: G+ peak is identified with TO-mode, and LO-mode has a lower frequency caused by strong electron-phonon interaction and Kohn anomaly [28].

Secondly, an important feature of the Raman spectra of carbon nanotubes is the presence of the so-called radial breathing mode (RBM) in low-frequency region that is

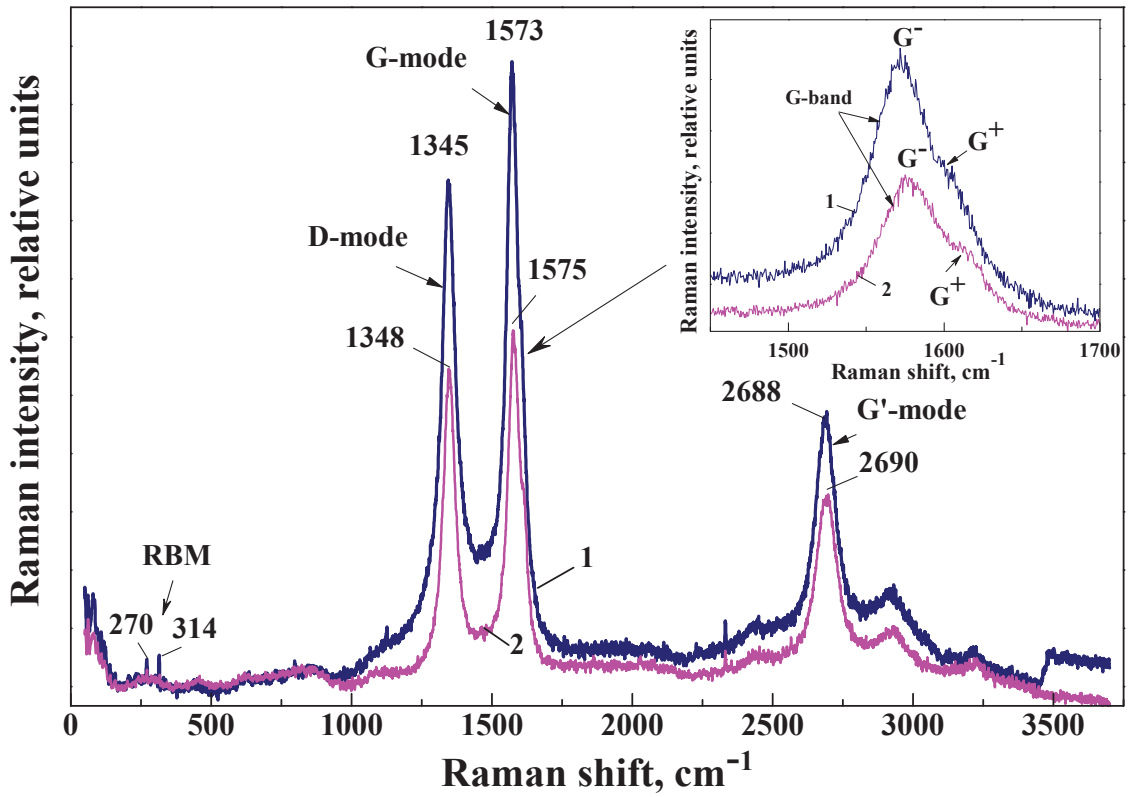

Fig. 4.3. Raman spectra of multiwalled carbon nanotubes: 1 – $MWCNTs_1$; 2 – $MWCNTs_2$. Insert presents a larger scheme of the absorption bands of G mode.

typical for nanotubes only and relates to symmetric vibrations of carbon atoms in radial direction (Fig. 4.4 b), i.e. it is the variation in diameter of nanotubes nearly the mean value. Oscillation frequency of the RBM-mode is inversely proportional to the radius of nanotube, thus the indicated part of the spectrum contains information about the distribution of nanotubes by diameter. However, in the multiwalled CNTs the radial vibrations of carbon atoms are hindered by the walls of adjacent tubes, so these vibrations in MWCNTs are virtually absent.

However, the data presented in Fig. 4.3 clearly show that in the spectra of both the types of nanotubes at 200 ÷ 350 $см^{-1}$ the characteristic bands (of low intensity) are present, which according to the literature [136] refer to symmetric vibrations (in radial direction) of

carbon atoms in double-wall nanotubes, or they are associated with the presence of internal CNTs with very small diameter (less than 2 nm) in the multiwall nanotubes.

Thirdly, this is the occurrence in the Raman-spectra of D-mode and G'-mode (with

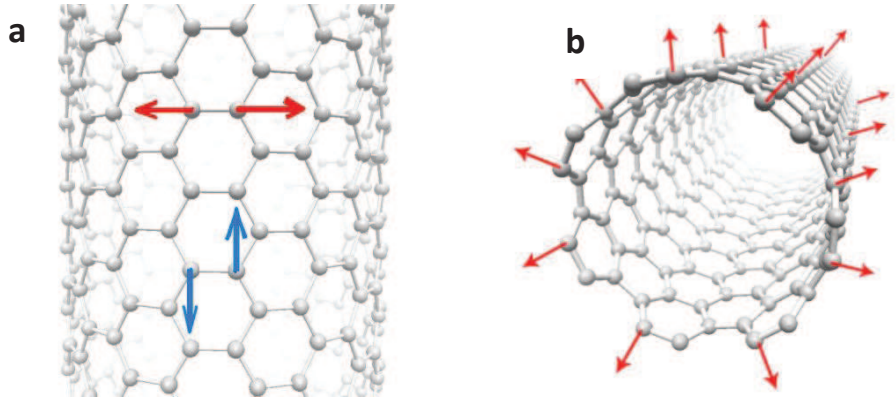

Fig. 4.4. Schematic view of carbon nanotubes: a – tangential modes; b – radial breathing mode (RBM) [30].

maxima at 1345-1348 and 2688-2690 cm^{-1}, respectively) that indicates the presence of certain defects in nanotubes, which may be caused by imperfection of the lattices of nanotubes and by the presence of impurities. It is seen that for both the types of nanotubes, the intensity of D-mode is high enough. Since the manufacturers report about the absence of any traces of amorphous carbon in the CNTs, the appearance of these bands can be explained by the presence of defects on the walls of nanotubes (Fig. 4.2) that is in a good agreement with the above given TEM data.

For these carbon nanotubes the so-called index of imperfection (D/G) and index of perfection (G'/G) were calculated by comparison of the areas under the peaks of D-mode and G-mode. The calculations have shown that for $MWCNTs_1$ D/G = 0.90 and G'/G = 0.84, for $MWCNTs_2$ D/G = 0.77 and G'/G = 1.12. Since the calculated indexes are close, therefore one can conclude that the carbon nanotubes used have similar structure.

Using FTIR spectroscopy chemical structure of $MWCNTs_1$ and $MWCNTs_2$ was investigated, the spectra are shown in Fig. 4.5. It is clearly seen that in the IR spectra the broad absorption band ν_{OH} at 3660 ÷ 3160 $см^{-1}$ appears that can be explained by the presence of a number of OH groups (functional groups on the surface of nanotubes or as a

part of the adsorbed water) in the structure of the investigated carbon nanotubes. Moreover, for $MWCNTs_2$ one can see the absorption band with maximum at 1105 cm^{-1}, which according to literature data corresponds to stretching vibrations of Si-O groups of the catalyst remained after synthesis of these nanotubes.

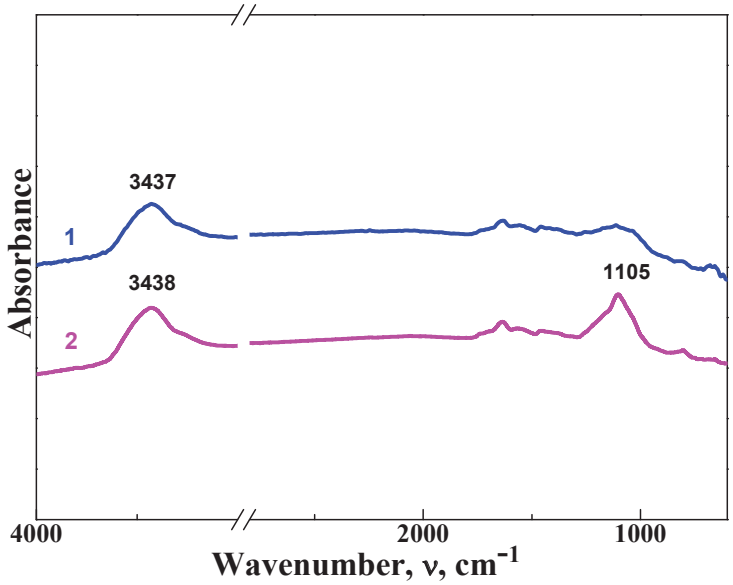

Fig. 4.5. FTIR spectra of individual carbon nanotubes: 1 – $MWCNTs_1$; 2 – $MWCNTs_2$.

The TGA studies have shown that resistance of the carbon nanotubes studied to thermal-oxidative degradation, as expected, was high (cf. Table 4.1 and Fig. 4.6). Thus, temperature of onset of thermal-oxidative degradation for $MWCNTs_1$ was $T_{d\ (onset)} \approx$ 791.6 K, and for $MWCNTs_2$ $T_{d\ (onset)} \approx$ 734.6 K. The $MWCNTs_1$ degradates with maximum rate at $T_{d\ (max)} \approx$ 917.2 K and the $MWCNTs_2$ has the maximum rate of degradation at $T_{d\ (max)} \approx$ 882.6 K. Thus the TGA data presented evidence that thermal stability of $MWCNTs_1$ is slightly higher than that of $MWCNTs_2$. It was also found that for both the

Table 4.1. Thermal characteristics ($O_2/N_2 \approx 1/1$) of the $MWCNTs_1$ and $MWCNTs_2$ studied

Sample	$T_{d\ (onset)}$, K	$T_{d\ (5\%)}$, K	$T_{d\ (max)}$, K	Δm_{max}, wt.%	$T_{d\ (50\%)}$, K	m_{char} (at 970 K), wt.%
$MWCNTs_1$	796.1	830.3	917.2	46.3	913.6	19.26
$MWCNTs_2$	734.6	800.9	882.6	37.2	872.5	6.27

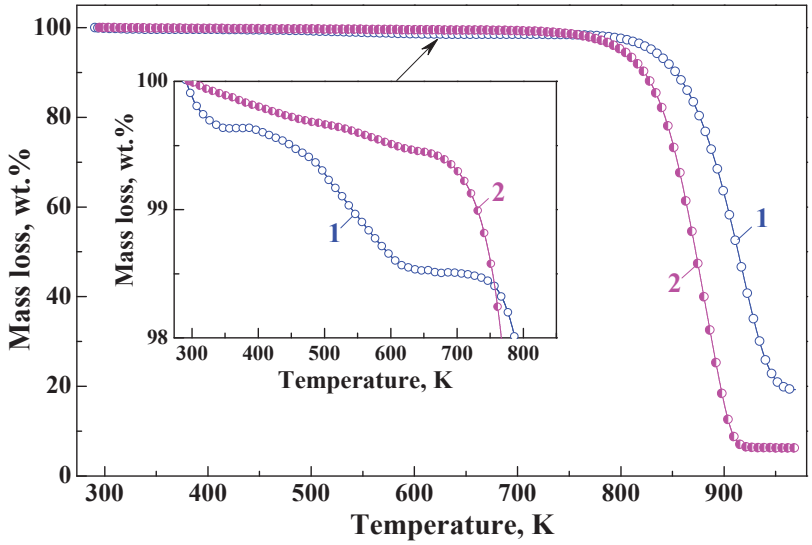

Fig. 4.6. TGA data (in $O_2/N_2 \approx 1/1$) for the samples of individual carbon nanotubes: 1 – $MWCNTs_1$; 2 – $MWCNTs_2$.

samples of MWCNTs, prior to the main stage of decomposition of carbon skeleton (at $T >$ 800 K), in temperature region of $T \approx 373 \div 473$ K a certain mass loss was fixed, namely: $\triangle m \approx 0{,}57$ wt. % (for $MWCNTs_1$) and $\triangle m \approx 0{,}32$ wt. % (for $MWCNTs_2$), that in certain temperature interval may be caused by the removal of adsorbed water out of the CNTs. Therefore, the samples of CNTs studied have small amount of the adsorbed H_2O.

For the both types of CNTs studied in temperature region of $T \approx 473 \div 720$ K another mass loss was also fixed: $\triangle m \approx 0.96$ wt. % (for $MWCNTs_1$) and $\triangle m \approx 0.53$ wt. % (for $MWCNTs_2$) (Fig. 4.6 and Table 4.1). It is known [30] that it is caused by destruction of functional groups, which usually present in a certain amount in the structure of the outer walls of most the types of carbon nanotubes. This conclusion correlates with the FTIR data above confirming the presence of OH groups in the structure of the carbon nanotubes studied.

4.3. Investigation of the effect of carbon nanotubes on polymerization of cyclic oligomers of butylene terephthalate

Literature review (cf. Chapter 1) have shown that chemical and physical properties of CNTs-containing polymeric nanocomposites are controlled, in the first place, by

dispersing degree of CNTs, at that the best physical-mechanical properties are demonstrated by nanocomposites with CNTs dispersed up to individual nanotubes.The presence of aggregates of CNTs results in lower effect of the nanofiller on final properties of nanomaterials obtained. However, according to the recently published series of works by Alig et al. [7, 141, 142], nanocomposites formed from the molten polymers at temperatures higher than T_m of polymer matrix had an improved electrical conductivity. The authors associated this effect with reaggregation of CNTs during their annealing at $T > T_m$ facilitated formation of three-dimensional CNTs-network. In this chapter the effect of aggregation of CNTs on electrical conductivity of nanocomposites obtained will be examined in more detail later in sect. 4.8.

It is known now [42], that the most effective way of introduction of CNTs into oligomeric or polymer matrix is mixing with a help of ultrasonic dispersers of different capacity (from 12 to 500 W) and frequency (20 ÷ 55 kHz), high-speed mixers (500 ÷ 3000 rpm), calenders (with rotation speed of rolls from 20 to 180 rpm), etc.

From the technological point of view, the most promising method of obtaining of polymer nanocomposites, including CNTs-containing ones, is reactive extrusion: simultaneous synthesis of polymer matrix from oligomer and effective dispersing of nanofiller in it. Since at reactive extrusion synthesis of polymer component is carried out in the presence of nanofiller, the viscosity of the reactive mixture increases significantly; that is why it is important to have quite low viscosity of the original reactive oligomer used.

As it was noted above, in the present work the cPBT/MWCNTs$_1$ nanocomposites were obtained by the reactive extrusion method using miniextruder (see sect. 2.2) through *in situ* synthesis of cPBT from CBT in the presence of MWCNTs$_1$. It is known that technological advantage of CBT over PBT is much lower viscosity of CBT in comparison with PBT: $\eta_{CBT} \sim 0.020$ Pa·sec (at T_{mCBT}) and $\eta_{PBT} \sim 4000$ Pa·sec (at T_{mPBT}). It is also important that CBT polymerizes even at temperatures lower the melting point of PBT ($T_{m\ PBT} \approx 503$ K). Therefore, to avoid crystallization of cPBT obtained synthesis of cPBT from CBT has to be carried out in isothermal conditions at $T > T_{m\ PBT}$ (Fig. 4.7).

Samples of the net cPBT were also synthesized using the reactive extrusion method at similar conditions as for synthesis of the nanocomposites (see sect. 2.2), while in one case the original mixture of cyclic oligomers of butylene terephthalate, CBT$_{in}$ (without vacuuming and drying) was used, otherwise CBT was prevacuumed and dried (at $T \approx 353$ K) to remove

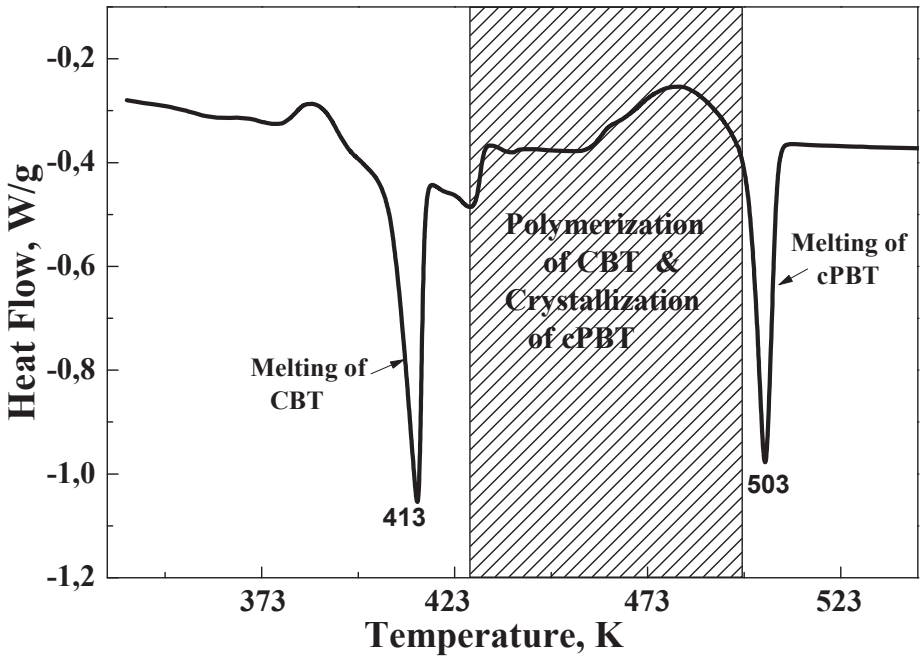

Fig. 4.7. Dynamic DSC data on synthesis of cPBT from CBT (heating rate 10 K/min).

the traces of volatile impurities that may remain at CBT production.

Using Size Exclusion Chromatography, SEC, the molecular weights of $cPBT_{in}$ and cPBT samples were determined and insignificant difference in their values of M_w, M_n and M_z were established (Table 4.2). In addition, using TGA it was found (sect. 4.6) that mass loss of $cPBT_{in}$ at heating in the temperature range of 373 ÷ 473 K (where evaporation of adsorbed water takes place) was extremely small (~ 0.15 wt. %).Thus, it was concluded that original CBT_{in} was also suitable for cPBT synthesis without additional purification.

Table 4.2. Size Exclusion Chromatography data for the synthesized samples of $cPBT_{in}$ and cPBT

Sample	M_n	M_w	M_z
$cPBT_{in}$	4 590	23 200	51 100
cPBT	5 600	26 500	43 800

Kinetics of the reaction of *in situ* polymerization of CBT oligomers in the presence of $MWCNTs_1$ depending on the content of the latter, was studied using method of melt rheology (sect. 3.8), the results are presented in Fig. 4.8. It was established that polymerization process of the individual CBT (at temperature $T \approx 503$ K) has a certain induction period ($\tau \approx 40$ sec), followed by a rapid increasing in viscosity due to growth of molecular weight of PBT formed. At the last stage of the process (at $\tau > 500$ sec) viscosity becomes almost stable ($\eta^* \approx 4400$ Pa · sec), indicating the termination of polymerization with formation of cPBT.

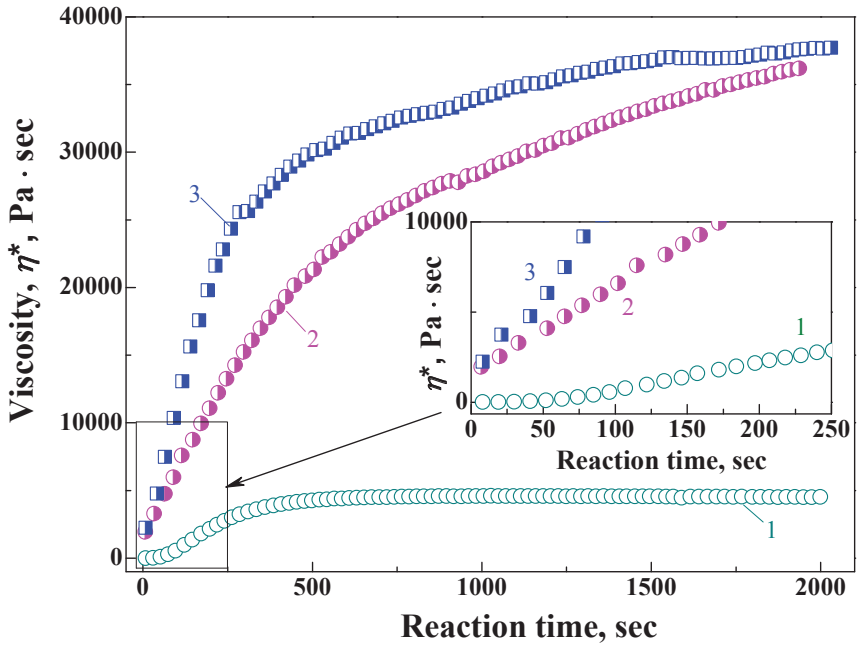

Fig. 4.8. Dependence of viscosity η^* on reaction time of polymerization of CBT and CBT/$MWCNTs_1$ at $MWCNTs_1$ content (wt. %): 1 – 0; 2 – 1.0; and 3 – 2.0.

During *in situ* polymerization of CBT in the presence of $MWCNTs_1$ the induction period disappears, and viscosity of the system starts growing dramatically within the first seconds of the extrusion and the slope angle of the viscosity curve increases indicating acceleration of polymerization of CBT-component in the presence of $MWCNTs_1$. Fig. 4.8 shows that increasing of nanofiller content from 1.0 to 2.0 wt. % results in significant increasing polymerization rate, especially in the early stages of the reaction.

Thus, one can conclude that carbon nanotubes possess significant catalytic effect in

CBT polymerization process even with just 1 ÷ 2 wt. % of CNT in the composition. In other words, $MWCNTs_1$ actually acts as catalyst for CBT polymerization.

The catalytic effect of CNTs observed in synthesis of the CBT-based nanocomposites may be caused by adsorption of the molecules of CBT oligomer onto the developed surface of nanotubes and probably by adsorption of catalyst $C_4H_9SnCl(OH)_2$ with its possible chemical grafting through the reaction with OH groups of $MWCNTs_1$ surface and so heterogeneous catalysis [112, 113] takes place in the system.

Furthermore, it is known [143] that even carbon nanotubes itself can participate in complex electronic interactions with different chemical functional groups on atomic level and interaction force significantly depends on electronic structure of functional groups reacting with CNTs.

4.4. Determination of morphology of cPBT/$MWCNTs_1$ nanocomposites using scanning and transmission electron microscopies

It is known that electron microscopy is one of the basic methods for nanomaterials research, as it enables direct visibility of the material morphology. For example, discovery of CNTs has become possible due to using TEM at their investigation [45]. Morphological features of cPBT/$MWCNTs_1$ nanocomposites with different content of nanotubes were studied by SEM and TEM, the corresponding microphotographs are presented in Fig. 4.9 and 4.10, respectively. It was established that $MWCNTs_1$ were effectively dispersed in all the samples of the nanocomposites obtained. The SEM micrographs clearly showed that CNTs were well distributed in the samples area, thus one could observe both isolated nanotubes (filiform light inclusion) and cross-section (light round spots) of nanotubes broken during preparation of the samples for SEM studies (samples were frozen in liquid nitrogen and subsequently splited, sect. 3.1). Sometimes dark spherical areas looking like pores were also noticed, these voids were formed after pulling out of the nanotubes at splitting at insufficient adhesion to polymer matrix as mentioned before [26].

Analysis of SEM data allows concluding about high adhesion between polymer matrix and carbon nanotubes. This inference is based on the fact that the majority of CNTs after splitting of the sample (in liquid nitrogen) remained in cPBT matrix, but were not

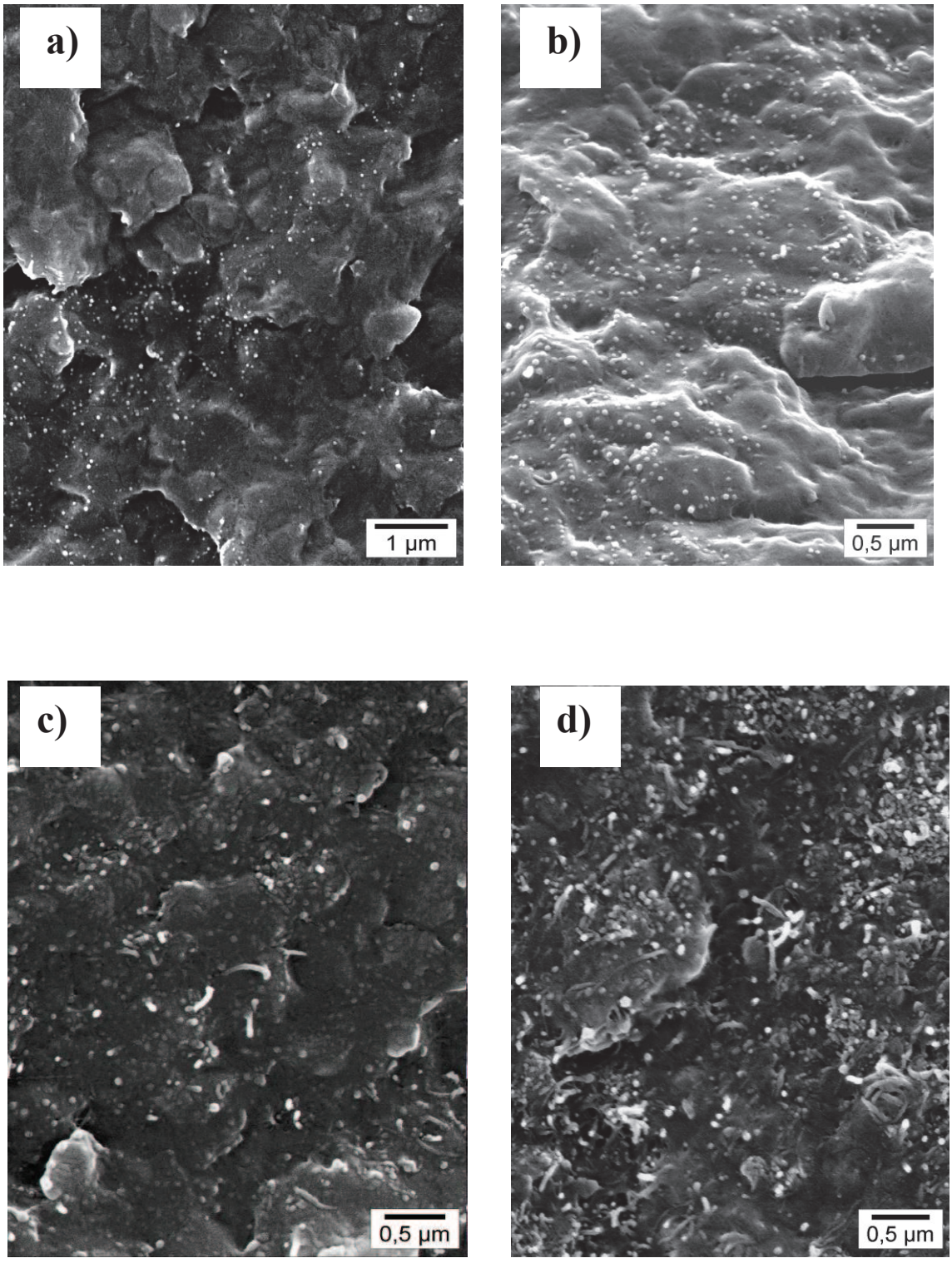

Fig. 4.9. SEM micrographs of nanocomposites of cPBT/MWCNTs$_1$ (samples were obtained by hot pressing of extrusion strand) with different MWCNT$_1$ content, wt.%: a – 0.1; b – 0.3; c – 2.0; and d – 2.0 (agglomerate zone).

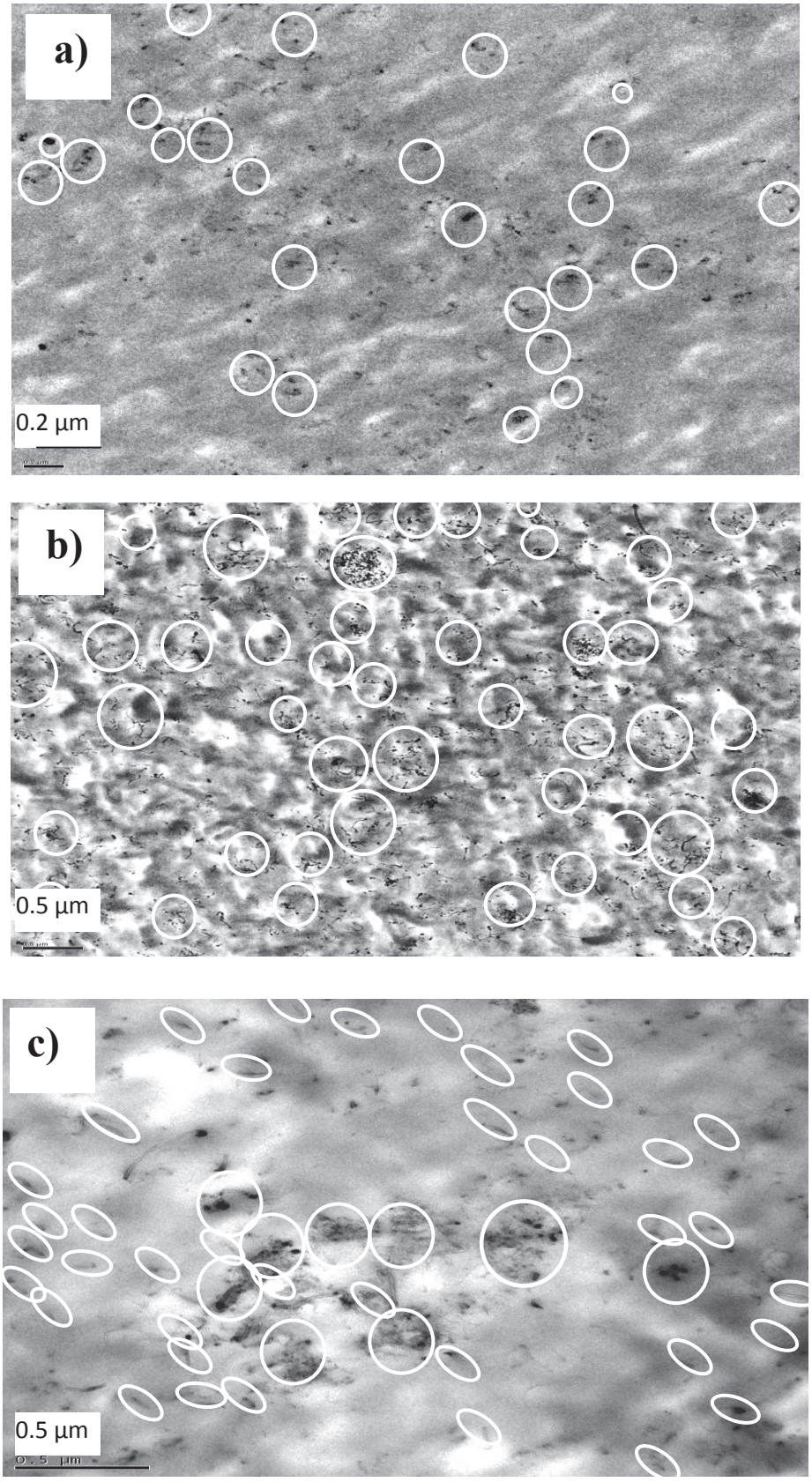

Fig. 4.10. TEM micrographs of cPBT/MWCNTs$_1$ nanocomposites (MWCNT$_1$ content was 2 wt. %) obtained by: a – extrusion strand; b – hot pressing of extrusion strand; c – injection molding.

pulled out from the matrix (that would take place in a case of poor adhesion between the matrix and CNTs). Moreover, the results of determination of outer diameter of nanotubes in the nanocomposites investigated using "Image J" software showed that their diameter was by ~ 5 ÷ 25 nm larger than the diameter of the initial $MWCNTs_1$. This is known as a phenomenon of "wrapping" of carbon nanotubes by polymer, and it occurs in systems with high adhesion between polymer matrix and CNTs only [26]. As far as carbon nanotubes possess electrical conductivity, the above mentioned phenomenon has to affect the conductivity of the nanocomposite obtained. The electrical properties of the $cPBT/MWCNTs_1$ nanocomposites will be discussed in detail below in sect. 4.8.

Thus, one can conclude that in the samples studied certain nanostructure looking like a “hot dog” is formed. However, taking into consideration that it belongs to the subjects of nanoworld, therefore, the structure formed can be conventionally called as “nano hot dog” (by analogy to “nanorose”, “nanonail”, “nanobrush”, “nanodandelion” etc. [145]). So, the composites studied can be considered in a certain way as nanostructured ones.

Similar results were obtained recently by Lusenkov et al. [146], where effect of CNTs on structure and the properties of PEG300 and PEG300/CNTs polyelectrolytes were investigated. Studying the impact of CNTs on electrical properties of the nanocomposites obtained, the authors have found that conductivity of the samples increases significantlywith increasing CNTs concentration in the system and proposed the model, whereby there are three basic components with different electrical properties in the systems studied, namely: ion-conductive polymer matrix (PEG-$LiClO_4$), dispersed filler (CNTs) and conductive surface layer, forming around the filler particles and having higher conductivity than the polymer matrix. The latter looks very similar to our observations. As a result three-dimensional conductive network consisting of nanostructures above-named as “nano hot dog” is formed.

Figs. 4.9 and 4.10 also display that along with isolated CNTs there are also agglomerates of CNTs in the systems studied. In SEM photomicrographs they look like clusters of light spots and filaments; in TEM - like dark threadlike inclusions). It was found that increasing of $MWCNTs_1$ content from 0.1 to 2 wt. % resulted to increasing agglomerates content. It is observed that in the samples studied there are the regions with high content of agglomerates of $MWCNTs_1$ and the regions without agglomerates at all. We consider that such situation may be caused by two reasons. First, as noted above in

sect. 2.2, there are some agglomerates remained in the system after dispersing CNTs in the matrix. Secondly, as it is known from the publications of Alig et al [7, 141, 142], at thermal treatment and shear stress of CNT-based polymer nanocomposites at $T > 500$ K (i.e. actually during annealing process) the processes of reaggregation of CNTs takes place.

Using analysis of TEM micrographs for the samples obtained by different ways (Fig. 4.10) one can conclude that a number of aggregates in the film samples obtained by pressing of extrusion strand is greater as compared with the composites of the other two serieses (Fig. 4.10 b). We believe that this is caused by the longest influence of the temperature aboveT_m of cPBT ($T \approx 513$ K, sect. 2.2) and additional pressure on the samples obtained by hot pressing, that, as mentioned above, results in reaggregation of CNTs in polymer matrix. It will be shown in sect. 4.8 that reaggregation of CNTs improves electrical properties of the nanocomposites significantly, however, decreasing storage modulus, E' will be also observed (sect. 4.5).

The analysis of Fig. 4.10 (c) evidences the occurrence of certain orientation of CNTs in the samples obtained by injection molding. Obviously, the orientation in this sample took place in the process of casting in the direction of flow of molten cPBT/MWCNTs$_1$ compositions.

As it will be shown below in the sect. 4.5 ÷ 4.8, the changes in morphology of the samples of the nanocomposites investigated cause significant changes in a number of their physical-chemical properties.

4.5. Viscoelastic properties of cPBT/MWCNTs$_1$ nanocomposites

It is known that Poly(butylenes terephthalate) is a partially crystalline polymer, therefore it was of a great interest to define the influence of the nanofiller on viscoelastic properties of the nanocomposites synthesized, and especially on characteristics of amorphous microphase of cPBT. DMTA is the most informative method to determine the relationships and changes occurring in macrochains of polymers from amorphous phase under the influence of various factors, including filling of polymer by fillers [137]. The effect of MWCNTs$_1$ on viscoelastic properties of the samples of the synthesized nanocomposites and formed by hot pressing of extrusion strands was investigated

depending on the nanofillers content (Fig. 4.11). Details of the research technique and preparation of the samples for the investigation were described in the sect. 3.6.

Fig. 4.11 representing temperature dependencies of storage modulus E' and loss modulus E'' (at temperatures $T \approx 133 \div 423$ K), shows that the presence of even small amounts (0,01 ÷ 2,0 wt. %) of carbon nanotubes in these nanocomposites, changes the glass transition temperature T_g (β-relaxation process) of cPBT matrix and the temperature of γ-relaxation process of the latter as well as the value of activation energy E_a of β-relaxation process, etc. (Table 4.3).

For example, introduction of 0.01 wt. % of $MWCNTs_1$ only caused significant increase in storage modulus E' at temperatures $T < 240$ K (Fig. 4.11 a), while for the nanocomposites containing 0.3 and 2.0 wt. % of nanotubes, E' values were lower as compared with the sample of the individual cPBT in the whole temperature range.

Obviously, during *in situ* synthesis of cPBT matrix in the presence of small amount of the nanofiller (0.01 wt. %) effective dispersing of CNTs occurr (probably mainly to individual nanotubes), aggregation of CNTs was insignificant, and therefore the sample was reinforced by the dispersed CNTs, as a result the value of storage modulus increases. However, increasing of CNTs content in 30 or more times (up to 0.3 ÷ 2.0 wt. %) results, first, in decreasing possibility of CNTs dispersing to individual nanotubes (Figs. 4.9 and 4.10) and, secondly, as noted above, at high temperature of cPBT synthesis ($T \approx 503$ K) the reaggregation of CNTs and, hence, reducing homogeneity of their dispersion in polymer matrix are observed, i.e. reinforcing effect of CNTs decreases. This results in the reduction of storage modulus E' and simultaneously of loss modulus E'' as far as the aggregates of CNTs hinder a segmental mobility of macromolecules of Poly(butylene terephthalate). Similar effects were observed by Alig et al. [7, 141, 142] at investigation of some MWCNTs-containing polymer nanocomposites.

It was found that for the dependence $E'' = f(T)$ obtained at different frequencies (1-15 Hz) a shift towards higher temperatures with increasing frequency is observed. According to the temperature-frequency superposition low [147], the higher frequency the greater the shift of the curve to higher temperatures. Such behavior of the dependence $E'' = f(T)$ can be explained as follows: the higher frequency of the forced dynamic oscillations, the lower wave energy is transmitted to the material for the same period of

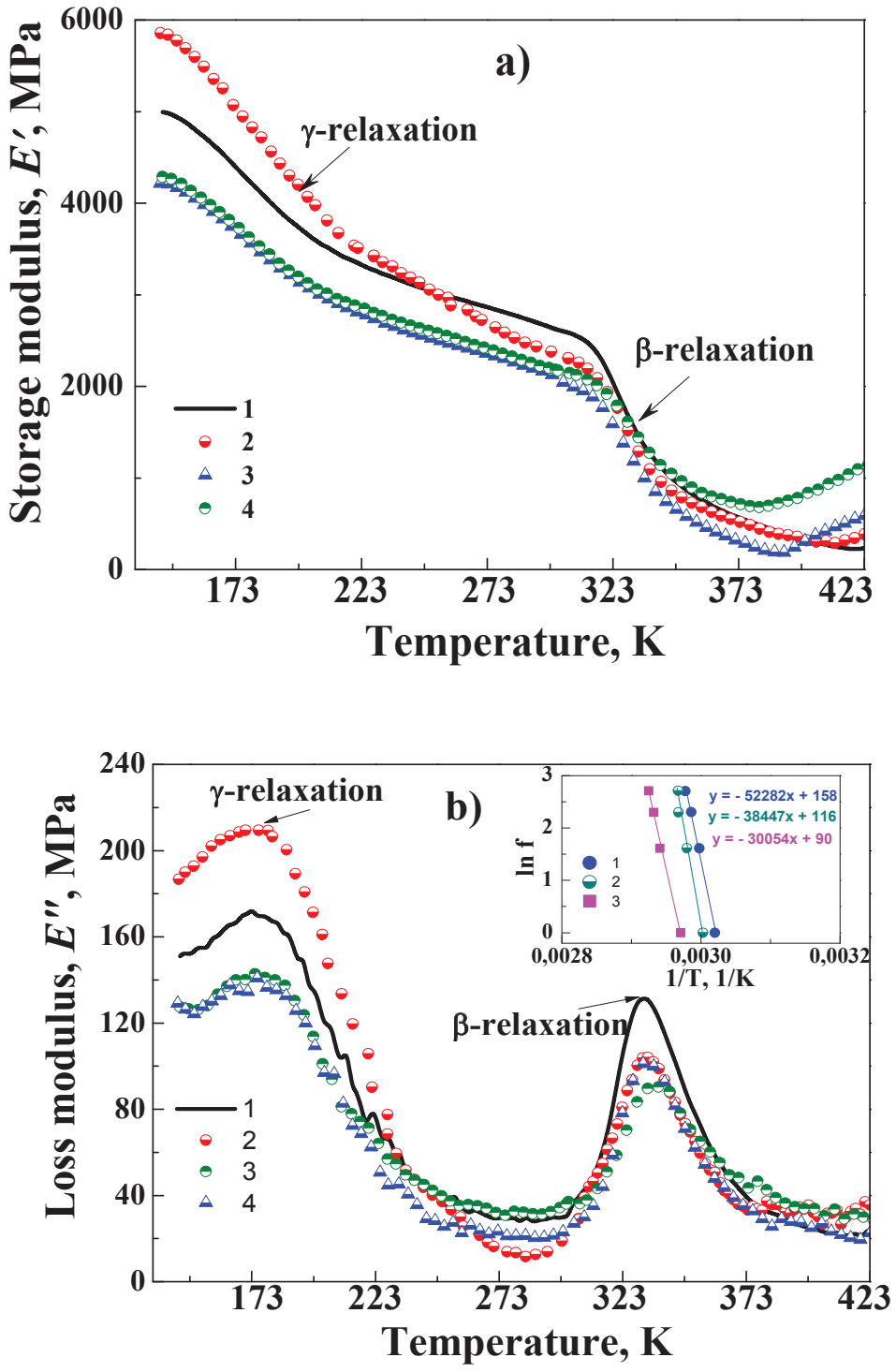

Fig. 4.11. Temperature dependencies of (a) storage modulus *E′* and (b) loss modulus *E″* (at frequency of 1 Hz) for cPBT/MWCNTs$_1$ nanocomposites with the content of MWCNTs$_1$, wt. %: 1 – 0; 2 – 0.01, 3 – 0.3, and 4 – 2.0. In framing the corresponding Arrenius plots are shown for the samples with the content of MWCNTs$_1$, wt. %: 1 – 0; 2 – 0.3; and 3 – 2.0.

Table 4.3. Effect of carbon nanotubes on viscoelastic properties of cPBT/$MWCNTs_1$ nanocomposites (frequency 1 Hz)

$MWCNT_1$content, wt.%	***E'*** **(at 273 K), MPa**	**T_γ, K**	**T_g (β-relaxation), K**	**Apparent activation energy, $E_{a(\beta)}$, kJ/mol**
0 (cPBT)	2871	173.0	331.7	47.5
0.01	2695	170.8	333.5	52.8
0.3	2360	175.2	333.7	60.6
2.0	2407	174.2	338.6	54.1

time and the higher amount of heat energy is needed to start any process, including relaxation. The DMTA data obtained were used to determine the values of apparent activation energy E_a of *β*–relaxation process in the samples, the calculations were made using well known Arrenius equation. It was found that the presence of carbon nanotubes in cPBT matrix results in increasing values of T_gs and of activation energy E_a of β–relaxation process (see Table 4.3) confirming the conclusion about the difficulties in cooperative mobility of kinetic segments of macromolecules of cPBT matrix (in comparison with unfilled cPBT) due to the presence in the samples of the nanofiller.

4.6. Effect of carbon nanotubes on thermal physical properties of nanocomposites

It is known that DSC method is one of the most informative and sensitive method for characterization of crystalline structure of polymers and polymer composites. Using DSC the changes in crystalline microphase of polymer systems occurred as a result, for example, of changes in composition, method of synthesis or sample molding are clearly recorded. Therefore, DSC method was chosen for determination of the impact of carbon nanotubes on such characteristics of crystalline structure of cPBT as melting temperature

T_m of crystallites, melting enthalpy, ΔH_m, degree of crystallinity, X_c, etc. Glass transition temperature T_g of the amorphous phase of cPBT in the samples studied was also determined.

During synthesis of cPBT from CBT using the method of reactive extrusion in miniextruder several processes occur simultaneously (temperature of synthesis $T \approx 503$ K): 1) melting of CBT; 2) dispersing of $MWCNTs_1$ in the molten CBT; 3) polymerization of CBT with formation of cPBT; 4) *in situ* dispersing (due to significant shear stress) of $MWCNTs_1$ in the cPBT being synthesized. After synthesis, during further cooling, crystallization of the cPBT formed takes place. All these stages form the final properties of the nanocomposites, and therefore the impact of nanofiller on their phase structure and properties is essential.

As it was noted above in sect. 2.2, the nanocomposite samples of cPBT/$MWCNTs_1$ were obtained in three ways: 1) as strand, coming out of the nozzle of miniextruder; 2) by pressing of the strands (after miniextruder), 3) by injection molding of the molten material obtained from miniextruder. DSC thermograms for the mentioned three serieses of cPBT/$MWCNTs_1$ nanocomposites are presented below in Figures 4.12 – 4.15 and in Tables 4.4 – 4.6. It is noteworthy that the first scans are mainly shown on the graphs (i.e., the data from the first heating of the samples), since it was interesting to determine the impact of the method of preparation of polymer material (i.e. thermomechanical history of the samples) on thermal-physical properties of the nanocomposites obtained.

The DSC thermograms presented show that depending on the composition and on preparation method the thermal-physical properties of amorphous and crystalline phases of cPBT-matrix in the synthesized cPBT/$MWCNTs_1$ nanocomposites are changed non-monotonically, namely, glass transition temperature T_g (by 1 ÷ 5 K), melting temperature T_m (by 0.1 ÷ 4.5 K, the tables list the value of T_m of the peak of maximal height), crystallization temperatureT_c (by 3,1 ÷ 18,2 K), melting enthalpy ΔH_m (by 1.1 ÷10.2 $J \cdot g^{-1}$), degree of crystallinity X_c (by1.0 ÷ 7.5 %) etc. Beside, the increase of CNTs content in the samples leads to changes in a shape of melting termograms of the cPBT-matrix crystallites, especially at second heating (Fig. 4.12 b).

In the DSC thermograms for most of the samples before the main melting peak, a second weaker peak of the cPBT crystallites melting [95] corresponding to the melting of

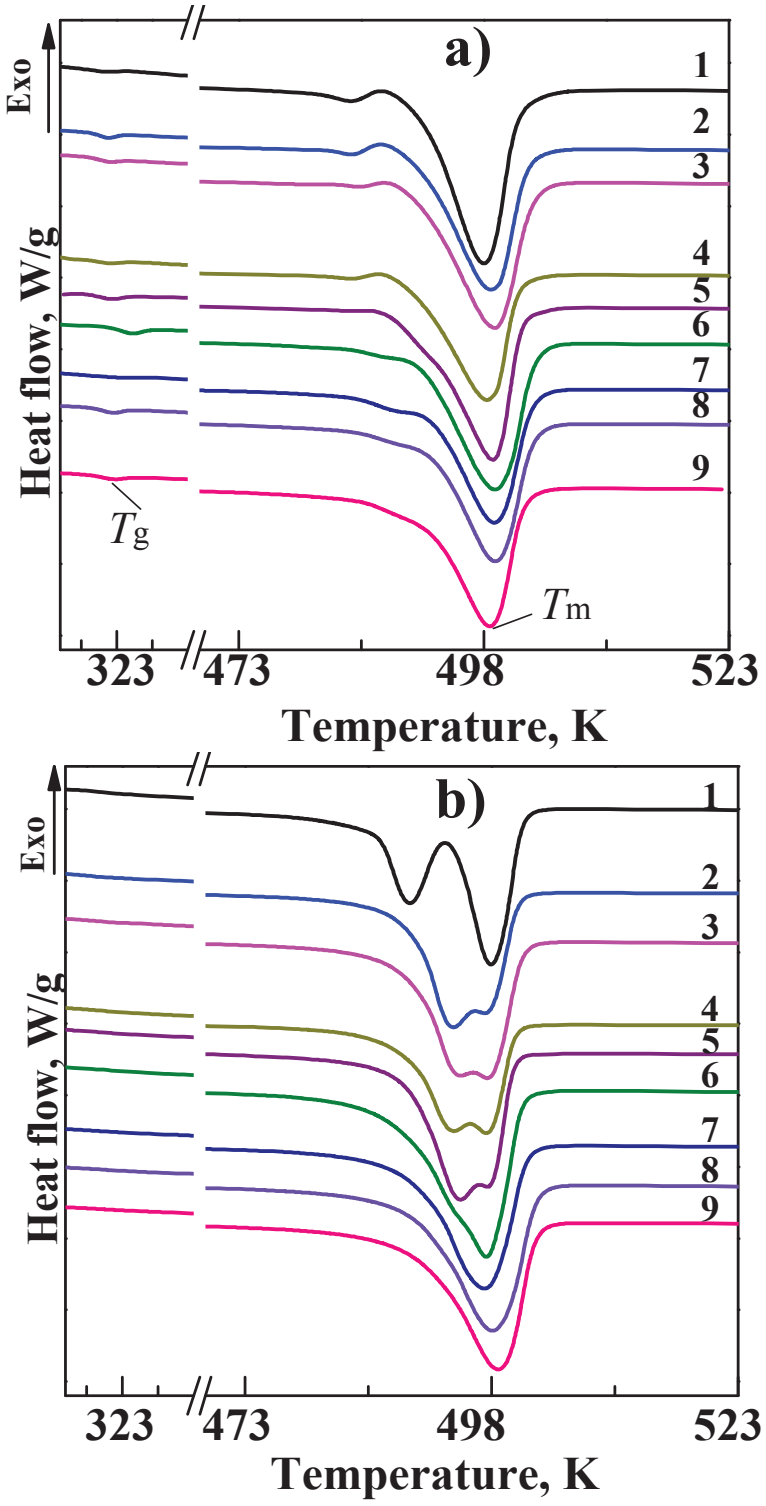

Fig. 4.12. DSC thermograms for cPBT/MWCNTs$_1$ nanocomposite samples obtained by injection molding of the molten material arrived from miniextruder with various content of MWCNTs$_1$, wt. %: 1 – 0, 2 – 0.01, 3 – 0.05, 4 – 0.1, 5 – 0.25, 6 – 0.3, 7 – 0.5, 8 – 1.0, 9 – 2.0; a) – first scan; b) – second scan.

Table 4.4. Thermal-physical properties for cPBT/$MWCNTs_1$ nanocomposites obtained by injection molding of the molten material obtained from miniextruder

$MWCNT_1$ content, wt.%	T_g, K	T_m, K	ΔH_m, J·g^{-1}	X_c, %
0	311	498.1	52.3	36.8
0.01	315	498.8	43.5	30.6
0.05	315	499.1	45.2	31.8
0.10	315	498.5	42.1	29.6
0.25	314	499.0	45.8	32.3
0.30	312	499.2	50.0	35.0
0.50	314	499.1	45.7	32.2
1.00	315	499.3	46.9	33.0
2.00	316	498.6	49.5	34.9

defective crystallites was observed. During the further heating recrystallization of the samples occurred and the larger or more perfect crystallites of cPBTwith higher melting temperature are formed. It can be seen from Fig. 4.12 ÷ 4.14 that in the thermograms of the nanocomposites with CNTs content ≥ 1 wt. % the melting peaks corresponding to smaller or defective crystallites are absent, thus it is clear that the higher $MWCNTs_1$ content in the system provides formation of more perfect or larger crystallites of cPBT.

It was found that during cooling of the samples after first heating of the nanocomposites (unlike unfilled cPBT) crystallization process started much earlier and at higher temperatures (by 3 ÷ 18 K, depending on the composition and the method of sample molding, Fig. 4.15). Moreover, it was established that the higher content of the nanofiller, the higher temperature of the cPBT crystallization onset. The character of changes in T_c values in the nanocomposites obtained allows concluding that carbon nanotubes play the

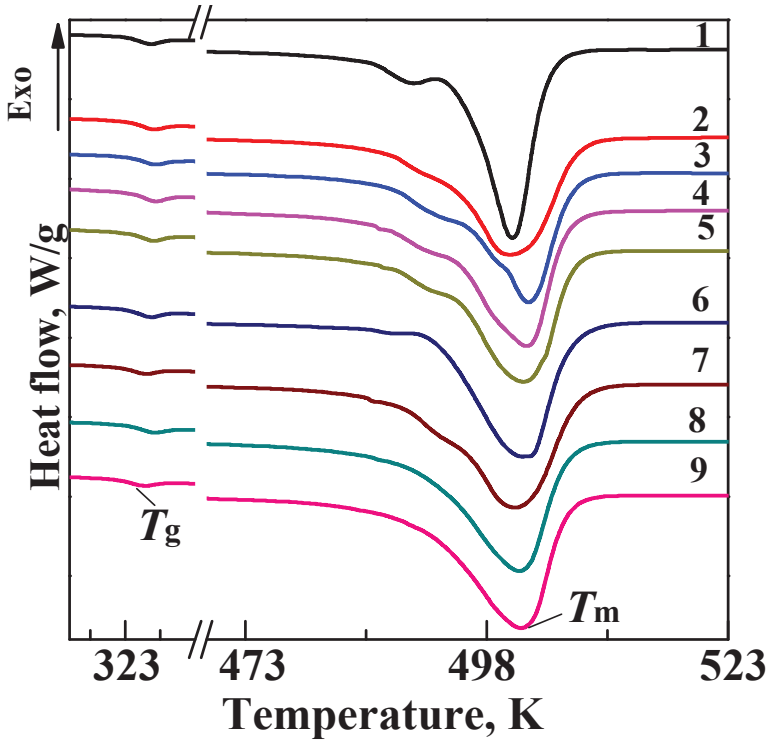

Fig. 4.13. DSC thermograms for cPBT/MWCNTs$_1$ nanocomposites obtained by hot pressing of extrusion strand with MWCNT$_1$content, wt. %: 1 – 0; 2 – 0.01; 3 – 0.05; 4 – 0.1; 5 – 0.2; 6 – 0.3; 7 – 0.5; 8 – 1.0; 9 – 2.0.

Table 4.5. Thermal-physical properties for cPBT/MWCNTs$_1$ nanocomposites obtained by reactive extrusion with further hot pressing of extrusion strand

MWCNT$_1$ content, wt.%	T_g, K	T_m, K	ΔH_m, J·g^{-1}	X_c, %
0	324	500.7	55.1	38.8
0.01	326	500.6	53.8	37.9
0.05	324	502.4	50.4	35.5
0.10	325	502.2	56.8	40.0
0.20	323	501.9	56.7	39.9
0.30	324	502.1	50.9	35.8
0.50	323	500.9	57.4	40.4
1.00	324	501.4	56.5	39.8
2.00	321	501.7	57.7	40.6

role of heterogeneous nuclei of crystallization. This conclusion correlates with the results of study published by Wu et al. [110].

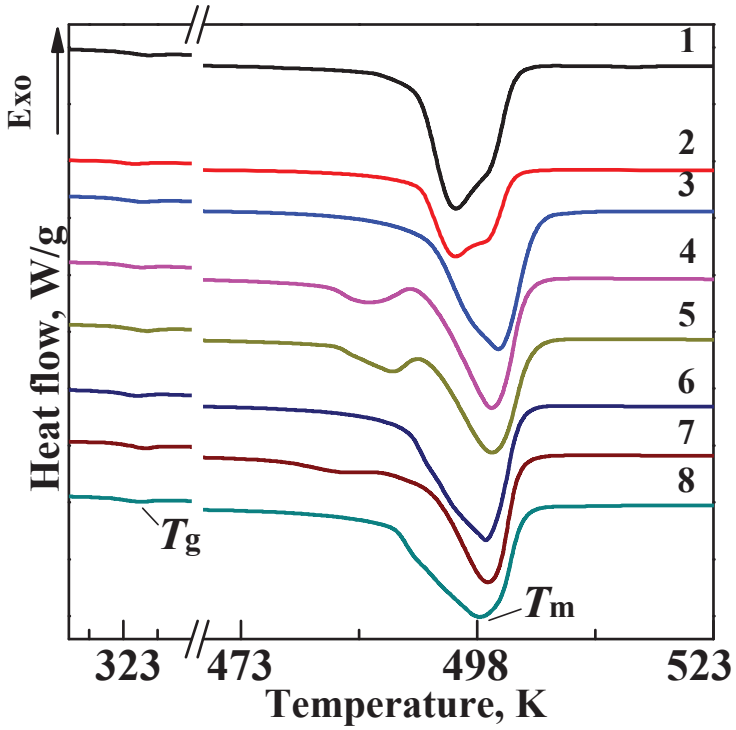

Fig. 4.14. DSC thermograms for cPBT/MWCNTs$_1$ nanocomposites obtained by extrusion with further hot pressing, with the MWCNTs$_1$ content, wt. %: 1 – 0; 2 – 0.1; 3 – 0.2; 4 – 0.25; 5 – 0.3; 6 – 0.5; 7 – 1.0, 8 – 2.0.

For the samples of nanocomposites formed by hot pressing method or by injection molding, increasing melting temperature T_m and degree of crystallinity X_c of cPBT matrix (compared to the unfilled cPBT) at increasing MWCNTs$_1$ content in the composition up to 1.0 ÷ 2.0 wt. % has been fixed (table 4.4 ÷ 4.6). However, for the nanocomposite samples with low MWCNTs$_1$ content (0.01 ÷ 0.05 wt. % fot hot pressing, and 0.10 ÷ 0.30 wt. % for injection molding) decreasing X_c value is found that evidences a hindrance of cPBT crystallization process by carbon nanotubes at these their concentrations in the systems, perhaps, in the final stages of the process. One can suppose that in these samples the effective dispersing of CNTs to single nanotubes (Fig. 4.9 a, b), where the filler is situated homogeneously in whole area of cPBT matrix, creates steric impediments to the front of crystallization. Similar conclusions were made by Wu et al. [110].

Table 4.6. Thermal-physical properties for cPBT/MWCNTs$_1$ nanocomposites obtained by extrusion technique with further hot pressing

MWCNT$_1$ content, wt.%	T_g, °C	T_m,K	ΔH_m, J·g^{-1}	X_c, %
0	321	495.8	58.1	41.0
0.10	318	495.5	50.5	36.0
0.20	320	500.3	62.0	43.7
0.25	323	499.6	56.1	39.5
0.30	322	499.7	55.9	39.4
0.50	321	498.7	60.5	42.6
1.00	323	499.2	59.7	42.0
2.00	321	498.6	68.0	47.9

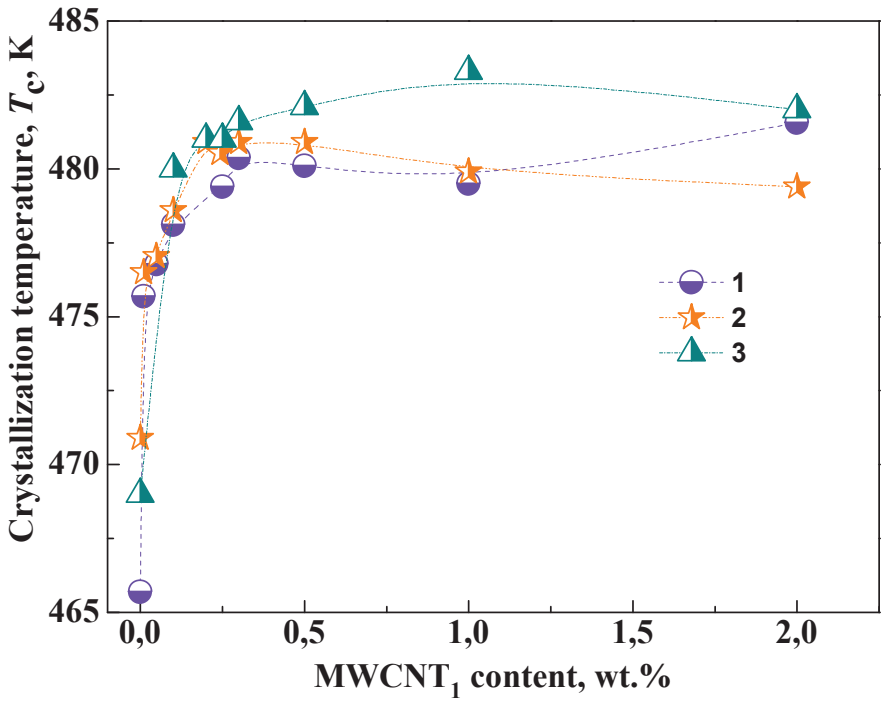

Fig. 4.15. Dependence of crystallization temperature T_c of the cPBT matrix crystallites in the nanocomposites studied on MWCNTs$_1$ content and on molding technique: 1 – extrusion strand; 2 – sample pressing; 3 –injection molding.

All these facts undoubtedly testify to a significant effect of the presence of carbon nanotubes at certain conditions of formation of the nanocomposites *in situ* with CNTs on crystallization process of cPBT matrix (at cooling of the samples after synthesis). Thus, one can conclude that in this case carbon nanotubes acts as particular crystallization nuclei that causes the acceleration of the onset of cPBT crystallization and other changes in formation of crystalline phase of the latter. Similar effect of CNT was found in [144]. Some non-monotonic changes in parameters of crystalline structure of the nanocomposites depending on the content of CNTs, obviously, was caused by imperfect dispersion of carbon nanotubes in cPBT matrix (Fig. 4.10), as well as by the difference in structure and properties of carbon nanotubes. It is clearly seen (Fig. 4.12 ÷ 4.14) that weaker T_m, corresponding to the melting of smaller and defective crystallites disappears at CNT concentration of ≥ 1 wt.%,so it can be concluded that increasing of concentration of $MWCNT_1$ promotes generation of more perfect cPBT crystallites.

4.7. Effect of $MWCNTs_1$ on stability to thermal-oxidative degradation of the nanocomposites of cPBT/$MWCNTs_1$ and $cPBT_{in}$/$MWCNTs_2$

Since Poly(butylene terephthalate) represents the class of thermostable polymers, it was interesting to determine the ability of carbon nanotubes to change thermal characteristics inherent to the individual cPBT. To determine thermal characteristics of the polymer nanocomposites obtained TGA method was used. TGA is the most sensitive for establishing mass loss of the samples under high temperatures. The influence of carbon nanotubes on resistance to thermal-oxidative degradation of cPBT/$MWCNTs_1$ nanocomposites in comparison with the nanocomposites of $cPBT_{in}$/$MWCNTs_2$ synthesized from original oligomer CBT (i.e. without pre-drying) and with carbon nanotubes of Ukrainian production ($MWCNTs_2$) has been studied. Both series of the samples were synthesized in miniextruder by the procedure described in sect. 2.2, and the samples studied were obtained as extrusion strands.

Since the original CBT oligomer was not prevacuumized, first the mass loss in temperature region at $T \sim 373 \div 473$ K indicating the presence of the adsorbed water was determined. The mass loss curves presented in Fig. 4.16 have shown that during heating of

CBT oligomer sample the mass lost was ~ 0.14 wt. %, therefore the water content in the initial CBT was insignificant that had not impede the polymerization process of CBT oligomer in $cPBT_{in}/MWCNT_2$ nanocomposites.

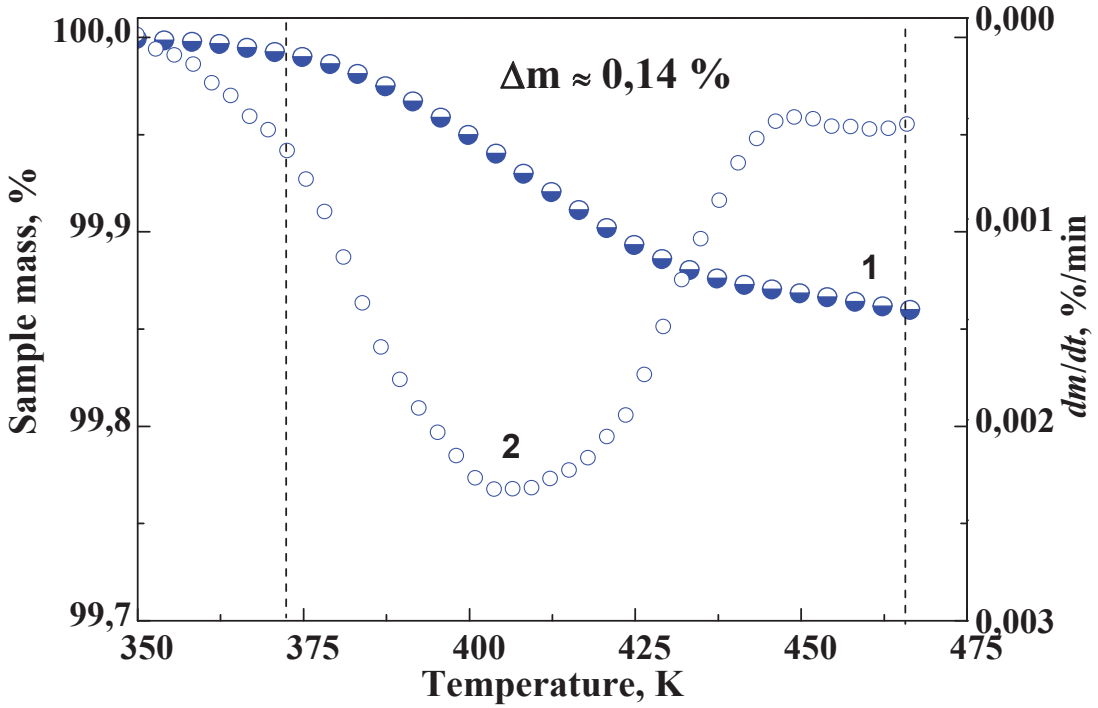

Fig. 4.16. The mass loss curves at heating of the initial CBT oligomer in temperature region T ~ 350 ÷ 470 K: 1 –TGA curve; 2 –corresponding differential curve (DTA).

It was established (Fig. 4.17 and 4.18, Tables 4.7 and 4.8) that in both the serieses of the samples of nanocomposites the presence of even negligible amount (0.01 ÷ 0.2 wt. %) of dispersed carbon nanotubes in polymer matrix increased the resistance to thermal-oxidative degradation of the samples investigated. The above-mentioned data showed that degradation of the nanocomposites obtained started at higher temperatures (temperatures of degradation, namely $T_{d(5\%)}$, $T_{d(max)}$, $T_{d(50\%)}$ increased), the char residue increased too. It was also found that the higher content of carbon nanotubes the lower mass loss of the composition as compared with individual cPBT.

Moreover, CNTs made their effective contribution to increasing stability of the nanocomposites to thermal-oxidative destruction, note that $T_{d(onset)}$ for the individual $MWCNTs_1$ is ~ 796.1 K and for $MWCNTs_2$ ~ 734.6 K (sect.4.1).

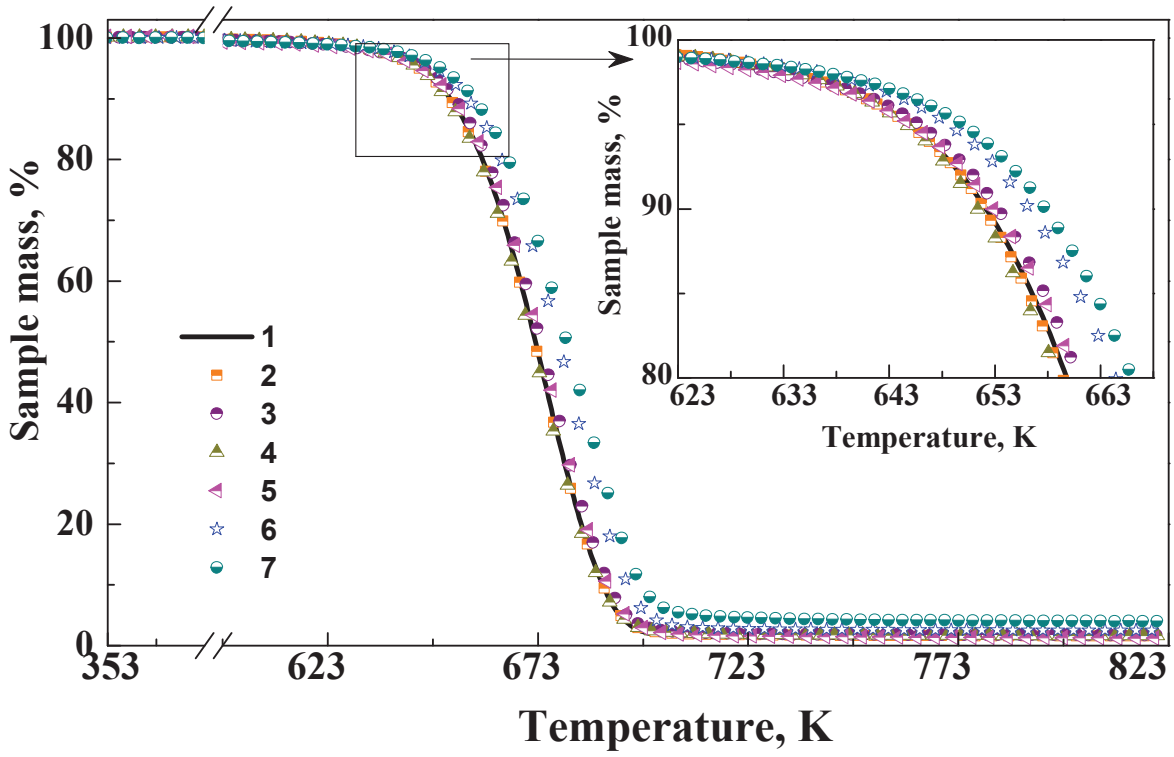

Fig. 4.17. TGA curves (in air) of the nanocomposites of cPBT/MWCNTs$_1$ with MWCNTs$_1$ content, wt. %: 1 – 0, 2 – 0,01. 3 – 0,05. 4 – 0.1, 5 – 0.2, 6 – 1.0, 7 – 2.0.

Table 4.7. Impact of MWCNTs$_1$ on resistance to thermal-oxidative degradation for the cPBT/MWCNTs$_1$ nanocomposites

MWCNT$_1$content, wt. %	$T_{d\,(5\%)}$, K	$T_{d\,(50\%)}$, K	$T_{d\,(max)}$, K	Δm (at$T_{d\,(max)}$), wt. %	m_{char}, wt. %
0 (cPBT)	645	672	676	59	1.32
0.01	645	672	676	60	1.60
0.05	646	674	676	56	1.74
0.10	645	672	674	53	1.67
0.20	645	673	678	64	1.64
1.00	649	678	680	55	2.49
2.00	650	680	684	61	4.00

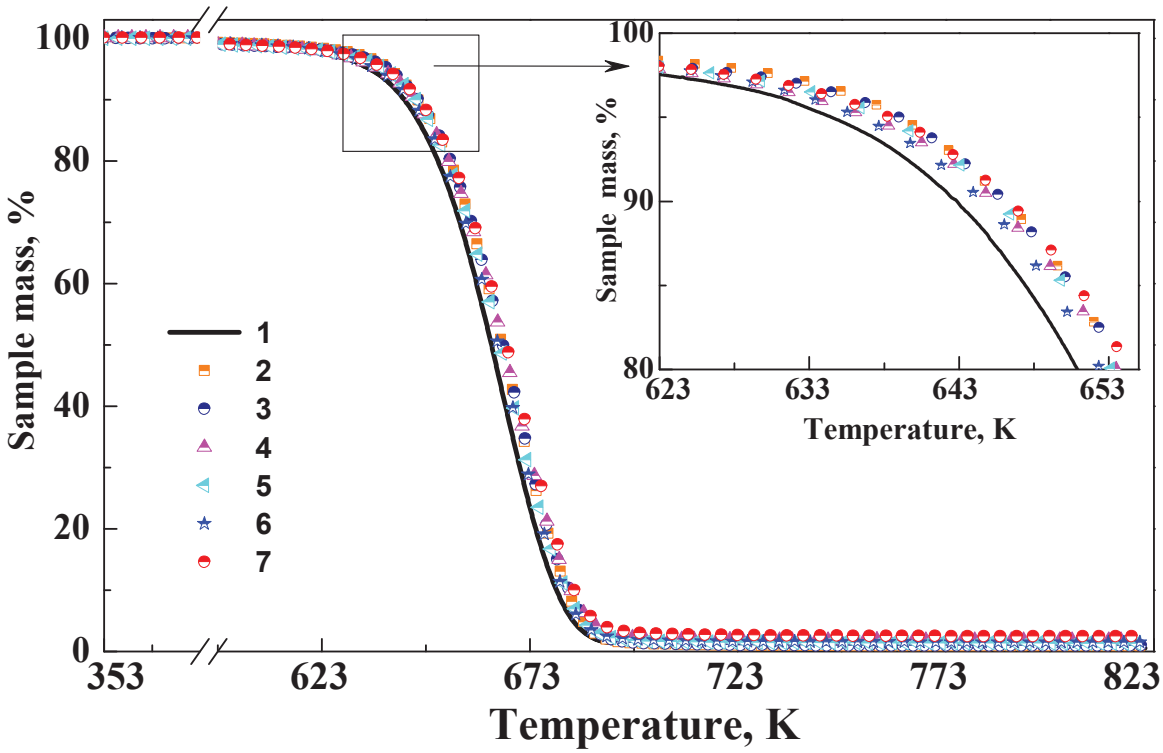

Fig. 4.18. TGA curves (in air) of $cPBT_{in}$/$MWCNTs_2$ nanocomposites with $MWCNTs_1$ content, wt. %: 1 – 0, 2 – 0.01, 3 – 0.5, 4 – 0.1, 5 – 0.2, 6 – 0.5, 7 – 1.0.

Table 4.8. Effect of $MWCNTs_2$ on stability to thermal-oxidative degradation of the $cPBT_{in}$/$MWCNTs_2$ nanocomposites

$MWCNT_2$ content, wt. %	$T_{d\,(5\%)}$, K	$T_{d\,(50\%)}$, K	$T_{d\,(max)}$, K	Δm (at $T_{d\,(max)}$), wt. %	m_{char}, wt. %
0 ($cPBT_{in}$)	634	664	667	59	0.57
0.01	639	666	669	57	0.89
0.05	639	667	669	58	0.96
0.10	637	667	669	58	1.32
0.20	638	666	668	57	1.51
0.50	636	666	669	59	1.89
1.00	638	667	670	58	2.57

Comparative analysis of the resistance to thermal-oxidative degradation of the samples of nanocomposites of cPBT/MWCNTs$_1$ and cPBT$_{init}$/MWCNTs$_2$ indicates that the samples from the first series are more thermally stable. This, perhaps, is due to lower thermal stability of the individual cPBT$_{init}$ (Tables 4.6 and 4.7) and MWCNTs$_2$ (sect. 4.1).

Certainly, increasing of resistance to thermal-oxidative degradation for the samples investigated is not very significant, but one can vary a CNTs content and the conditions of synthesis of the nanocomposites in order to improve the influence on thermal stability of the cPBT-based nanocomposites.

4.8. Determination of the effect of carbon nanotubes on electrical performance of the nanocomposites synthesized

Recently, much attention has been paid to the use of CNTs in polymer nanocomposites to provide (or improve) their electrical properties, moreover introduction of carbon nanotubes enables to obtain conductive materials with low concentration of filler, i.e.to achieve lower percolation threshold (p_c) as compared with utilization of traditional fillers-conductors such as carbon black, graphite, dispersed metals [147-156]. To develop the electroconductive CNTs-containing polymer composites, the CNTs are dispersed in polymer matrix. Using the so-called percolation theory one can describe quantitatively electrical properties and the transition "insulator-conductor" in polymer composites containing "filler-conductor", dispersed in a "matrix-insulator" [14, 67, 157-161]. It is known that electrical conductivity of the composite strongly depends on filler content, since continuous three-dimensional network of conductive filler in polymer phase is formed. One of the main technological tasks is to achieve as lower percolation threshold in the composite as possible. The greater ratio of length to diameter of conductive nanofiller (nanotube), the lower content of the later is required to achieve percolation threshold, i.e. to get conductive material [159]. Therefore, carbon nanotubes, having a great ratio of L/D ($L/D \geq 1000$) and unique electrical properties, are potentially attractive nanofillers in generation of polymer nanocomposites with controllable conductibility in a wide range (from dielectric to electroconductive material).

Until recently it was believed that in order to achieve maximal benefits while using CNTs as effective nanofiller for high-performance nanocomposites, the nanotubes should be well dispersed and do not form aggregates [10]. Undoubtedly, it works in case of enhancing of mechanical properties of CNTs-containing nanocomposites. However, as noted above, in the recent works [7, 141, 142] it was determined that reaggregation of CNTs dispersed in a polymer occurring as a result of high-temperature and shear stress exposure at synthesis or molding of the samples (extrusion, pressing, injection molding ect.) results in increasing electrical conductivity of the composite.

One of the objectives of the research fulfilled was to determine electrical properties of the synthesized cPBT/MWCNTs$_1$ nanocomposites and to establish the impact of MWCNTs on electrical conductivity of the materials obtained (experimental technique was described in sect. 3.10).

According to the percolation theory, at low filler content, a conductivity of material is determined by a polymer matrix [67, 158, 160], while at certain critical volume fraction of conductive filler a percolation threshold, p_c, is achieved. As a result, the conductivity grows by many orders instantly and rapidly, even with very slight increase in filler content. When content of nanofiller is lower as compared with the value of p_c, the system has no the so-called "linked" conductive channels, but when the filler content is higher than the p_c, a great number of continuous conductive channels is formed, resulting in generation of conductive composite. Classical percolation theory assumes that the conductivity (σ) should be described by exponential law as follows [161]:

$$\sigma = \sigma_0 (p - p_c)^t \tag{4.1}$$

where σ_0 – scale factor, p_c– the value of percolation threshold, t – universal exponent, depending on dimension and topology of the system (t = 1.33 for two-dimensional systems, t = 2.0 for three-dimensional systems [161]).

It is known, that experimental values of t described for the CNT-filled polymer nanocomposites are within t = 0,7 ÷ 7,5 [14]. It should be noted that since the density of carbon nanotubes can be determined only approximately (according to [162] $\rho_{CNT} \approx 1{,}4 \div 1{,}9$ g/cm^3, and in [67] $\rho_{CNT} \approx 2{,}045$ g/cm^3), it is reasonable for calculations to use mass fraction (instead of volume one) of MWCNTs.

Fig. 4.19, representing the dependencies of conductivity σ_{DC} (direct current) for cPBT/MWCNTs$_1$ nanocomposites on MWCNTs$_1$ content (the samples were formed by hot pressing of extrusion strands), shows that conductivity σ_{DC} exhibits percolation behavior, namely at low concentrations of MWCNTs (from 0 to ~ 0.2 wt. %), the σ_{DC} value does not change essentially and is equal to $\sigma_{DC} \sim 10^{-16}$ S/cm. Increasing MWCNTs concentration in the composites results in abrupt increase of conductivity σ_{DC} by 10 orders of magnitude in a narrow concentration range at around ~0,2–0,3 wt. %. Using equation 4.1, the experimental dependence of $\sigma_{DC} = f(C_{MWCNTs})$ (Fig. 4.19) was theoretically approximated, for this purpose the dependence of $lg\sigma_{DC} = f(lg)(p - p_c)$ was plotted. Changing the p_c value allowed to find the best linear approximation of the experimental data obtained. One can see (Fig. 4.19) that theoretical and experimental data of conductivity are in a good agreement with each other, the value of the calculated percolation threshold p_c and of the critical exponent t are given in Table 4.9.

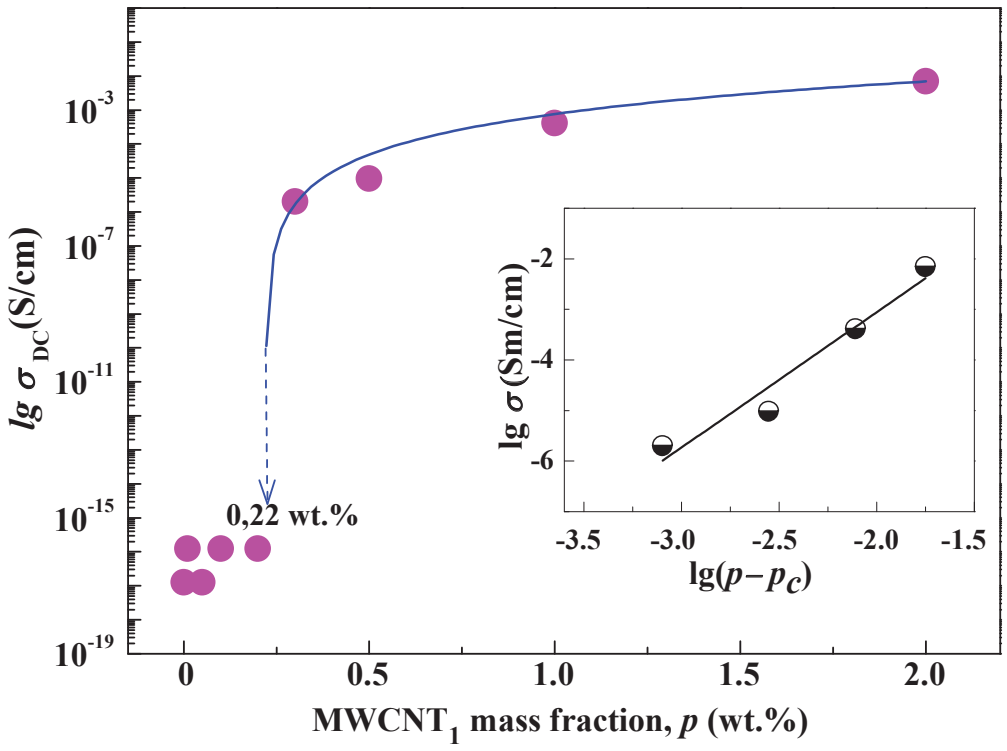

Fig. 4.19. Dependence of conductivity σ_{DC} (direct current) for cPBT/MWCNTs$_1$ nanocomposites on MWCNTs$_1$ content; dots represent experimental data; lines shows theoretical values (according to equation 4.1); insertion reflects the dependence curve of $lg\sigma_{DC} = f(lg)(p - p_c)$ for $p > p_c$; the samples were prepared by hot pressing.

Table 4.9. Percolation threshold p_c and critical exponent t for the composites of cPBT/MWCNTs$_1$ and cPBT/CF

Percolation parameters	cPBT/MWCNTs$_1$	cPBT/CF
p_c	0.0022	0.0260 (AC); 0.0254 (DC)
t	2.68	2.55 (AC); 2.51 (DC)

Thus, the percolation area for the system of cPBT/MWCNTs$_1$ is in the concentration range of MWCNTs$_1$ around 0.2–0.3 wt. %, and, consequently, percolation behavior of the system can be characterized by two values of critical concentration: corresponding to the beginning of formation of conductive cluster (at $p_c \approx 0.22$ wt. %) and to the completion of the process (at $p_c^* \approx 0.3$ wt. %).

The value of critical exponent t is slightly higher as compared with theoretical prediction ($t_t = 2.00$) that, apparently, is because the statistical percolation theory describes an ideal systems containing homogeneously dispersed identical electroconductive particles. Due to the variation in characteristics of CNTs (different size, chirality, complexity, aggregation, defects, etc.) the investigated nanocomposites are far from being considered as the systems with ideal filler.

Thus, a new approach to the synthesis of CNTs-containing nanocomposites from low-viscosity cyclic oligomers of butylene terephthalate allows to obtain nanocomposites with low percolation threshold ($p_c \sim 0.22$ wt. % or 0.0022) and, hence, with improved electrical properties. Such low values of percolation threshold in the nanocomposites are provided by specific characteristics of carbon nanotubes (large value of L/D ratio) and by the effective dispersing of filler in polymer matrix during the synthesis of the latter. One can conclude that deliberately changing the content of MWCNTs, a series of MWCNTs-containing nanocomposites and materials with the properties varying from insulator to conductor can be synthesized.

In the present work for comparison the composites based on cPBT and carbon fibers, CF, having diameter value around ~7 μm and L/D ratio nearly ~ 900 were synthesized. CF content was varied from 0.5 to 10.0 wt. %, preparation technique of the

composites was described in sect. 2.5. Electrical conductivity of cPBT/CF samples was investigated at constant and alterating current (σ_{DC} and σ_{AC}, respectively, Fig. 4.20).

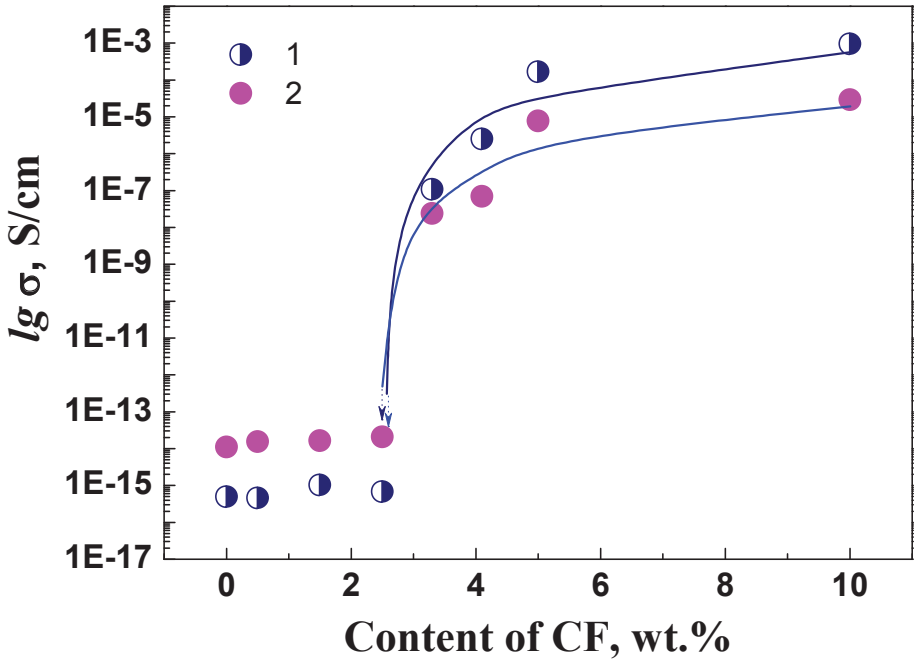

Fig. 4.20. Concentration dependence of conductivity of cPBT/CF composites: 1–σ_{AC} (alterating current); 2 –σ_{DC} (direct current).

It is clearly seen that, in the samples obtained the electrical conductivities σ_{DC} and σ_{AC} also show percolation behavior. In concentration range of CF from 0 to ~ 2.5 wt. % the values of σ_{DC} and σ_{AC} are practically constant and are equal to $\sigma_{DC} \approx 10^{-14}$ S/cm and $\sigma_{AC} \approx 10^{-16}$ S/cm, respectively. Increasing CF concentration in the compositions results in abrupt increase of conductivity (σ_{DC} by 6 orders of magnitude and σ_{AC} by 9 orders of magnitude) in a narrow concentration range ≈2.5–3.0 wt. %. Further growth of CF concentration causes slight increase of σ value by ~ 3 orders of magnitude in the concentration range ≈ 3.0–10.0 wt. %. Thus, for the samples of cPBT/CF percolation area can be identified in the concentration range of CF around ~ 2.5–3.0 wt. %.

Comparing these results with identical data for the cPBT/MWCNTs$_1$ nanocomposites (Table 4.9), one can conclude that percolation threshold in the nanocomposites is more than by 1 order of magnitude lower compared to that for

composites, comprising the conventional conductive filler, namely carbon fibers, instead of nanofiller. Undoubtedly, utilization of carbon nanotubes as a conductive filler in the production of special-purpose polymer materials, for example, conductors of electric current, is more promising and cost-effective method as compared to using traditional electroconductive fillers.

Since in industrial conditions different techniques of molding polymer materials based on Poly(butylene terephthalate) are applied, investigation of the effect of molding method used on electrical properties of the materials produced was of interest. The corresponding data are presented in Table 4.10. It was found that the samples formed by hot pressing had higher electroconductivity ($\sigma_{DC} \approx 6.97 \cdot 10^{-3}$) that could be explained by generation of a three-dimensional percolation conductive network due to reaggregation of carbon nanotubes during hot pressing under high temperatures and pressure, as mentioned above.

Table 4.10. Effect of $MWCNTs_1$ on electroconductivity of the cPBT/$MWCNTs_1$ nanocomposites (CNTs content was 2 wt. %) formed by different methods

Method of sample molding	σ_{DC}, S/cm
Hot pressing	$6.97 \cdot 10^{-3}$
Extrusion strand	$3.02 \cdot 10^{-4}$
Injection molding	$2.04 \cdot 10^{-8}$

As it is shown in Table 4.10, the sample formed by injection molding does not conduct electricity at all ($\sigma_{DC} \approx 2.04 \cdot 10^{-8}$) that is very unusual for the nanocomposites with such a high CNTs content. We believe that this fact can be explained by orientation of carbon nanotubes during injection process in the direction of flow of molten cPBT/$MWCNTs_1$, that is confirmed by TEM microscopy data. Obviously, the orientation of nanotubes impedes the generation of three-dimensional percolation conductive network and, as a result, the samples do not conduct electrical current.

Electrical conductivity is one of the most important properties in the polymer/CNTs composites for characterization of their electronic structure and determination of possible applications. In the reviews [163, 164] electrical properties in heterogeneous organic polymer systems as well as basic concepts and equations for mechanisms of charge transport controlled by percolation processes are discussed in details. Authors present theoretical models from the point of view of their experimental implications. Among the many possible conduction mechanisms, including hopping and tunneling, especial attention is paid to Fluctuation-Induced Tunneling (FIT) model proposed by Sheng [165]. The theory was applied for description of charge carrier transport in our materials. Generally, this can be applied to heterogeneous materials, in which relatively large conducting islands (or long conducting pathways) are separated by small insulating barriers. The main idea of this model is that thermal noise can induce strong voltage fluctuations over a tunnel junction, which effectively narrow and lower the barrier analogous to the effect of an externally applied electric field. The analytical expression for the temperature dependence of the Fluctuation-Induced Tunneling conductivity is presented by the following equation [165]:

$$\sigma = \sigma_0 \exp\left(\frac{-T_1}{T+T_0}\right) \quad , \tag{4.2}$$

where

$$T_1 = \frac{wA\varepsilon_0^2}{8\pi k_B} \tag{4.3}$$

$$T_2 = \frac{2T_1}{\pi w \chi} \quad , \tag{4.4}$$

where σ_0 is a constant, T is the absolute temperature, T_0 is a temperature below which the tunneling is a simple elastic and temperature independent process, and T_1 is the temperature above which the conductivity is thermally activated, k_B is the Boltzman's constant, $\chi = (2mV_0/h^2)^{1/2}$, $\varepsilon_0 = 4V_0/ew$, m is the electron mass, V_0 is the potential barrier height, w is the insulating layer width, and A is the aria of capacitance formed at the junction.

The temperature dependence of electrical conductivity of the nanocomposites has been investigated in temperature range from 10 to 320 K for concentrations above the percolation threshold (Fig. 4.21). The fitting of the experimental results to FIT model (see Eq. (4.2-4.4) gives a good description of conductivity data variation within whole the range of temperatures. It has been found that the conductivity value of polymer nanocomposites developed rises with increasing weight fraction of MWCNTs. Increase of the filler content results in the enhanced number of intertube connections; consequently numerous conductive paths are available.

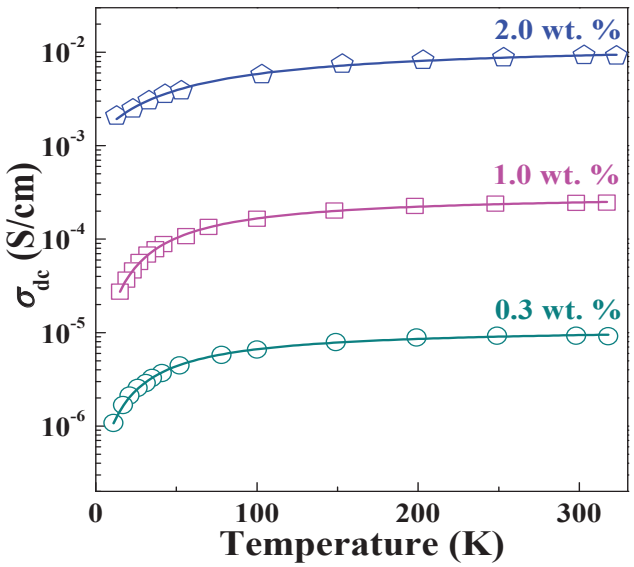

Fig. 4.21. Temperature dependence of dc conductivity of cPBT/MWCNTs$_1$ nanocomposites (MWCNTs$_1$ content in the samples is indicated in the plot).

The fittings of experimental data to FIT model give data values of T_1 and T_0 for each curve of both the types of the nanocomposites that are listed in Table 4.11. The calculated parameters of T_0 and T_1 have reasonable values and are consistent with the Arrhenius plots, *i.e.* one can correlate the T_1 values with the temperatures above which the experimental points yield straight lines in the Arrhenius plots. The values of T_0 and T_1 are much smaller than that reported by Kymakis et al. [152]. Note, that the authors investigated the samples with SWCNTs concentrations in the range of 8.0-25.0 wt. %. Our data are in the same range with the values reported by Zhang et al. [166] for the samples of nanocomposites with MWCNTs contents from 0.5 to 1.0 wt. %.

Table 4.11. Activation energy E_a and fitting parameters T_0, T_1 for cPBT/MWCNTs$_1$ nanocomposites studied

MWCNTs$_1$ content, wt. %	***E_a*, eV**	***T_0***	***T_1***
0.3	0.0007	16	64
1.0	0.0011	14	71
2.0	0.0004	49	119

Weak temperature dependence of conductivity of the polymer nanocomposites studied can find an explanation in nanotubes' chirality, their structural characteristics and polymer nanocomposite morphology. Basically, one can roll up the graphene sheet along one of the symmetry axis: this gives armchair, chiral or zig-zag nanotube [167]. Chirality of CNTs affects the conductance of the nanotube [168]. CNTs can be metallic (armchair type) or semiconducting zheretzo-thirds of CNTs are semi-conductung (chiral and zig-zag). Very weak temperature dependence of conductivity for the nanocomposites presented in this study indicates metallic conducting behavior of MWCNTs at low temperatures suggesting armchair nanotubes' type. The conductivity of CNTs can be determined by the electron mobility, which can be affected by different structural defects formed during the synthesis of nanotubes that promotes the electron dissipation and as a result lower conductivity [169]. Along with such structural defects the presence of adsorbates i.e. different molecules or radicals attached to CNTs surface change their electronic structure. The nature of above mentioned damages of CNTs structure depends on synthesis method of CNTs [169-171]. Based on these considerations and taking into account very weak temperature dependence of conductivity of the CNTs networks, we can suppose that MWCNTs used in the present study have small amounts of defects. This seems reasonable for non-functionalized CNTs. In polymer/CNTs composites nanotubes are much entangled and form continuous networks within polymer matrix, where CNTs are covered by the layer of polymer which acts a barrier in bundle to bundle hopping. That is why some decrease of conductivity at low temperatures is observed. According to FIT theory [165] this polymer layer is rather thin, so electrons can tunnel through the barrier (even without physical bonding between conducting regions).

The electrical behavior of polymer/CNTs nanocomposites under the low temperatures has not been studied enough yet. Only a few works on investigation of charge transport in polymer/CNTs composites at low temperatures have been recently published [58, 152-156, 166]. A detailed characterization of the electrical properties of alumina/MWCNTs composites in the temperature range from 5 to 300 K is presented [172]. Taking into account the influence of the structural features on CNTs electrical behavior, the synthesis way of nanocomposites can explain the percolation threshold as well as conductivity behavior under broad ranges of temperatures. Kim et al. [153] dispersed MWCNTs in toluene with PMMA through stirring and sonication during 24 h and have observed a percolation threshold p_c = 0.4 wt. %. The conductivity of studied samples strongly depended on MWCNTs content and varied widely within the temperatures ranging from 0.5 to 300 K. Probably such behavior can be interpreted by the break-down of MWCNTs under the heavy dispersion conditions. It is reported [164, 166] that long nanotubes can be damaged or even broken up into shorter segments at using long time sonication. In our case the temperature dependence of the conductivity is rather weak and smooth treatment condition were applied for nanocomposites preparation, so carbon nanotube structure is probably not damaged that result in observed conductivity behavior under low temperatures.

Among the recently published papers only Kymakis et al. [152] give some explanation of electrical behavior of polymer/CNTs nanocomposites under the low temperatures. Authors correlate the electrical behavior under the broad range of temperatures of nanocomposites to the CNTs structure. Authors explain weak temperature dependence of conductivity of the samples based on poly(3-octylthiophene) (PO3T) filled by single-wall CNTs (SWCNTs) by the fact that SWCNTs consist of a mixture of semiconducting and metallic nanotubes. At very low temperatures the contribution of semiconducting nanotubes is frozen out. As a result, only the metallic SWCNTs contribute to the conductivity at very low temperatures. Here we should note that PO3T is a semiconducting polymer [173], which also contributes to the complex conductivity behavior of PO3T/SWCNTs composites. It should be noted that SWCNTs show lower conductivity than that of MWCNTs (in spite of less defect structure), because of participation of multiple walls in the electrical transport and the large diameter [169, 174, 175].

The Fluctuation-Induced-Tunneling mechanism was efficiently applied to model the nanocomposites' temperature dependent conductivity. The elaborated polymer nanocomposites have very interesting conductivity properties for practical applications (such as antistatic materials of automobile parts, in electronics, as details of aircraft and space constructions): by changing the content of MWCNTs one can get the materials with varying conductivity values, but with similar and very weak temperature dependences of the conductivity.

So one can conclude that both the factors, namely the content of carbon nanotubes and the method of molding of composite material, affect substantially the ability of the samples studied to conduct electrical current, i.e. electrical properties of the nanocomposites synthesized can be controllably changed depending on customer's needs.

* * *

Thus, in the present work comprehensive research on determination of the influence of multi-wall carbon nanotubes on structure and main physical-chemical properties of the nanostructured polymer composites based on linear Poly(butylene terephthalate), cPBT, synthesized from cyclic butylene terephthalate by the reaction of ring-opening polymerization using the reactive extrusion was firstly carried out. Catalytic effect of carbon nanotubes on CBT polymerization process generating cPBT was firstly established. It was shown that due to the presence of active surface on the outer walls of nanotubes the introduction of nanofiller reduced the induction period of reaction and increased polymerization rate. It was found that using reactive extrusion for cPBT synthesis from CBT as well as the presence of CNTs contributes to the formation of the nanocomposites with enhanced resistance to thermal-oxidative degradation. Positive effect of nanofiller on viscoelastic properties of the synthesized cPBT/MWCNTs$_1$ nanocomposites was established, namely the increase of glass transition temperature T_g of cPBT matrix by $\sim 2 \div 7$ K (depending on MWCNTs$_1$ content) and the growth of storage modules *E"* were observed. Significant influence of carbon nanotubes on generation of crystalline structure of cPBT matrix was firstly revealed. It was found that increasing CNTs concentration in the composition resulted to increasing melting temperature T_m and degree of crystallinity X_c of cPBT matrix.

Moreover, it was also determined that crystallization process (during cooling of the samples) started at higher temperatures than in case of individual cPBT and increasing concentration of CNTs from 0.01 to 2.0 wt. % resulted in increasing crystallization temperature T_c by 3 ÷ 18 K (depending on the composition and molding technique). It was concluded that carbon nanotubes acted as crystallization nuclei of cPBT. It was established that depending on the CNTs content electrical properties could be purposefully changed from insulators to conductors. It was determined that the percolation threshold for cPBT/$MWCNTs_1$ nanocomposites was low and equal to p_c ~0.22 wt.% of $MWCNTs_1$ indicating the formation of three-dimensional percolation conductive network of carbon nanotubes. Therefore, in summary, in the present work the technique of CNTs dispersing, method of synthesis of cPBT from CBT oligomers in the presence of CNTs and molding procedure of polymer cPBT/$MWCNTs_1$ nanocomposites with enhanced physical-chemical properties were optimized.

Chapter 5

In situ nanostructured composites based on crosslinked polycyanurates and multiwalled carbon nanotubes

5.1. Catalytic effect of carbon nanotubes on the polycyclotrimerization process of dicyanate ester of bisphenol A

5.2. Study of morphological features of $PCN_2/MWCNT_2$ nanocomposites depending on the nanofiller content

5.3. Determination of influence of carbon nanotubes on thermal conductivity of nanocomposites based on polycyanurate network

5.4. Effect of $MWCNT_2$ on viscoelastic properties of the nanocomposites and their mechanical characteristics

5.5. Study of the effect of $MWCNT_2$ on the thermophysical characteristics of nanostructured composites

5.6. Influence of $MWCNT_2$ on resistance to thermooxidative destruction of nanocomposites $PCN_1/MWCNT_2$ and $PCN_2/MWCNT_2$

5.1. Catalytic effect of carbon nanotubes on the polycyclotrimerization process of dicyanate ester of bisphenol A

This section presents the results of investigation of structure and basic physical-chemical properties of nanocomposites of polycyanurate networks and multiwalled carbon nanotubes $MWCNTs_2$. These nanocomposites were obtained in the presence of different content of carbon nanotubes by in situ polycyclotrimerization: 1) oligomer of dicyanate ester of bisphenol A, DCBA previously synthesized from monomer DCBA ("Primaset BADCy") with conversion of cyanate groups α ~ 28 %, or 2) industrial oligomer DCBA ("Primaset BA-230S 75") with conversion of cyanate groups α ~ 52 %. In the first series of samples polycyanurate component was marked as PCN_1, in the second series of samples - as PCN_2. Description of initial components, details of synthesis and forming of nanocomposite samples are given in sections 2.1, 2.3 and 2.4.

For the first time, the catalytic effect of unfunctionalized $MWCNTs_2$ on kinetics of polycyclotrimerization reaction of DCBA was established by us [176], and this work has been patented [177]. The conversion of cyanate groups was determined on changes of absorbance of the band with maximum at 2236-2272 cm^{-1}, corresponding to the valence vibrations of the −O−C≡N group. As a standard band the band at 2968 cm^{-1} of the valence vibrations of CH_3-group in FTIR spectra of the reactive composition. In Fig. 5.1 the FTIR spectra of DCBA monomer, DCBA oligomer and PCN_1 synthesized without using any catalyst are shown. It is seen that at polymerization of the DCBA an intensity of the peaks of cyanate groups at 2236-2272 cm^{-1} decreases and the peaks at 1367 and 1564 cm^{-1} corresponding to polycyanurate cycle [117] appear in the FTIR spectra.

The conversion of the PCN resin was calculated using the Equation (5.1):

$$\alpha(t) = 1 - \frac{A_{(t)2236-2272}/A_{(0)2236-2272}}{A_{(t)2968}/A_{(0)2968}} \qquad (5.1)$$

where $A_{(t)2236\text{-}2272}$ is the area under absorbance peak of −O−C≡N at 2236-2272 cm^{-1} at time t; $A_{(t)2968}$ is the area under absorbance peak of $-CH_3$ at 2968 cm^{-1} at time t; $A_{(0)}$ are the areas under absorbance peaks of corresponding groups in initial DCBA monomer.

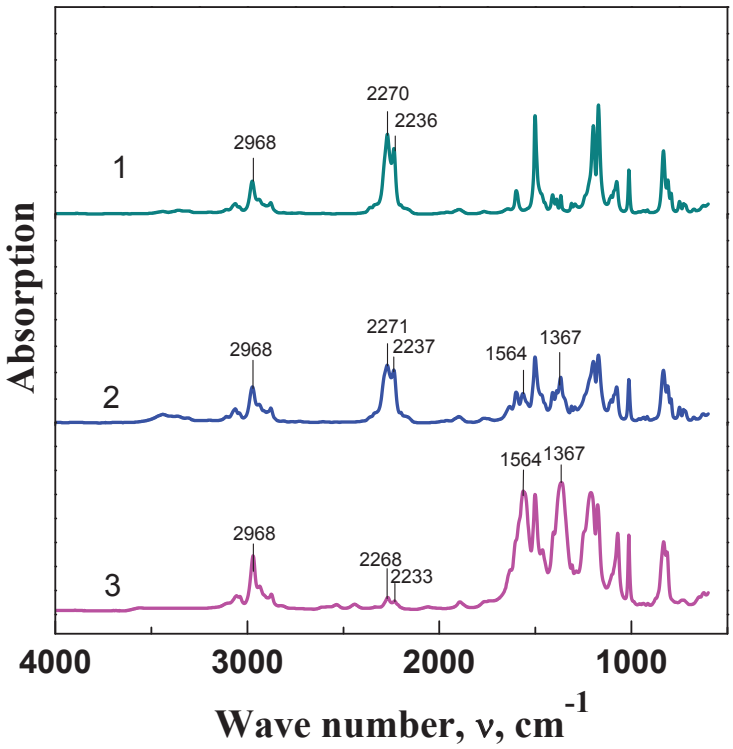

Fig. 5.1. FTIR-spectra: 1 – DCBA monomer; 2 – DCBA oligomer; 3 – individual PCN_1.

The conversion of cyanate groups in DCBA oligomer was found to be ~ 28% and that in PCN sample – 92.5 %. It should be noted here that for achieving full conversion post-curing is needed at 270-300 °C even at using conventional catalysts [117].

For kinetic measurements the system based on DCBA oligomer (with conversion of the cyanate groups, α ~ 28 %, synthesized according to the method described in chapter 2) containing 0.01 and 0.1 wt. % of $MWCNTs_2$ was used. The kinetics of polycyclotrimerization of DCBA oligomer as well as in the presence of $MWCNTs_2$ through the schedule with step by step temperature increase was studied by FTIR method (Figs. 5.2 and 5.3).

In Fig. 5.4 the conversion of cyanate groups of DCBA oligomer as well as in the presence of the small amounts of $MWCNTs_2$ *versus* time is shown. The FTIR data evidence an acceleration effect of MWCNTs on kinetics of the early stages of PCN formation. The higher the MWCNTs content in the system the higher the conversion of the

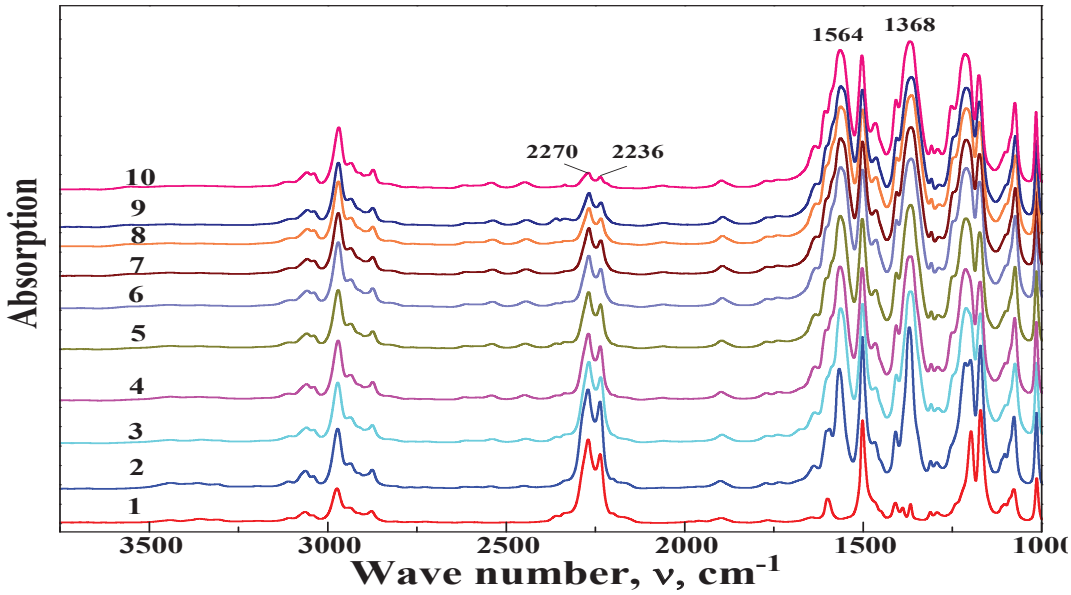

Fig. 5.2. FTIR–spectra of polycyclotrimerization process of DCBA oligomer, synthesis schedule (with step by step temperature increase): 1 – 423 K, 40 h; 2 – 453 K, 1 h; 3 – 453 K, 2 h; 4 – 453 K, 3 h; 5 – 483 K, 30 min; 6 – 483 K, 1 h; 7 – 503 K, 30 min; 8 –503 K, 1 h; 9 – 523 K, 30 min; 10 – 523 K, 1 h.

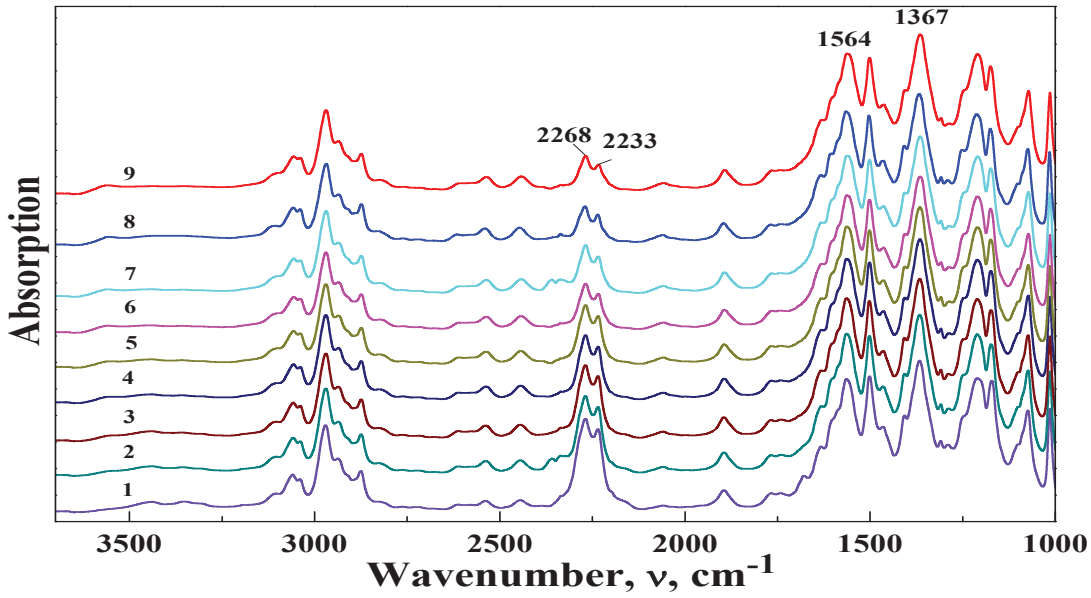

Fig. 5.3. FTIR–spectra of polycyclotrimerization process of DCBA oligomer *in situ* in the presence of $MWCNTs_2$ (0.01 wt. %), synthesis schedule (with step by step temperature increase): 1 – 423 K, 5 h (individual DCBA oligomer); 2 – 453 K, 1 h; 3 – 453 K, 2 h; 4 – 453 K, 3 h; 5 – 483 K, 30 min; 6 – 483 K, 1 h; 7 – 503 K, 1 h; 8 –523 K, 30 min; 9 – 523 K, 1 h.

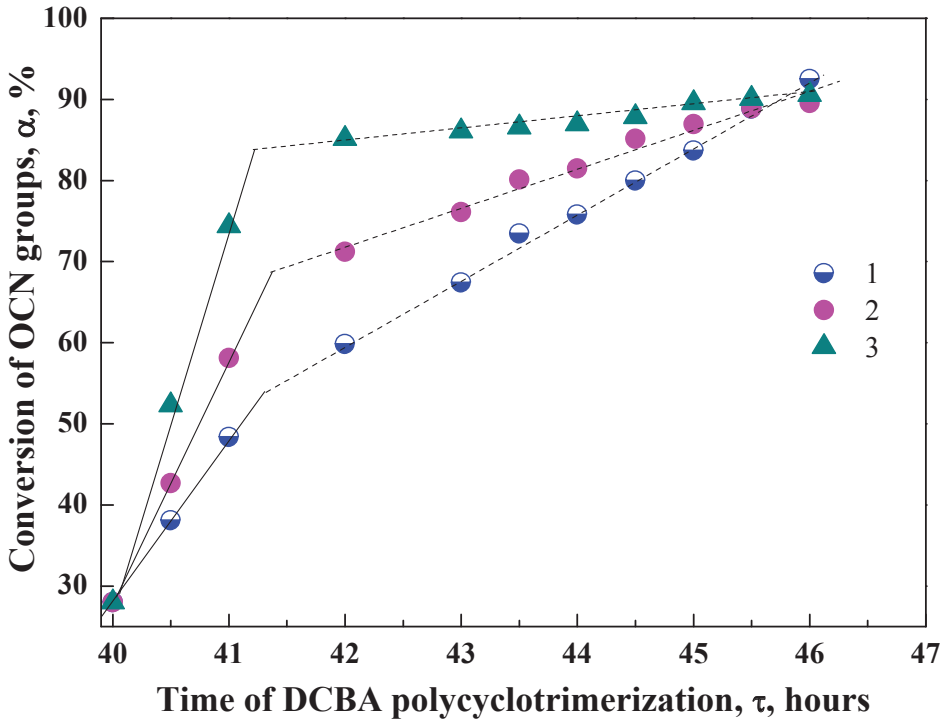

Fig. 5.4. Kinetic curves of PCN formation from DCBA at $MWCNTs_2$ content, wt. %: 1 – 0; 2 – 0.01; 3 – 0.1.

cyanate groups into cyanurate cycles at least in the range of the concentrations used. The attempt to study the system with 0.5 wt. % of MWCNTs resulted in vitrification as early as in a stage of components blending in 2 min after starting ultrasound action.

However, as can be seen from Table 5.1, in spite of the higher reaction speed of the polycyclotrimerization process of the cyanate ester in the presence of $MWCNTs_2$ the final conversion of −O−C≡N groups for the temperature/time schedule used was some lower compared to that for neat PCN_1.

One can suppose that the acceleration effect of carbon nanotubes on polymerization of cyanate ester is due to adsorption of DCBA oligomer molecules on highly developed surface of $MWCNTs_2$. However, this phenomenon can play negative role in the final stage of PCN_1 network formation, when some unreacted molecules are not easy accessible, and the probability of elementary reaction act is very low (as can be seen from Fig. 1.12c three molecules of cyanate ester have to meet each other to react with cyanurate cycle formation).

Table 5.1. Influence of $MWCNTs_2$ content on conversion of cyanate groups of DCBA and activation energy E_a at formation of $PCN_1/MWCNTs_2$ nanocomposites

$MWCNTs_2$ content , wt. %	**Conversion of −O−C≡N groups, %**	**E_a (kJ/mol)**
0	92.5	32.7
0.01	89.1	27.3
0.10	88.8	16.9

As it was above mentioned this problem can be solved by post-curing of the polymer product at higher temperatures, when the mobility of the reactive molecules and polymer fragments is higher.

The manufacturer of MWCNTs used in this study reports that catalyst residue in MWCNTs is the mixture of SiO_2, Al_2O_3, Fe_2O_3, MoO_3. For the moment, there are no references in the literature that describe the catalytic action of such oxides on reaction of cyclotrimerization of cyanate esters. Normally, reaction of cyclotrimerization of the aryl dicyanates can be catalyzed by the mixture of catalyst and co-catalyst. The most common types of catalyst are carboxylate salts and chelates of transition metal ions (Cu^{2+}, Co^{2+}, Zn^{2+}, Mn^{2+}...) [117] that facilitate the reaction of cyclotrimerization by formation of co-ordination complexes. The co-catalyst serves a dual purpose of acting as a solvent for catalyst and completing ring closure of the triazine ring via hydrogen transfer. The most commonly used co-catalyst is nonylphenol.

The data obtained from FTIR studies for DCBA oligomer as well as filled with 0.01 and 0.1 wt. % of $MWCNTs_2$ were analyzed using an empirical equation 5.2 [117]:

$$\frac{\partial \alpha}{\partial t} = k(1-\alpha)^n, \qquad (5.2)$$

where k is the rate constant and n is the order of overall reaction. The parameters k and n are evaluated from the data region where the reaction rate depends on monomer concentration and sharp increase in conversion is observed. Equation (5.2) was integrated and fitted to experimental concentration profiles of both the unfilled and the filled with MWCNTs systems. It was observed that the data calculated from FTIR spectra is in a good

agreement with Equation (5.2) when the order of reaction n = 1. This means that DCBA oligomer or DCBA oligomer/$MWCNTs_2$ systems can be described by a first-order autocatalytic rate law.

The values of the observed rate constants obtained from the first-order reaction analysis for DCBA and DCBA/MWCNTs nanocomposites are listed in the Table 5.2. The values of kinetic constants for unfilled DCBA are lower than the values reported for the catalyzed DCBA [178]. The results show that the kinetic constant increases with the addition of $MWCNTs_2$ on each isothermal step of polymerization of DCBA oligomer.

The activation energies E_a were determined from Arrhenius plots (cf. Table 5.1). The activation energies E_a for the reaction ranged from 32.7 to 16.9 kJ/mol for pure DCBA oligomer and for that filled with $MWCNTs_2$ and agree with the values reported earlier [178, 179]. The E_a values for the samples of DCBA oligomer cured in the presence of $MWCNTs_2$ are much lower than the values obtained for virgin DCBA oligomer and they decrease with increasing $MWCNTs_2$ content. This effect is quite similar to the decrease of activation energy with adding catalysts in reactive systems [180].

Table 5.2. Rate constant of polycyclotrimerization reaction for individual DCBA oligomer and that in a mixture of DCBA oligomer/ $MWCNTs_2$

Temperature, K	**Reaction rate constant, k x 10^4 (conc. · sec)$^{-1}$**		
	DCBA	DCBA oligomer/$MWCNTs_2$ (0.01 wt. %)	DCBA oligomer/$MWCNTs_2$ (0.1 wt. %)
423	0.02	0.02	0.02
453	0.05	0.06	0.09
483	0.08	0.10	0.12
503	0.10	0.12	0.14

Presence of low molar mass compounds (for example, conventional catalysts) in polymer networks can influences negatively on thermal properties of the final material. In this work we have shown that synthesis of PCN/CNTs nanocomposites can be effectively realized without using the conventional catalysts.

Tang et al. [116] using method of dynamic DSC has fixed acceleration of polycyclotrimerization process of cyanate esters of bisphenols at additions of $MWCNTs_2$ too. At that, shifting of maximum of the exothermic peak to the lower temperatures has been observed. The authors have explained the catalytic effect found by the presence on the surface of carbon nanotubes of reactive OH-groups, which, as known [117, 181], can catalyze polycyclotrimerization reaction.

As far as the existence of OH-groups on a surface of $MWCNTs_2$ has been confirmed in our work too (sect. 4.2), one can suppose the same nature of the catalysis.

5.2. Study of morphological features of $PCN_2/MWCNTs_2$ nanocomposites depending on the nanofiller content

Using SEM and TEM methods the changes of morphological features of $PCN_2/MWCNTs_2$ nanocomposites were investigated depending on the content of the nanofiller, the corresponding microphotographs are presented in Figs. 5.5 and 5.6. From the analysis of SEM microphotographs one can conclude that in these nanocomposites the $MWCNTs_2$ are effectively dispersed throughout the sample. The isolated nanotubes (the thread like light includings) as well as the nanotubes broken during preparation of samples for their study by SEM method (at cracking of the sample in liquid nitrogen, section 3.1) are observed too. The latter is confirmed by the presence of a large number of cross cutover of nanotubes (light points). There dark spherical areas, which (as it was noted above in section 4.2) refer to the voids formed after pulling (at breaking sample) the nanotubes out, are also observed. Thus one can conclude of high adhesion between the polymer matrix and the carbon nanotubes.

This conclusion is confirmed by the estimations carried out using the computer program "Image J", which allows to measure precisely the size of any visible inclusions on the microphotographs. The estimations carried out using SEM and TEM microphotographs of nanocomposite samples have shown that the diameters of the nanotubes is larger than that the initial $MWCNTs_2$ by ~ 5÷45 nm. This evidences wrapping of carbon nanotubes by the polymer that is only possible in systems with high adhesion between the polymer

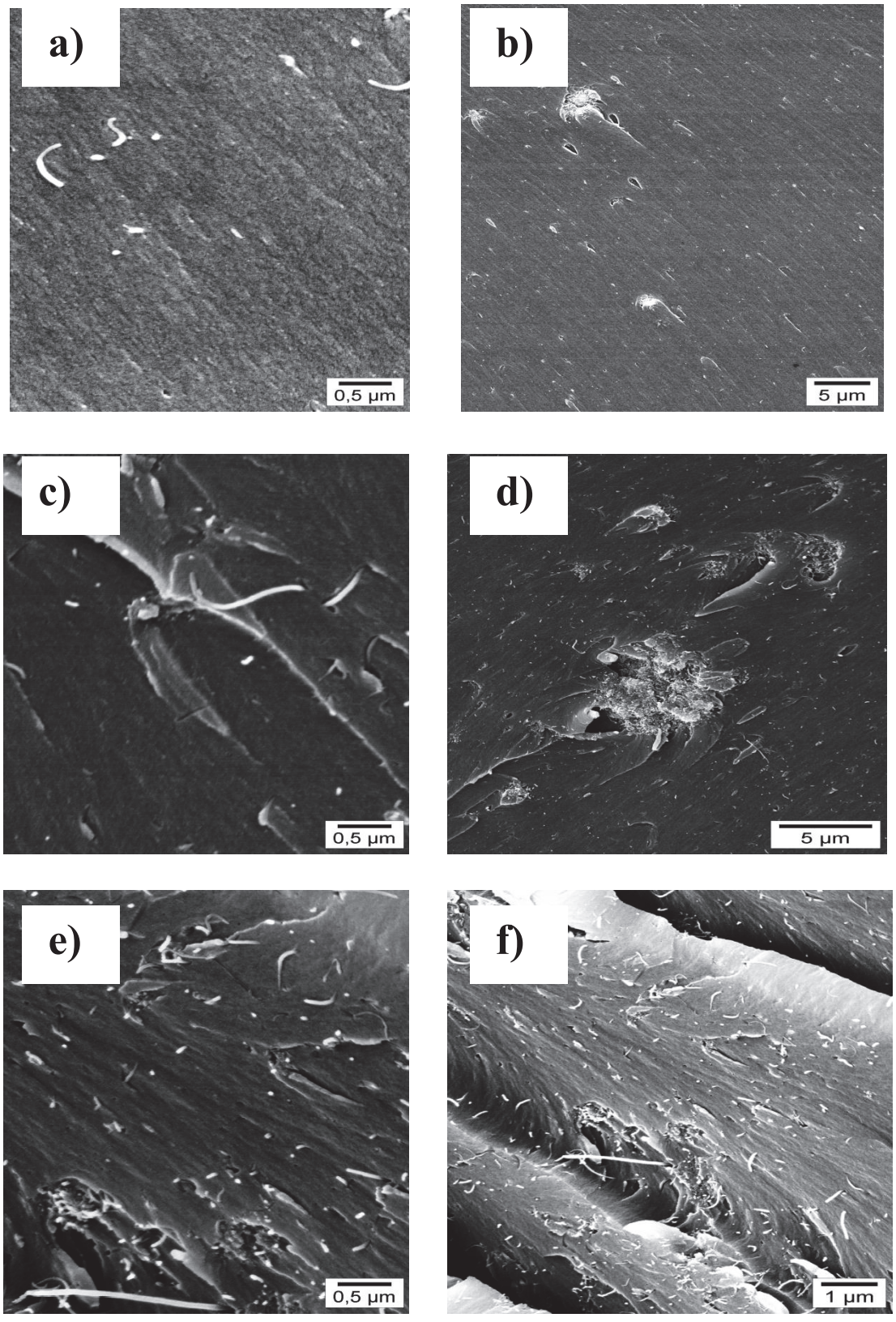

Fig. 5.5. SEM microphotographs of PCN_2/$MWCNTs_2$ nanocomposites with $MWCNTs_2$ content, wt. %: a, b - 0.08; c, d - 0.50; e, f - 1.20.

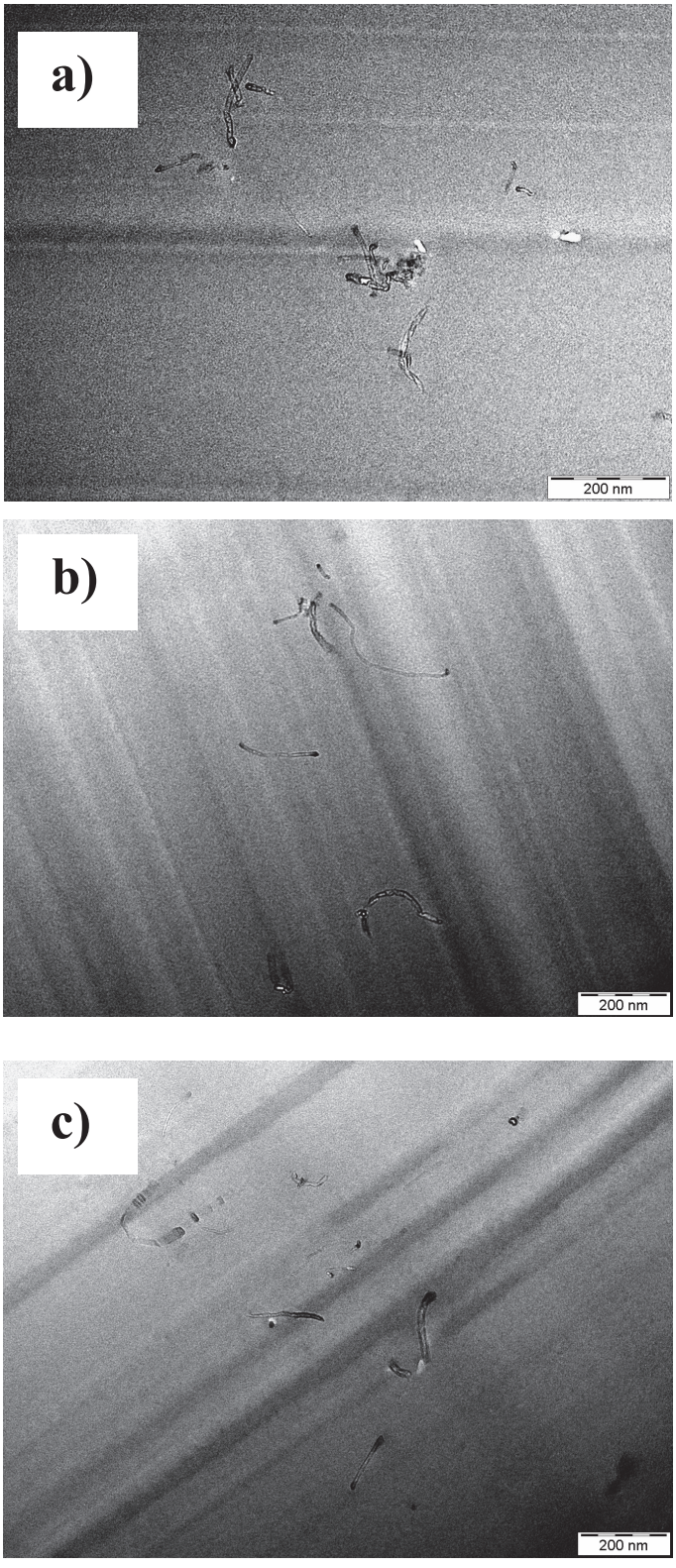

Fig. 5.6. TEM microphotographs PCN_2/$MWCNTs_2$ nanocomposites with $MWCNTs_2$ content, wt. %: a - 0.05; b - 0.10; c - 0.20.

matrix and CNTs. However, as it is seen from the SEM and TEM microphotographs (Figs. 5.5 and 5.6), there are agglomerates of CNTs in all the samples along with the isolated CNTs: in the SEM pictures one can observe the clusters of light points or threads, in the TEM microphotographs the clear clews of CNTs can be seen. It has been found that with increasing content of $MWCNTs_2$ from 0.08 to 1.2 wt. % the content of agglomerates increases too (Fig. 5.5 d, e). This can be explained by 2 reasons, as it was done for the series of samples cPBT/ $MWCNTs_1$ (see chapter 4): 1) an inclination of carbon nanotubes to self-agglomeration at increasing their content in the nanocomposite sample due to their extended surface and significant Van der Waals forces, 2) as for the previous series of the samples (sect. 4.2) during high-temperature synthesis of polymer (here polycyanurate) matrix the re-aggregation of the dispersed carbon nanotubes occurs, probably because at high temperature CNTs have higher mobility that promotes their re-aggregation. As it will be shown below in the section 5.3 ÷ 5.7, such change in the morphology of the nanocomposite samples studied leads to some improvement in their physical-chemical properties.

5.3. Determination of influence of carbon nanotubes on thermal conductivity of nanocomposites based on polycyanurate network

It is known that the introduction of CNTs to matrix of a linear polymer significantly (by several times) enhances thermal conductivity of material obtained, drastic increase in thermal conductivity is achieved if in the nanocomposite structure formed, the particles of nanofiller are fixed in a highly oriented position [182, 183]. One can expect that in a combination of highly regular polymer network PCN - CNTs the nanotubes will be situated with some regularity that can provide high thermal conductivity. In Fig. 5.7 the temperature dependence of thermal conductivity (λ) of the nanocomposites studied is presented. It is seen that at addition of a small (ω = 0.02 wt. %) amount of CNTs to the PCN matrix thermal conductivity λ of the material is slightly reduced (compared with individual PCN), while at $\omega \geq 0.03$ wt. % a sharp increase in the λ value is observed [184]. Simultaneous increase of the temperature coefficient $d\lambda/dT$ from $1.07 \cdot 10^{-4}$ to $1.13 \cdot 10^{-3}$ $W/(m \cdot K^2)$ in the same range of CNTs concentrations may reflect changes in composition of

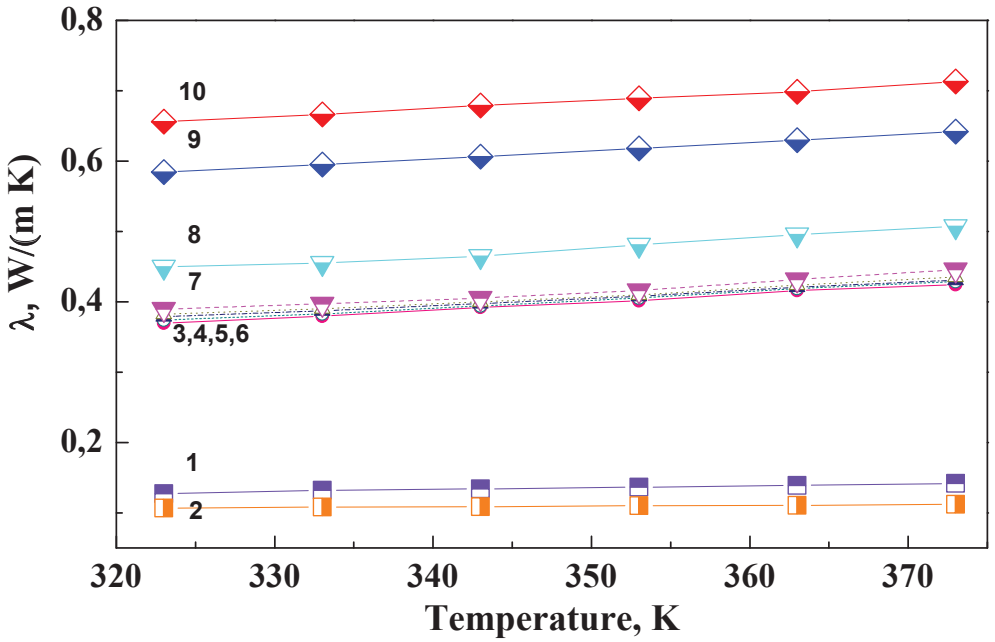

Fig. 5.7. Temperature dependence of thermal conductivity λ for PCN_2/$MWCNTs_2$ samples with $MWCNTs_2$ content, wt. %: 1 – 0; 2 - 0.02; 3 - 0.03; 4 - 0.04; 5 - 0.05; 6 - 0.06; 7 - 0.08; 8 - 0.5; 9 - 1.0; 10 - 1.2.

the structural elements (one-dimensional, two-dimensional, three-dimensional) responsible for thermal conductivity [185]. Then the thermal conductivity at w ≥ 0.03 wt. % can be presented as follows [186]:

$$\lambda = \lambda_c + A_1(\omega - \omega_c) + A_2(\omega - \omega_c)^2 + A_3(\omega - \omega_c)^3, \qquad (5.3)$$

where w_c - critical concentration, λ_c - thermal conductivity at ω_c, $A_1(\omega - \omega_c)$ corresponds to one-dimensional structural elements, $A_2(\omega - \omega_c)^2$ - two-dimensional ones, and $A_3(\omega - \omega_c)^3$ – to three-dimensional structural elements.

The calculations have shown that the experimental data throughout the temperature range investigated are described satisfactorily by equation (5.3) (the relative error of the calculations is less than 3 %). In Fig. 5.8, as example, the plots of λ *versus* content of nanotubes, ω, determined at temperatures T = 323 K and T = 373 K are given. Extrapolation of the values of thermal conductivity λ obtained to content of the polymer

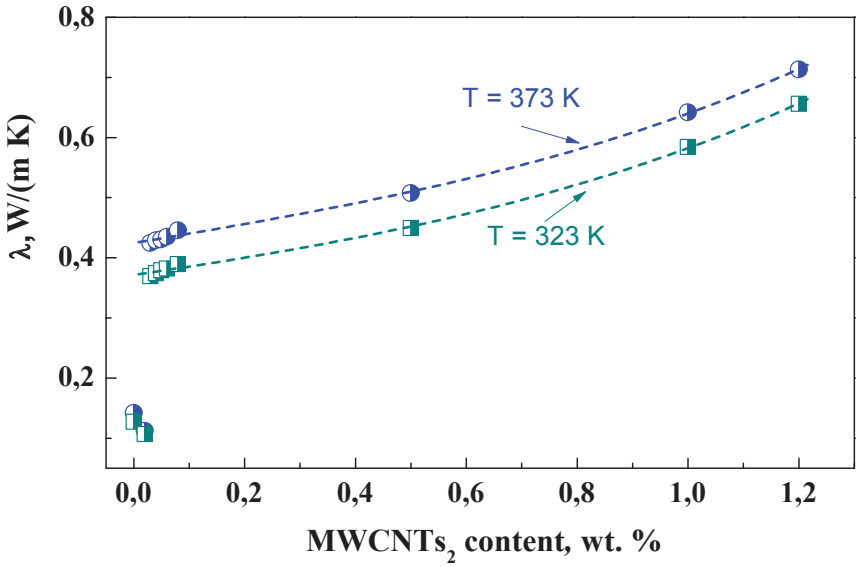

Fig. 5.8. The dependence of thermal conductivity λ for the samples of PCN_2/$MWCNTs_2$ on the $MWCNTs_2$ content in nanocomposite; dotted line corresponds to the values obtained using equation 5.3.

0% has allowed to estimate thermal conductivity of pure $MWCNTs_2$ and to obtain the dependence λ = f (*T*) for the nanofiller (Fig. 5.9). The obtained value of thermal conductivity of carbon nanotubes is in good agreement with literature data [187, 188]. On

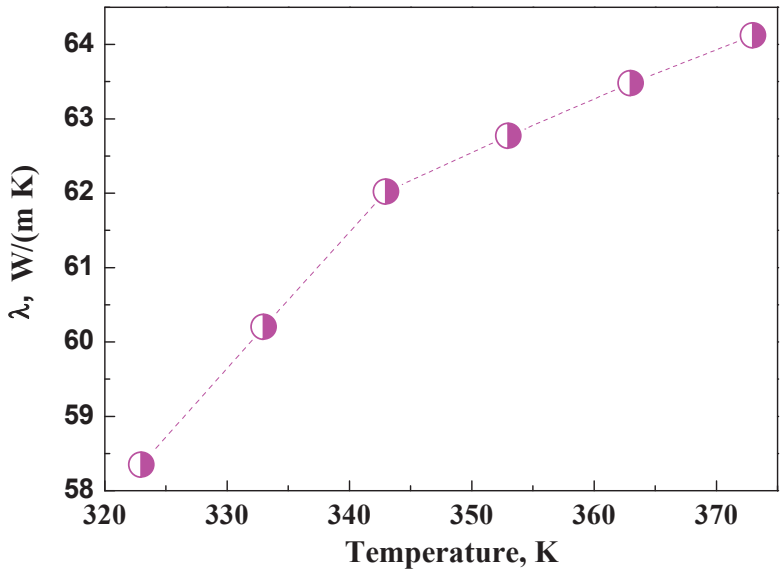

Fig. 5.9. Temperature dependence of thermal conductivity λ for individual $MWCNTs_2$.

the other hand, the mutual correlation between the coefficients A_1, A_2 and A_3 can serve as a measure of the contribution of each structural element to the total thermal conductivity of the material. The calculations have shown that the highest content of linear structural elements from the beginning is due to the geometry of CNTs used.

The relatively high contribution to the thermal conductivity of three-dimensional structural elements may be caused by the presence of agglomerates of CNTs in the samples of nanocomposites (Fig. 5.10). And, finally, the unlikely formation of the two-dimensional structural elements leads to their smallest contribution to the overall thermal conductivity.

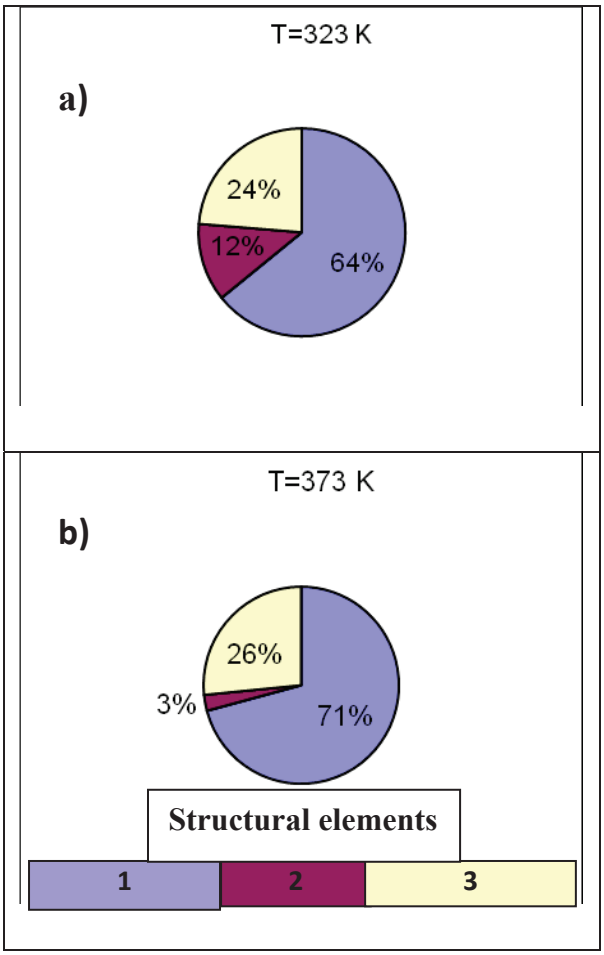

Fig. 5.10. The contribution of different structural elements at: a) T = 323 K, b) T = 373 K, 1 - one-dimensional elements; 2 – two-dimensional elements; 3 – three-dimensional elements.

At temperature increase to 373 K a further reducing contribution of two-dimensional structural elements at the expense of increasing contribution of the other components, mainly the linear ones (Fig. 5.10b) occurs.

Thus, as a result of this study a sharp increase in thermal conductivity of the nanocomposites for the compositions of PCN_2/$MWCNTs_2$ with $MWCNTs_2$ content > 0.02 wt. % has been found. The value of thermal conductivity of the individual CNTs as well as the temperature dependence of thermal conductivity has been estimated. The contribution of the linear, planar and three-dimensional structural elements in the total thermal conductivity of the nanocomposites has been analized. It is supposed that the high thermal conductivity of the nanocomposites investigated is achieved due to a successful combination of regular thermostable non-defective polycyanurate network + nanofiller with a high degree of anisotropy.

5.4. Effect of $MWCNT_2$ on viscoelastic properties of the nanocomposites and their mechanical characteristics

Viscoelastic characteristics of the original polycyanurate network and the nanocomposites based on them with different content of carbon nanotubes were investigated by DMTA technique (details of the methodology of measurements and preparation of samples for the study are described in section 3.6), the experimental results are presented in Figs. 5.11−5.13 and in Table 5.3. Two series of nanocomposite samples were investigated: 1) the samples of PCN_1/$MWCNTs_2$ prepared from DCBA oligomer synthesized at the lab; 2) the samples of PCN_2/$MWCNTs_2$ prepared from the industrially available oligomer DCBA (the details of synthesis of the samples are described above in sections 2.3 and 2.4, respectively).

It is seen (Fig. 5.11) that addition of even a small amount (0.01 ÷ 0.1 wt. %) of carbon nanotubes changes viscoelastic properties of the PCN-matrix (in comparison with unfilled PCN_1). In the dependencies $E' = f(T)$ and $tg\ \delta = f(T)$ one can see redistribution of intensities and shift of the tg δ peak maxima along the temperature axis, narrower glass transition temperature interval (ΔT_g), reduced modulus of elasticity E'. It should

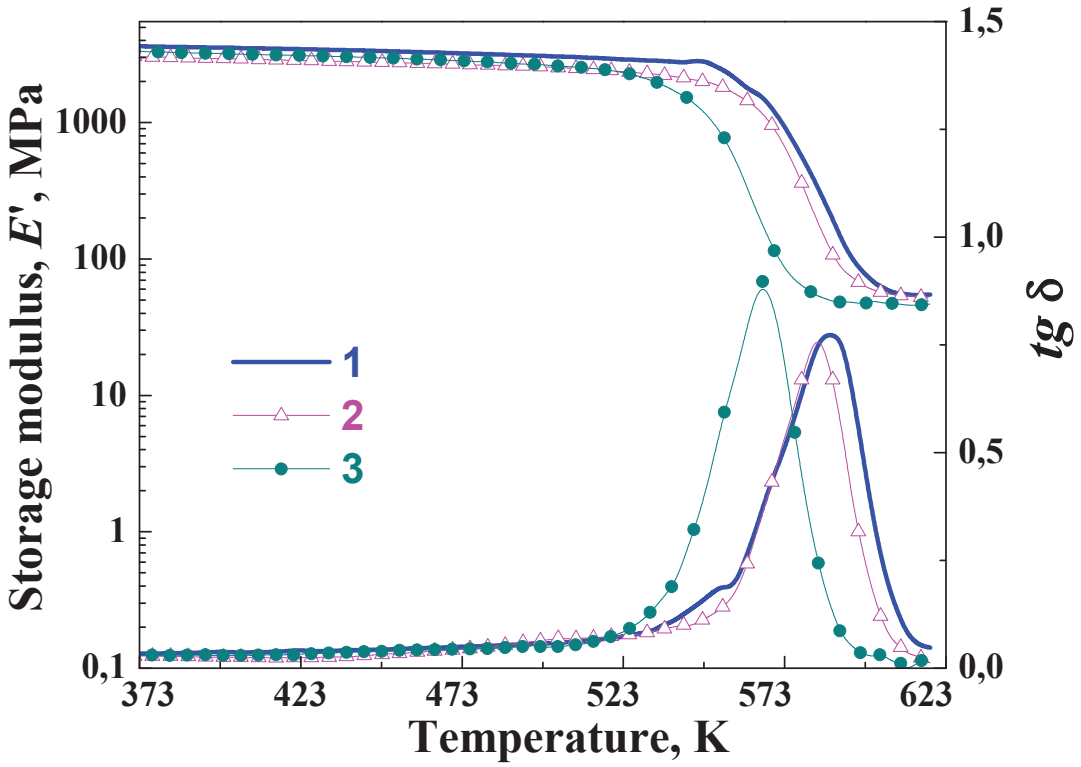

Fig. 5.11. Temperature dependence of storage modulus *E*'and tan δ (at frequency 1 Hz) for the PCN_1/$MWCNTs_2$ nanocomposites with $MWCNTs_2$ content, wt. % 1 – 0; 2 – 0.01; 3 – 0.10.

be noted here that the introduction of the nanofiller ($MWCNT_2$) and increase of its content leads to decreasing glass transition temperature (T_g) value of the amorphous polycyanurate matrix (Table 5.3).

As it is well known [189, 190] the T_g value for the polycyanurate networks depends directly on the network crosslink degree and, therefore, depends on the conversion of cyanate groups, α: the lower the value of the conversion α, the lower the crosslink degree of PCN-network and lower T_g (Fig. 5.12). It was shown above (sect. 5.1) that despite the catalytic effect of CNTs in the initial stages of the DCBA polycyclotrimerization process, the ultimate conversion of cyanate groups in the nanocomposites is slightly lower than in the individual PCN_1 (Table 5.1), and for all the samples $\alpha < 100$ %.

So unlike the series of samples of nanocomposites of linear cPBT, the study of PCN-containing samples by methods (for example DMTA, DSC, etc.) that provide some heating at temperatures > T_g, the properties of the samples may change due to chemical

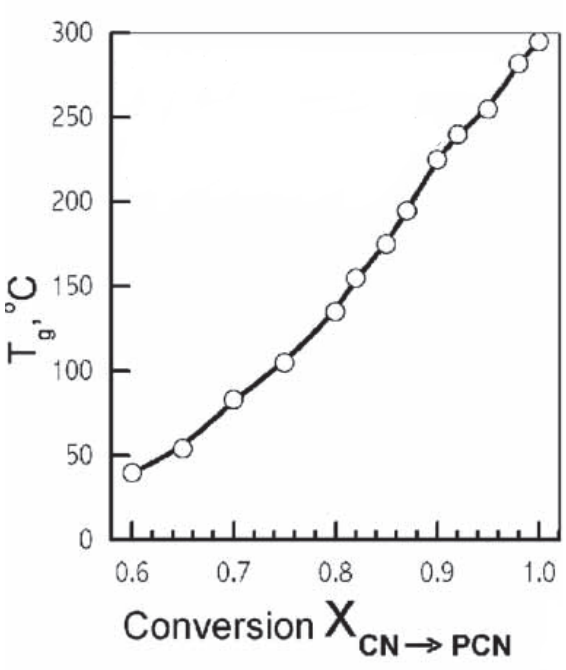

Fig. 5.12. Glass transition temperature T_g *versus* conversion of cyanate groups for DCBA curing process according to work [189].

Table 5.3. Viscoelastic properties of $PCN_1/MWCNTs_2$ and $PCN_2/MWCNTs_2$ nanocomposites

$MWCNTs_2$ content, wt. %	***T_g, K***	***ΔT_g, K***	***E', MPa (at 373 K)***	***$h_{tg\,\delta}$***
$PCN_1/MWCNTs_2$				
0 (PCN_1)	552; 588	92	3632	0.40; 0.77
0.01	583	73	3034	0.76
0.1	566	70	3336	0.90
$PCN_2/MWCNTs_2$				
0 (PCN_2)	545; 560; 578	79	2876	0.16; 0.19; 0.29
0.03	534; 546; 566	85	4226	0.11; 0.14; 0.37
0.04	524; 545; 565	93	3654	0.11; 0.12; 0.32
0.10	552; 572	81	3652	0.32; 0.24
1.20	560	63	3301	0.46

interactions of cyanate groups of PCN-matrix, which were not able to react at lower temperature because of steric hindrance. During step by step synthesis (the details can be found in sect. 2.3) at temperatures > T_g the mobility of kinetic segments in the polycyanurate network increases and the unreacted cyanate groups can react to each other with further formation of cyanurate cycles providing post-curing process [117, 181]. Occurrence of post-curing in the PCN_1 sample is evidenced by an appearance of a small peak in the curve of $E' = f(T)$ dependence in the temperature range of T = 540 ÷ 550 K, and a similar maximum on the curve of $tg\ \delta = f(T)$ dependence (cf. Fig. 5.11), which indicate increasing mobility of kinetic segments of macromolecules of the PCN_1 in this temperature region. At further heating of the sample the crosslink degree of polycyanurate network increases (due to post-curing), and a new higher glass transition temperature T_g is fixed for this PCN_1 (Table 5.3).

The lower values of T_g and moduli of elasticity E' for the nanocomposites investigated are explained, first of all, by the formation during synthesis in the presence of $MWCNTs_2$ of more defective and less crosslinked PCN_1 matrix (in comparison with the sample of individual PCN_1). As it was shown above in sect. 5.1 the carbon nanotubes hinder achieving higher conversion of cyanate groups of PCN_1 matrix that cause formation of the less crosslinked network. The formation of the network of lower crosslink density is confirmed by an increasing intensity of the $tg\ \delta$ maximum (at T_g, cf. Fig. 5.13, curve 3) that reflects the greater mobility of kinetic segments in the less-crosslinked PCN_1 matrix of the nanocomposites. However in general, the results indicate that the nanocomposites of $PCN_1/MWCNTs_2$ have high glass transition temperature T_g and module of elasticity E' that is important in terms of their possible practical application.

In Fig. 5.13 the temperature dependencies of E' and $tg\ \delta$ for nanocomposites of $PCN_2/MWCNTs_2$ with different $MWCNTs_2$ content are shown, it is clear seen that for the individual PCN_2 synthesized from the industrial oligomer DCBA three T_gs are clearly fixed (Fig. 5.13 b, Table 5.3) and in the curve of its temperature dependence of E' at temperatures T > 540 K (Fig. 5.13) a new broad maximum is observed. Both of these facts evidence the above mentioned post-curing process, which occur at heating of the sampleat the temperature $T > T_g$, providing increasing crosslink density of PCN_2 and, as a result, increasing value of glass transition temperature T_g. Note that during the second study

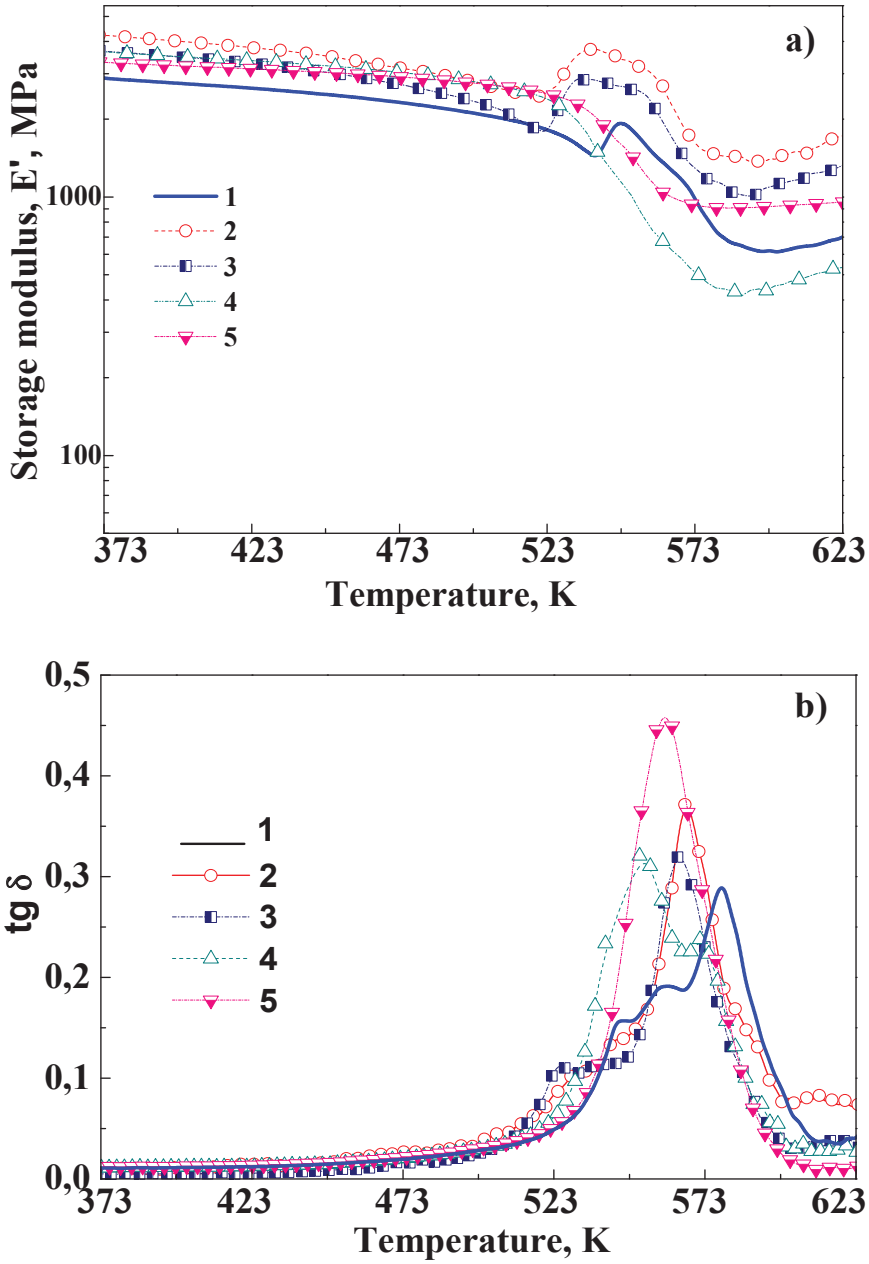

Fig. 5.13. Temperature dependences of (a) modulus *E*' and (b) *tan* δ (at frequency 3 Hz) for the PCN_2/$MWCNTs_2$ nanocomposites with $MWCNTs_2$ content, wt. %: 1 – 0; 2 – 0.03; 3 – 0.04; 4 – 0.1; 5 – 1.2.

(heating) of the same sample (the plot is not given) the single glass transition temperature T_g ~ 578 K is found that obviously evidences achieving complete conversion of cyanate groups and maximal degree of crossliking (according to Fig. 5.12).

It can be seen from the curves of *E' = f (T)* and *tan* $\delta = f(T)$ for $PCN_2/MWCNTs_2$ nanocomposites (Fig. 5.13) that at addition of carbon nanotubes $MWCNTs_2$ into the polycyanurate matrix and increase of their content from 0.03 to 1.2 wt. % the visible changes in viscoelastic properties occur: redistribution of intensities and shift of the maxima for *tan* δ along the temperature axis (decreasing T_g value), changing the glass transition temperature interval (ΔT_g), increase of moduli of elasticity *E*' in a wide temperature range, and so on.

It can be concluded that increasing concentrations of carbon nanotubes in $PCN_2/MWCNTs_2$ nanocomposites cause reduced crosslink density of PCN_2 formed in their presence that leads to lower values of T_g. This conclusion is confirmed by the growth of the intensity maxima for *tan* δ (Fig. 5.13 b, curves 2-5). In other words, the carbon nanotubes in the synthesis of these nanocomposites to some extent prevent the formation of a regular three-dimensional polycyanurate matrix. This is also confirmed by the fact that at increase in nanocomposites the $MWCNTs_2$ content to 0.1 ÷ 1.20 wt. % simultaneously with decreasing T_g values, the number of relaxation transitions is reduced (from three to one, Table. 5.3), indicating impediments in the process of post-curing in samples with high content of carbon nanotubes. Note that during the second study (heating) of all the nanocomposite samples the only single T_g (the highest value for each sample, Table. 5.3) is observed. However, because the value of T_g is less than that for the unfilled PCN_2 sample, we believe that due to the presence of carbon nanotubes in PCN_2 matrix the complete conversion of cyanate groups is not achieved and the polycyanurate network of lower regularity is formed.

Unlike the series of samples $PCN_1/MWCNTs_2$ for all the $PCN_2/MWCNTs_2$ nanocomposites a significant increase in the values of elastic modulus *E*' is observed (Fig. 5.13 a). For example, the value of *E'* at $T \sim 273$ K for the nanocomposite sample with small $MWCNT_2$ content (0.03 wt. %) is ~ 63 % higher than the *E'* value for unfilled PCN_2 that, as it is known, indicates reinforcement of PCN-matrix by carbon nanotubes, which are effectively dispersed to individual nanotubes (Fig. 5.5).

Additionally, perhaps there is some contribution to increasing modulus of elasticity *E'* in these nanocomposites of the indicated above (sect. 5.2) nanostructuring of the samples (the appearance of the structures of the type, which can be called as "nano hot

dog"), since it is clear that reinforcing effect of carbon nanotubes is increased with contributions in some way of the oriented thin polymer layer wrapping the carbon nanotubes. In other words in covalently crosslinked polycyanurate network the physical network of carbon nanotubes "wrapped" by the polymer is formed that, as known [137], promotes growing modules of elasticity *E'*.

Increasing concentrations of nanofiller leads to lower values of *E'* in the whole temperature range (Fig. 5.13 a), but the values of *E'* modulus for the nanocomposites synthesized are larger than that for the pure PCN_2. As it was noted above, in these nanocomposites during high-temperature synthesis of PCN-matrix a secondary reaggregation of carbon nanotubes occurs, resulting in reduced uniformity of dispersion of carbon nanotubes in a polymer matrix, there are areas where there is no physical network of carbon nanotubes "wrapped" by the polymer (section 5.2) that leads to decreasing values of *E'* modulus [137].

Comparison of viscoelastic properties of two series of the investigated nanocomposites based on crosslinked polycyanurates indicates that using of the industrial oligomer DCBA for synthesis of PCN_2-matrix allows to obtain of the nanocomposites with high modulus of elasticity *E'* that is important in terms of their possible practical application.

Using the "TA Instruments DMA 2980" equipment the "stress-strain" dependence for samples of the nanocomposites PCN_2/$MWCNTs_2$ was recordered and the value of tensile strength at break, σ_b was determined depending on the content of the nanofiller (cf. Fig. 5.14 and Table. 5.4).

Table 5.4. The impact of the nanofiller on the value of tensile strength at break σ_b for PCN_2/$MWCNTs_2$ nanocomposites

$MWCNTs_2$ content, wt. %	**σ_b, MPa**
0 (PCN_2)	115.9
0.03	187.6
0.06	225.1

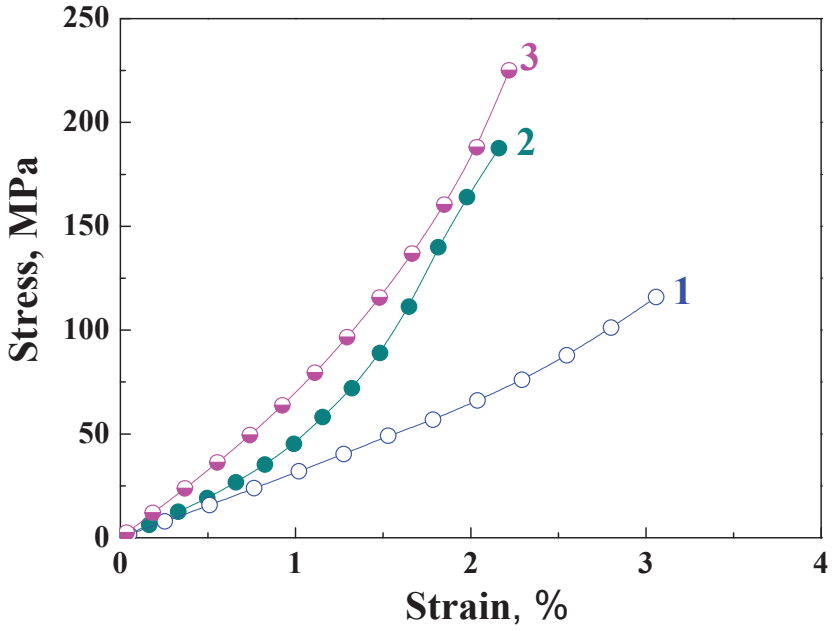

Fig. 5.14. Stress - strain curves for samples of the nanocomposites based on PCN_2 with $MWCNTs_2$ content, wt. %: 1 – 0; 2 - 0.03; 3 - 0.06.

It is obvious that with the introduction of the nanofiller to the unfilled polymer matrix the value of the ultimate strength σ_b significantly increases, the higher content of $MWCNTs_2$, the greater the value of σ_b: for example, introduction of 0.03 and 0.06 wt. % of $MWCNTs_2$ increases the value of σ_b by ~ 62 % and ~ 94%, respectively (compared to the value for pure PCN_2, Table. 5.4).

It can be concluded that at the conditions of forming PCN_2-matrix used even a small amount (0.03 ÷ 0.06 wt. %) of $MWCNTs_2$ significantly improves the strength of the nanocomposites obtained that is associated with features of the structure of carbon nanotubes as nanofiller.

5.5. Study of the effect of $MWCNTs_2$ on the thermophysical characteristics of nanostructured composites

As it was found (sect. 5.1 − 5.4), the presence of the nanofiller significantly affects the kinetics of the DCBA polycyclotrimerization process, it was interesting to investigate thermophysical properties of the $PCN_1/MWCNTs_2$ and $PCN_2/MWCNTs_2$ nanocomposites.

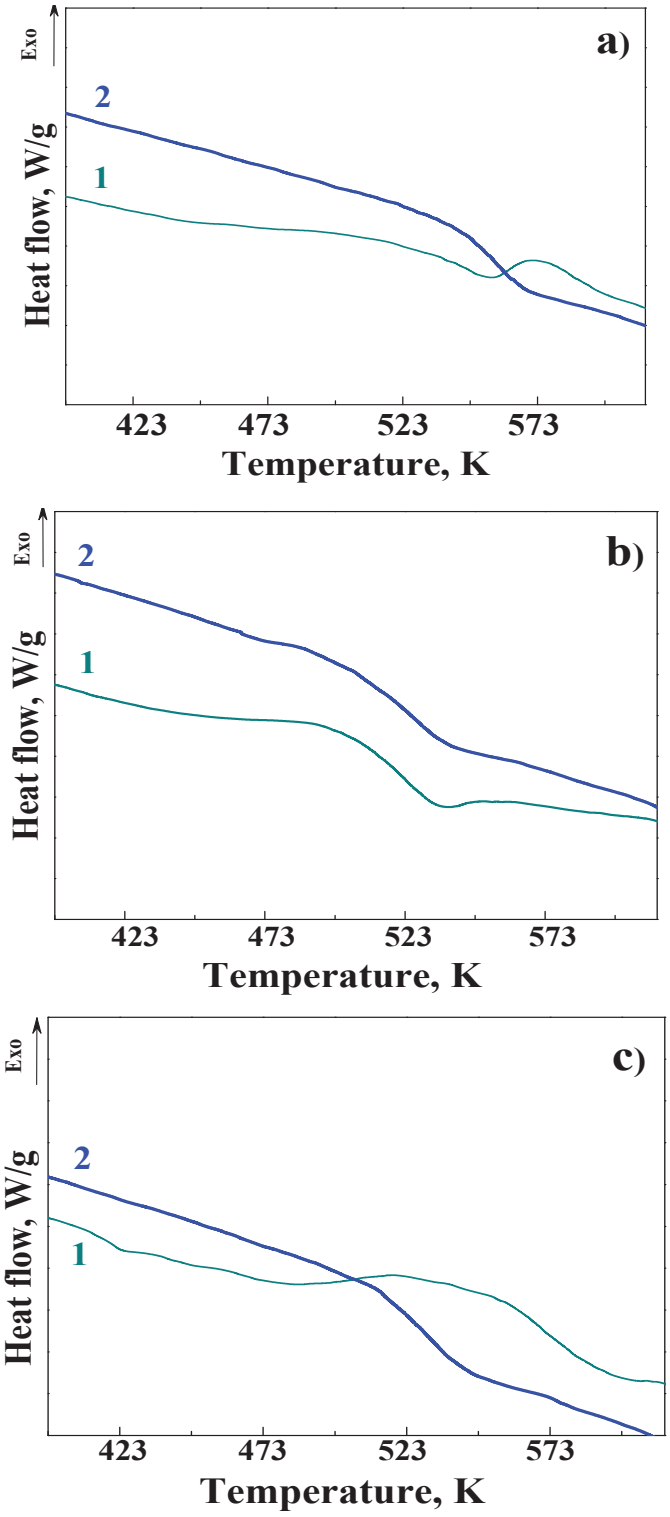

Fig. 5.15. DSC-thermograms for the $PCN_1/MWCNTs_2$ nanocomposites with $MWCNTs_2$ content, wt. %: a – 0; b - 0.01; c - 0.1; 1 - first heating scan; 2 - second heating scan.

The character of DSC-thermograms (cf. Fig. 5.15) obtained during the first scan (heating) of the samples of the nanocomposites $PCN_1/MWCNTs_2$ allows to determine that in all the samples studied the formation process of polycyanurate matrix is incomplete, it is clear seen that after the endothermic transition, corresponding to T_g of PCN_1-matrix, an intensive exothermic process starts, which is known [181] to appear when the reaction of post-curing of PCN-matrix through the interactions of unreacted (at the synthesis of the matrix) cyanate groups occur. This finding correlates with the above kinetic data (sect. 5.1) and the results of DMTA study (sect. 5.4).

From the DSC-thermograms recordered during the second heating of the same samples it can be seen (Fig. 5.15, curves at number 2) that the exothermic effects on thermograms disappear, indicating the absence of chemical reactions in these systems [133]. The thermophysical parameters are summarized in Table 5.5, it is seen that the values of T_g for PCN-matrix are slightly higher for the nanocomposite samples after their second scan (heating), certainly due to the increase of the crosslink density of PCN network after chemical reactions (interactions) of cyanate groups of PCN-matrix during the first scan (heating). It is also established that with increasing content of carbon nanotubes in the samples the value of heat capacity jump ΔC_p increases, indicating some disordering in highly regular polycyanurate matrix under the influence of the nanofiller. This conclusion is consistent with the above DMTA data (sect. 5.4).

For samples of the nanocomposites $PCN_2/MWCNTs_2$ the similar DSC-thermograms have been obtained, they are shown in Fig. 5.16. It is found that, as for the previous series of samples in these nanocomposites the formation of polycyanurate matrix was not complete, it is evidenced by the appearance in the temperature region $T > 500$ K an intensive exothermic peak, which, as noted above (sect. 5.1), corresponds to post-curing polycyclotrimerization reaction of the residual cyanate groups of the PCN-matrix, which were not able to react during the matrix synthesis. It should be noted that in comparison with the first series of samples of $PCN_1/MWCNTs_2$ in the series of $PCN_2/MWCNTs_2$ nanocomposites the exothermic effect is somewhat higher (Fig. 5.16) and it even makes impossible to fix the T_g value of the nanocomposites after first heating of the samples.

Comparison of the T_g values for post-cured individual PCN_1 and PCN_2 (Tables 5.5 and 5.6) has shown that the value of glass transition temperature T_g for the latter is lower

Table 5.5. Thermophysical parameters for PCN_1/$MWCNTs_2$ nanocomposites

$MWCNTs_2$ content, wt. %	***T_g, K***		***ΔT_g, K***		***ΔC_p, J/(K· g)***	
	1 scan	2 scan	1 scan	2 scan	1 scan	2 scan
0 (PCN_1)	538.5	557.8	16.7	20.0	0.106	0.224
0.01	522.6	525.8	25.7	32.8	0.282	0.304
0.10	-	529.7	-	26.4	-	0.299

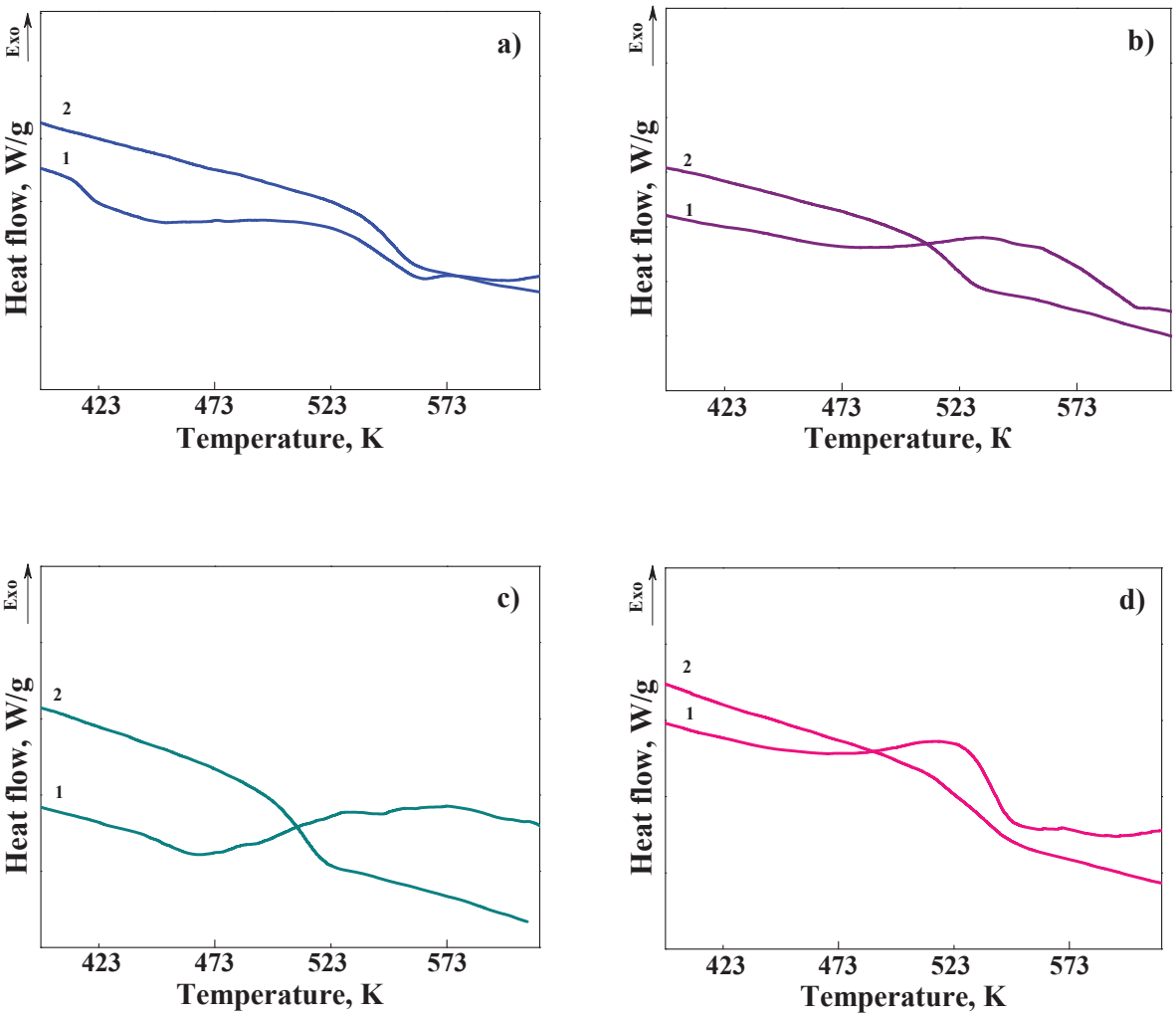

Fig. 5.16. Typical DSC-thermograms for PCN_2/$MWCNTs_2$ nanocomposites with $MWCNTs_2$ content, wt. %: a – 0; b - 0.03; c - 0.50; d - 1.20; curve 1 - first heating scan; curve 2 - second heating scan.

Table 5.6. Thermal-physical parameters for PCN_2/$MWCNTs_2$ nanocomposites

$MWCNTs_2$ content$_2$, wt. %	***T_g, K***		***ΔT_g, K***		***ΔC_p, J/(K· g)***	
	1 scan	2 scan	1 scan	2 scan	1 scan	2 scan
0 (PCN_2)	416.2; 542.5	551.1	17.8; 33.3	17.1	0.200; 0.276	0.204
0.03	-	545.5	-	29.0	-	0.249
0.10	-	538.3	-	11.2	-	0.291
0.50	-	512.4	-	17.0	-	0.227
1.20	-	537.1	-	29.5	-	0.218

by 6.7 K. This finding correlates with the above results of the DMTA study of the nanocomposites (sect. 5.4). As it was discussed above the lower T_g value of the PCN network is explained by the lower its crosslink density arising from the lower final conversion of the cyanate groups in the resulting network. We suppose that at synthesis of the industrial DCBA oligomer the producer used a special catalyst, and it is known that catalyst accelerates the reaction of polycyclotrimerization of cyanate ester monomers in first steps of curing, but leads to formation of the final network with lower conversion of the cyanate groups. The higher rate of network formation hinders formation of the network regular structure.

In the DSC-thermograms for all the PCN_2/$MWCNTs_2$ studied nanocomposites, obtained during the second scan (heating), there are no exothermic peaks (Fig. 5.16, curves at number 2), indicating the completion of the post-curing process [133]. It has been found (Table 5.6) that with increasing content of carbon nanotubes in the samples the value of heat capacity jump ΔC_p increases (non-monotonically) indicating some disordering of polycyanurate matrix under the influence of the nanofiller. This conclusion is consistent with the above data obtained using DMTA technique (sect. 5.4).

Thus, we can conclude that the basic thermophysical characteristics, such as glass transition temperature T_g, the heat capacity jump ΔC_p, glass transition interval ΔT_g of PCN-matrix in the nanocomposites PCN_1/$MWCNTs_2$ and PCN_2/$MWCNTs_2$ change non-

monotonically and non-additively under the influence of carbon nanotubes that evidences a complex reorganization of the phase structure of the nanocomposites during their synthesis.

5.6. Influence of $MWCNT_2$ on resistance to thermooxidative destruction of nanocomposites $PCN_1/MWCNTs_2$ and $PCN_2/MWCNTs_2$

Since the polycyanurate networks are thermostable polymers, it was certainly interesting to evaluate the influence of carbon nanotubes on thermal behaviour of PCN-matrix in air, the corresponding experimental TGA-curves, obtained for nanocomposites $PCN_1/MWCNTs_2$ and $PCN_2/MWCNTs_2$, are shown in Figs. 5.17 and 5.18. The appropriate thermal characteristics for the nanocomposite samples studied have been summarized in Tables 5.7 and 5.8.

It should be noted that the character of the TGA curves does not change at introduction of carbon nanotubes to the PCN-matrix since the trend of curves, the number of degradation stages for $PCN_1/MWCNTs_2$ nanocomposites are similar to that for individual PCN_1. For all the TGA curves the intense mass loss is observed in the temperature range of 700-750 K, which is associated with the destruction of the carbon backbone of PCN network. Samples of the nanocomposites of series $PCN_1/MWCNTs_2$ as well as the individual PCN_1 show a slightly higher resistance to thermooxidative destruction than the corresponding samples from the second series ($PCN_2/MWCNTs_2$), certainly due to the difference in the structure formed of polycyanurate matrix. As it was discussed above in section 5.5, in the samples based on PCN_1 the degree of polycyclotrimerization completeness and, correspondingly, the crosslink density of the resulting PCN-matrix are higher and thermal stability is higher too.

It has been found that for the series of samples $PCN_1/MWCNTs_2$ the presence of carbon nanotubes dispersed in polymer matrix in an amount of 0.01 and 0.10 wt. % slightly increases the resistance of these nanocomposites to thermal degradation in air. As it is seen from the data of Table 5.7, destruction of these samples starts at higher temperatures

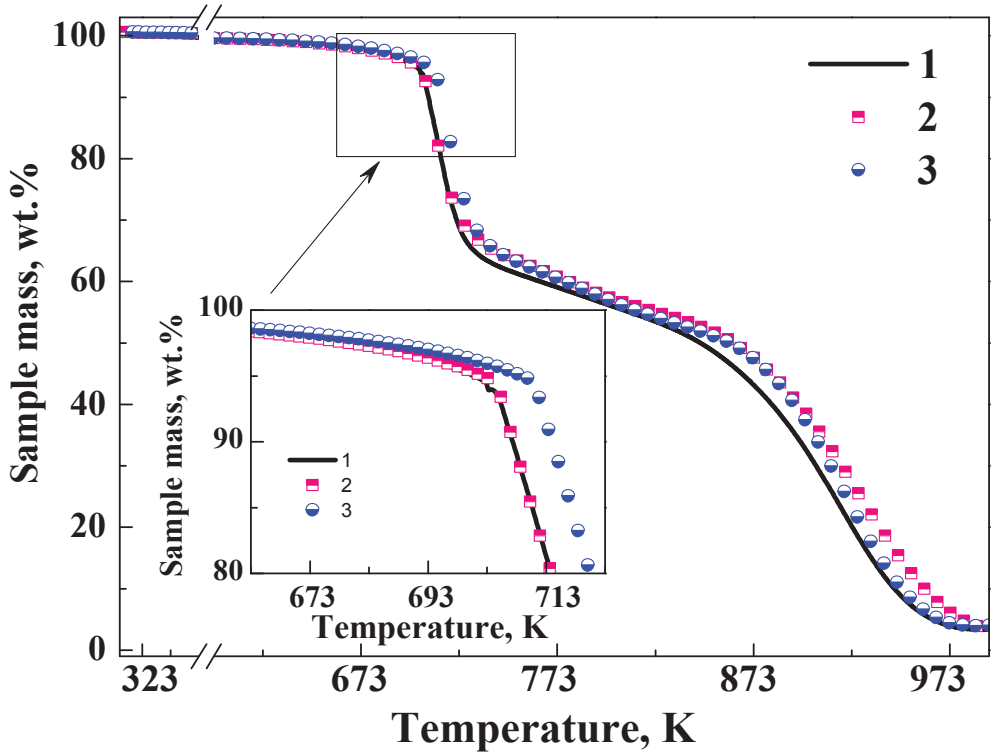

Fig. 5.17. TGA curves (in air) for the PCN_1/$MWCNTs_2$ nanocomposite samples with $MWCNTs_2$ content, wt. %: 1 – 0; 2 – 0.01; 3 – 0.10.

Table 5.7. Influence of $MWCNTs_2$ on resistance to thermooxidative destruction of PCN_1/$MWCNTs_2$ nanocomposites

$MWCNTs_2$ content$_2$, wt. %	***$T_{\partial\,(5\%)}$, K***	***$T_{\partial\,(50\%)}$, K***	***$T_{\partial 1\,(max)}$, K***	***$T_{\partial 2\,(max)}$, K***	***Δm, wt. %***		***m_{char}, wt. %***
					at $T_{\partial 1\,(max)}$	**at $T_{\partial 2\,(max)}$**	
0 (PCN_1)	701	846	714	912	20	74	3.11
0.01	702	863	715	926	20	74	3.57
0.10	709	861	720	920	19	74	4.25

compared to the pure PCN_1 (the values of $T_{d(5\%)}$, $T_{d(max)}$ and $T_{d(50\%)}$ are higher). This is connected with some contribution of CNTs themselves, which have very high own thermal stability (cf. Fig. 4.6). However, on the other hand it is known that the polycyanurate

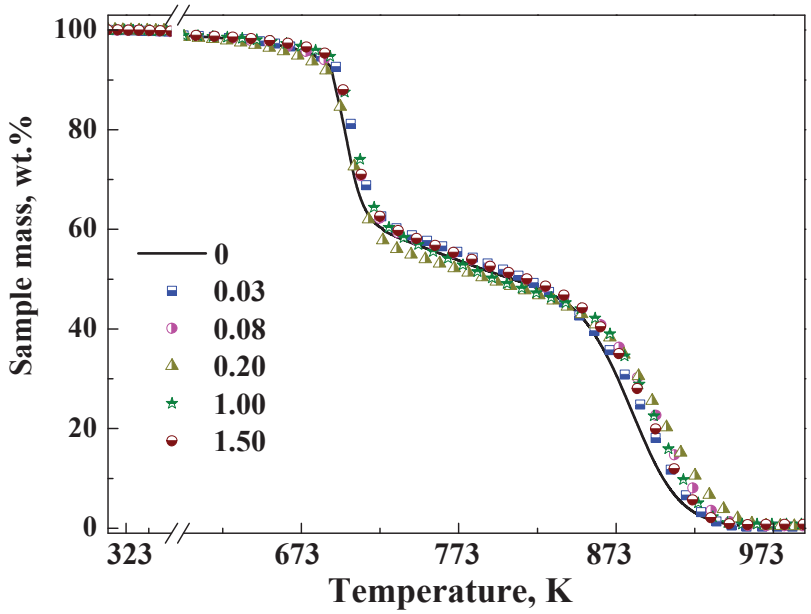

Fig. 5.18. Typical TGA curves (in air) for samples of the PCN_2/$MWCNTs_2$ nanocomposites with $MWCNTs_2$ content, wt. %: 1 – 0; 2 – 0.03; 3 – 0.08; 4 – 0.20; 5 – 1.00; 6 – 1.50.

Table 5.8. Influence of $MWCNT_2$ on resistance of PCN_2/$MWCNTs_2$ nanocomposites to thermooxidative degradation

$MWCNTs_2$ content$_2$, wt. %	*$T_{\partial\,(5\%)}$, K*	*$T_{\partial\,(50\%)}$, K*	*$T_{\partial 1\,(max)}$, K*	*$T_{\partial 2\,(max)}$, K*	*Δm, wt. %*		*m_{char}, wt. %*
					at $T_{\partial 1\,(max)}$	at $T_{\partial 2\,(max)}$	
0 (PCN_2)	680	807	702	884	22	77	0.63
0.03	683	816	708	890	24	82	0.34
0.08	682	816	706	899	23	78	0.54
0.20	670	792	704	903	24	78	0.47
1.00	663	766	699	883	25	80	0.56
1.20	689	796	708	899	23	78	0.98
1.50	690	816	706	894	22	77	0.79

networks have higher heat resistance and resistance to thermooxidative destruction at higher crosslink density [117].

In section 5.1 it was shown that the increase of $MWCNTs_2$ content in samples of the nanocomposites slightly decreased the final conversion value of cyanate groups, resulting to lower crosslink density of the final PCN network. Therefore it was logical to assume that the thermal properties of the nanocomposites would be worse than that of the individual PCN. Surprisingly, the experimental results show the opposite. Thus it can be assumed that the improved resistance to thermooxidative degradation in these nanocomposite samples is associated not only with a certain additive contribution of thermally resistant CNTs, but probably also with the post-curing process of PCN-matrix due to additional heating to high temperatures ($T > T_g$) during TGA measurements (the same observations were fixed by DMTA and DSC methods, sect. 5.4 and 5.5, correspondingly), increasing the density of PCN-matrix and hence the stability of nanocomposites to thermooxidative destruction.

Investigation of resistance to thermooxidative degradation for series of samples $PCN_2/MWCNTs_2$ has shown that their thermal stability in air depends non-monotonically on the $MWCNTs_2$ content (Fig. 5.18 and Table. 5.8). For example, the presence of 0.03 ÷ 0.08 wt. % of the dispersed in the polymer matrix $MWCNTs_2$ increases the resistance to thermooxidative destruction of these nanocomposites: increasing degradation temperatures $T_{d(5\%)}$, $T_{d(max)}$ and $T_{d(50\%)}$, simultaneously the reduced mass loss for these samples has been fixed in comparison with the individual PCN_2). In general we can conclude that the synthesized nanocomposites $PCN_1/MWCNTs_2$ and $PCN_2/MWCNTs_2$ have high resistance to thermooxidative destruction.

5.7. Study of influence of carbon nanotubes on electrical properties of $PCN_2/MWCNTs_2$

As it was noted above in section 4.8, carbon nanotubes in addition to the unique thermal and mechanical properties possess high electrical conductivity, thus they are very

attractive for use as conductive filler at creation of polymer nanocomposites. Therefore it is interesting to assess, first, in which limits the electrical properties of polycyanurates (which are recognized as dielectrics with low dielectric constant, 2.5 ÷ 3.2) can be purposefully altered; secondly, it is useful to determine the percolation threshold, p_c, above which the $PCN_2/MWCNTs_2$ nanocomposites exhibit properties of conductive material. Research technique is described in section. 3.10. Fig. 5.19 shows the concentration dependence of conductivity σ_{DC} for $PCN_2/MWCNTs_2$ nanocomposites, it is clear that the σ_{DC} value demonstrates percolation behavior [158, 160, 161], namely: at low concentrations of $MWCNTs_2$ from 0 to ~ 0.3 wt. % in nanocomposites σ_{DC} value does not change and is equal $\approx 10^{-16}$ Sm/cm; with increasing content of nanotubes in composites the value of σ_{DC} conductivity sharply increases by ~ 10 orders of magnitude in a narrow concentration range of $MWCNTs_2$ ~ 0.3 – 0.5 wt. %. A further increase in concentration of $MWCNTs_2$ in these samples causes slow growth of σ_{DC} value by ~ 3 orders of magnitude in the concentration range ~ 0.3-1.5 wt. %.

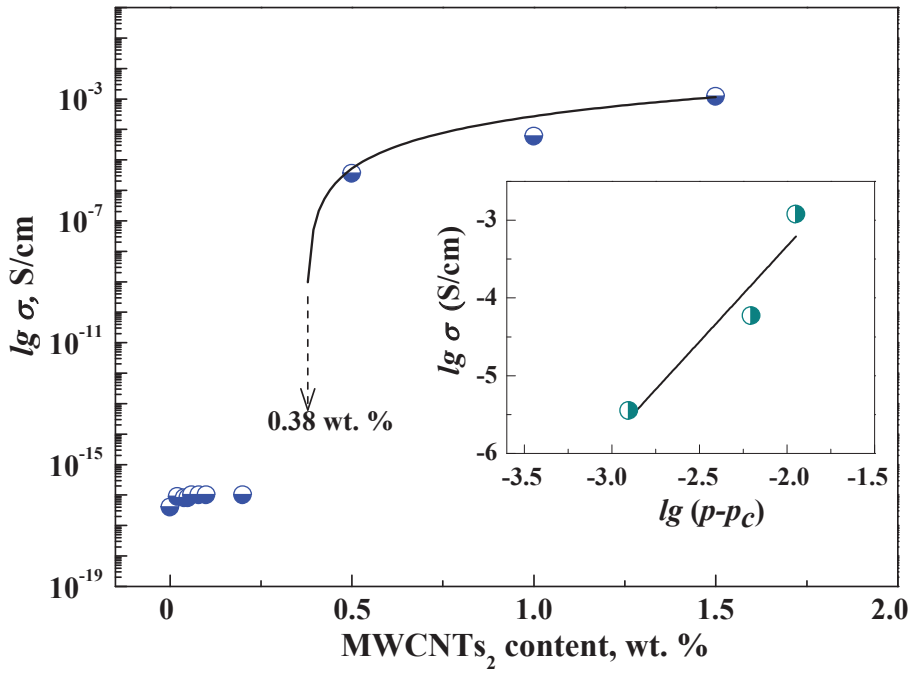

Fig. 5.19. Dependence of conductivity σ_{DC} (direct current) for $PCN_2/MWCNTs_2$ nanocomposites on $MWCNTs_2$ content; dots represent experimental data; lines shows theoretical values (according to equation 4.1); insertion reflects the dependence curve of $lg\sigma_{DC} = f(lg)(p - p_c)$ for $p > p_c$.

Experimental dependence of $\sigma_{DC} = f(C_{MWCNTs2})$ shown in Fig. 5.19 was theoretically approximated using equation 4.1 (sect. 4.8), the dependence of $\lg \sigma = f \lg (p - p_c)$ was built and step by step by changing the value of p_c the best linear approximation of the experimental data was achieved. As shown in Fig. 5.19, theoretical and experimental data agree well with each other. The percolation threshold p_c and the value of t are given in Table 5.9. One can see that the percolation area for $PCN_2/MWCNTs_2$ system is fixed in the concentration range of $MWCNTs_2$ content of 0.38 – 0.50 wt. %. Therefore the percolation behavior of this system can be characterized by two critical values of concentration: $p_c \approx 0.38$ wt. % when the conducting cluster begins to form and $p_c^* \approx 0.50$ wt. %, corresponding to the end of formation of spatial conducting cluster.

Table 5.9. Percolation threshold p_c and critical exponent t for $PCN_2/MWCNTs_2$ nanocomposites

Percolation parameters	***$PCN_2/MWCNTs_2$***
p_c	**0.0038**
t	**2.46**

Note that the percolation parameters obtained for $PCN_2/MWCNTs_2$ nanocomposites differ from similar characteristics for the nanocomposite samples of $cPBT/MWCNTs_1$ (sect. 4.8) because of differences in the chemical structure of the polymer matrix, the method of CNTs dispersing, methods of synthesis and the formation of nanocomposites samples, etc. [8, 12, 160, 161].

In order to determine the mechanism of conductivity in $PCN_2/MWCNTs_2$ nanocomposites for the samples with the $MWCNTs_2$ content higher than the percolation threshold found, (similarly to the $cPBT/MWCNTs_1$ nanocomposites) the temperature dependence of dc conductivity at temperatures close to the temperature of 0 K was investigated. In Fig. 5.20 the experimental temperature dependence of dc conductivity of nanocomposites with different $MWCNT_2$ content is shown and the theoretical values of σ_{DC} calculated using the FIT theory (equations 4.2 ÷ 4.4, sect. 4.8) are given. The

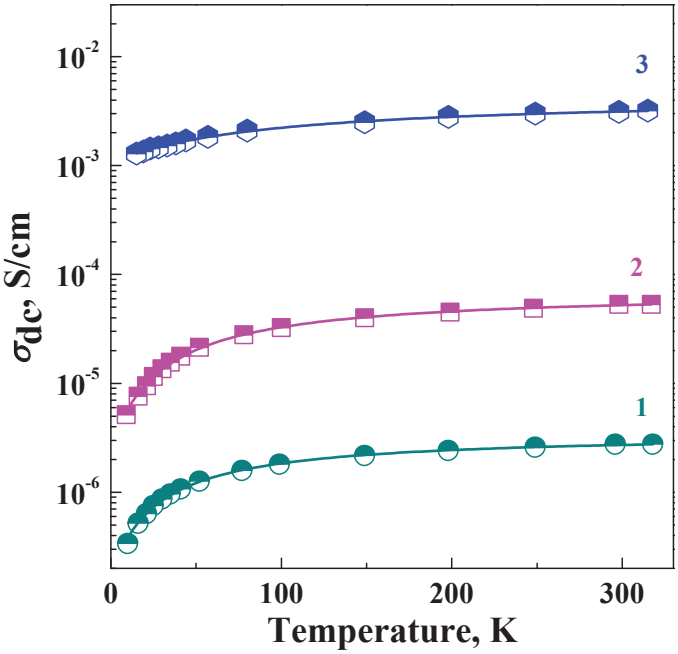

Fig. 5.20. Temperature dependence of dc conductivity of PCN_2/$MWCNTs_2$ nanocomposites with $MWCNTs_2$ content, wt. %: 1 – 0.5; 2 – 1.0; 3 – 1.2; symbols – experimental data, lines – theoretically calculated using FIT model.

calculations have shown that the experimental and theoretically calculated values of σ_{DC} obtained with a help of FIT model agree well in the whole temperature range measured, it is seen that at temperatures close to 0 K a weak temperature dependence of σ_{DC} is observed. It is explained by the above mentioned contribution to σ_{DC} of electrical conductivity of metallic carbon nanotubes, because at so low temperatures the semiconducting CNTs cannot conduct electrical current [152]. So $MWCNTs_2$ similar to $MWCNTs_1$ contain semiconducting nanotubes as well as a significant part of carbon nanotubes with a structure of "chair", which are characterized by metallic conductivity [42]. This finding correlates well with the data of Raman spectroscopy shown in section. 4.1. So we can conclude that the conductivity in these nanocomposites is mainly created by electrons through the tunnel mechanism, and the "wrapping" of carbon nanotubes with polymer described in section 5.2 does not hinder this process. Similarly to the cPBT/$MWCNTs_1$ nanocomposites, increasing concentration of $MWCNTs_2$ in

PCN_2/$MWCNTs_2$ nanocomposites causes growth in dc conductivity that is certainly explained by increasing number of the conducting channels [158].

* * *

Thus, in this work first the comprehensive study was carried out to determine the impact of multiwall carbon nanotubes $MWCNTs_2$ on structure and basic physical-chemical properties of polymer composites synthesized from oligomers of dicyanate ester of bisphenol A, DCBA, by in situ polycyclotrimerization of DCBA in the presence of MWCNTs, using the method of reaction forming. For the first time it is found that at synthesis of the crosslinked polycyanurate matrix the presence of $MWCNTs_2$ in the first stages of the process accelerates the reaction of polycyclotrimerization of DCBA oligomer, but in the final stages of the process the nanofiller hinders achieving high conversion of DCBA cyanate groups, leading to the formation of PCN-matrix with a lower degree of crosslinks. This conclusion is confirmed by the results of measurements by DMTA technique, as for the nanocomposites with higher content of $MWCNTs_2$ a significant reduction in T_g values for PCN-matrix has been fixed. Using TGA method it was determined that all the synthesized PCN_2/$MWCNTs_2$ nanocomposite samples retained high resistance to thermal-oxidative degradation inherent to this class of polymers, some increase in thermal performance of the nanocomposites compared to the individual PCN_2 was observed. It has been found that in these nanocomposites the value of tensile strength at break σ_b increases by 62 and 94% for the samples with 0.03 and 0.06 wt. % of $MWCNTs_2$, respectively, compared with unfilled PCN_2 ($\sigma_b \approx 115.9$ MPa) . It is found that by introducing of carbon nanotubes into the dielectric PCN-matrix the electrical properties of the nanocomposite can be purposefully alter from dielectric to the conductor with varying conductivity in a wide range (depending on the CNTs content), it has been determined that the percolation threshold for PCN_2/$MWCNTs_2$ nanocomposites is low and equal ~ 0.38 wt. % of $MWCNTs_2$ indicating the formation of three-dimensional percolation conducting network of carbon nanotubes in the system. In summary, the efficient methods of synthesis of PCN/MWCNTs nanocomposites with improved physical-chemical properties were developed.

CONCLUSIONS

Studies on synthesis and determination of properties of nanostructured polymer composites obtained by *in situ* polymerization of the oligomers of heterocyclic esters in the presence of carbon nanotubes, which are characterized by high thermal and mechanical resistance and elctrical conductivity, have been just started. Therefore, development of efficient methods for synthesis and formation of such polymer nanocomposites is an actual task of Macromolecular Chemistry. Solving of this task is addressed to an extension of the range of polymer products to meet the growing demands of high-tech industries.

The results obtained allow the following conclusions:

1. **For the first time**, the optimal conditions of synthesis of novel thermostable nanostructured polymer composites from oligomers of cyclic butylene terephthalate using method of reactive extrusion and from oligomers of dicyanate ester of bisphenol A using method of reactive forming in the presence in reactive mixture of effectively dispersed nanofiller, multiwall carbon nanotubes, were determined. It was established that using of low viscosity heterocyclic esters for synthesis of cPBT and PCN and the methods of *in situ* polymerization provide effective dispersing of nanofiller in the forming polymer matrix.

1. **For the first time**, catalytic effect of carbon nanotubes in reactions of Ring-Opening Polymerization of CBT oligomers and polycyclotrimerization of DCBA oligomers have been established. It has been shown that in the presence in reactive mixture of the dispersed MWCNTs the induction period of these reactions reduces, the rate of transformation of CBT to cPBT increases, the conversion of cyanate groups of DCBA is accelerated, i.e. the nanofiller at *in situ* polymerization of oligomers of heterocyclic esters play the role of catalyst due to interaction of the oligomers wth active surface of the outer walls of carbon nanotubes.

2. It is found that effective dispersing of $MWCNTs_1$ in the forming cPBT stipulates the non-additive increase in resistance to thermal-oxidative destruction, in apparent activation energy E_a of β-relaxation process and in glass transition temperature T_g. Significant influence of $MWCNTs_1$ on formation of crystalline structure of cPBT matrix in the

nanocomposites has been observed. This appers in non-additive changing value of melting enthalpy ΔH_m of crystallites, degree of crystallinity X_c, and melting temperature T_m of crystallites. Essential increase in value of crystallization temperature T_c (by 3 ÷ 18 K) with increasing of $MWCNTs_1$ content from 0.01 to 2.0 wt. % has been fixed. The changes found in the structure of the crystalline phase of film samples of $cPBN/MWCNTs_1$ nanocomposites obtained by hot pressing of extrusion strand or by injection molding of the melted extrudate evidence that in process of crystallization of cPBN matrix the dispersed carbon nanotubes play the role of heterogeneous nucleation centers.

4. **For the first time**, it has been found that during synthesis of $PCN_1/MWCNTs_2$ nanocomposites in the final stages of the reaction the nanofiller hinders achieving high conversion of cyanate groups that results in the formation of polymer networks with a lower crosslink degree (compared to the unfilled PCN_1), and this is confirmed by the decrease in glass transition temperature T_g, however, it is not accompanied by a drop in the other physical-chemical properties of the nanocomposites. It has been established that the $PCN_2/MWCNTs_2$ nanocomposites possess high stability to thermal-oxidative destruction, thermal conductivity and storage modulus E', the increase in value of tensile strength at break σ_b by 62-94 % compared to unfilled PCN_2 ($\sigma_r \approx 115{,}9$ MPa) for the samples with $MWCNTs_2$ content of 0.03-0.06 wt. % is fixed too.

5. It has been found during high temperature synthesis of the nanocomposites of PCN/MWCNTs and cPBT/MWCNTs as well as at forming of film materials by method of hot pressing from the latter, inside the polymer matrix the reaggregation of CNTs occurs resulting in some reduction in the values of storage modulus E', but at that the ability of the nanocomposites to conduct electrical current is improved significantly due to formation of the spatial percolation cluster of CNTs. It has been determined that the percolation thresholds for conductivity for the obtained nanocomposites is low and equal to 0.22 wt. % for $cPBT/MWCNTs_1$ and 0.38 wt. % for $PCN/MWCNTs_2$. Thus for these nanocomposites the possibility to change the electrical properties in wide range by varying the MWCNTs content has been established.

References

[1]. Crandall B.C. and Lewis J., *Nanotechnology: research and perspectives*, Proceedings from the first foresight conf. on nanotechnology, Cambridge : MIT Press; (1992) 381 p.

[2]. Schwarz J.A., Contescu C.I., and Putyera K., *Dekker Encyclopedia of Nanoscience and Nanotechnology*, New York : Dekker Inc.; (2004) 4014 p.

[3]. Wei B. Q, Vajtai R., and Ajayan P.M., *Reliability and current carrying capacity of carbon nanotubes*, Applied Physics Letters **79** (2001) 1172–1174.

[4]. Durkop T., Kim B.M., and Fuhrer A.M.S., *Properties and applications of high-mobility semiconducting nanotubes*, Journal of Physics : Condensed Matter. **16** (2004) 553–580.

[5]. Ajayan P. M., Stephan O., and Colliex C., *Aligned carbon nanotube arrays formed by cutting a polymer resin–nanotube composite*, Science **265** (1994) 1212–1214.

[6]. Andrews R. and Weisenberger M. C. *Carbon nanotube polymer composites*, Current opinion in solid state & materials science **8** (2004) 31–37.

[7]. Alig I., Skipa T., Lellinger D., and Pötschke P. *Destruction and formation of a carbon nanotube network in polymer melts: rheology and conductivity spectroscopy*, Polymer **49** (2008) 3524–3532.

[8]. Spitalsky Z., Tasis D., Papagelis K., and Galiotis C. *Carbon nanotube–polymer composites: chemistry, processing, mechanical and electrical properties*, Progress in polymer science **35** (2010) 357–401.

[9]. Tasis D., Tagmatarchis N., Bianco A., and Prato M., *Chemistry of carbon nanotubes*, Chemical Reviews **106** (2006) 1105–1136.

[10]. Coleman J. N., Khan U., BlauW.J., and Gun'koY.K., *Small but strong: a review of the mechanical properties of carbon nanotube–polymer composites*, Carbon **44** (2006) 1624–1652.

[11]. Yu M., Lourie O., Dyer M. J., Moloni K., Kelly T. F., and Ruoff R. S., *Strength and breaking mechanism of multiwalled carbon nanotubes under tensile load*, Science, **287** (2000) 637–640.

[12]. Grossiord N., Loos J., Regev O., and Koning C.E., *Toolbox for dispersing carbon nanotubes into polymers to get conductive nanocomposites*, Chemistry of materials **18** (2006) 1089–1099.

[13]. Al-Saleh M. H. and Sundararaj U. *A review of vapor grown carbon nanofiber/polymer conductive composites*, Carbon **47** (2009) 2–22.

[14]. Bauhofer W. and Kovacs J. Z., *A review and analysis of electrical percolation in carbon nanotube polymer Composites*, Composites Science Technology **69** (2009) 1486–1498.

[15]. Pinnavaia T. J. and Beall G.W., *Polymer-clay nanocomposites*, Chichester: John Wiley & Sons; (2001) 370 p.

[16]. Biswas M. and Sinha R. S., *Recent progress in synthesis and evaluation of polymer– montmorillonite nanocomposites*, Advances in Polymer Science **155** (2001) 167–221.

[17]. Shpak A. P, Kunitskiy Yu. A., and Karbovsky V.L., *Claster and nanostructural materials*, Kyiv: Akademperiodika; (2001) 588 p. (in Russian).

[18]. Schmidt H., *Nanoparticles by chemical synthesis, processing to materials an innovative applications*, Applied organometallic chemistry **15** (2001) 331–343.
[19]. Fischer H., *Polymer nanocomposites: from fundamental research to specific applications*, Materials Science and Engineering : C **23** (2003) 763–772.
[20]. Jordan J., Jacob K. I., Tannenbaum R., Sharaf M. A., and Jasiuk I., *Experimental trends in polymer nanocomposites – a review*, Materials science and engineering: A **393** (2005) 1–11.
[21]. Silberglitt R. and *Nanomaterials: new trends*. Dekker encyclopedia of nanoscience and nanotechnology. eds. J. A. Schwarz, C. I. Contescu, K. Putyera, New York : Dekker Inc.; (2004) 13 p.
[22]. Trefilov V. I., Shchur D. V., and Tarasov B. P. *Fullerenes – the base for future materials*, Kyiv: ADEF-Ukraine; (2001) 148 p. (in Russian).
[23]. Bugachenko F. L. *Nanochemistry – the direct way to high technologies of the new century*, Uspekhi khimii **72** (2003) 419–437. (in Russian).
[24]. Paul D. and Robeson L. M., *Polymer nanotechnology: nanocomposites*, Polymer **49** (2008) 3187–3204.
[25]. *Polymer nanocomposites,* eds. May Y. Y., Gong Y. G. (translation), Moscow: Technosfera; (2008) 238 p. (in Russian)
[26]. Mittal V. *Polymer Nanotube nanocomposites: synthesis, properties, and applications*, New Jersey: Wiley; (2010) 460 p.
[27]. Breuer O. and Sundararaj U., *Big returns from small fibers: areview of polymer/Carbon nanotube composites*, Polymer Composites. **25** (2004) 630–645.
[28]. Dresselhaus M.S., Dresselhaus G., and Eklund P.C., *Science of fullerenes and carbon nanotubes*, New York: Academic Press; (1996) 922 p.
[29]. Eletsky A. V., *Carbon nanotubes*, Uspekhi fizicheskikh nauk, **167** (1997) 945–972. (in Russian).
[30]. Dresselhaus M. S., Dresselhaus G., and Avouris Ph., *Carbon nanotube*, Berlin : Springer; (2000) 462 p.
[31]. Thess A., Lee R., Nikolaev P., Dai H., Petit P., Robert J., Xu C., Lee Y-H., Kim S-G., Rinzler A. G., Colbert D. T., Scuseria G. E., Tománek D., FischerJ. E., and Smalley R. E., *Crystalline ropes of metallic carbon nanotubes*, Science **273** (1996) 483–487.
[32]. Pan Z. W., Xie S. S., Chang B. H., Wang C.Y., Lu L., Liu W., Zhou W. Y., Li W. Z., and Qian L. X., *Very long carbon nanotubes*, Nature **394** (1998) 631–632.
[33]. Rakov E. G., *Methods of producing of carbon nanotubes*, Uspekhi khimii **69** (2000) 41–59. (in Russian).
[34]. Zhang X. F., Cao A., Wei B., Li Y., Wei J., Xu C., and Wu D., *Rapid growth of well-aligned carbon nanotube arrays*, Chemical Physics Letters **362** (2002) 285–290.
[35]. Zhu H. W., Xu C. L., Wu D. H., Wei B. Q., Vajtai R., and Ajayan P. M., *Direct synthesis of long single-walled carbon nanotube strands*, Science **296** (2002) 884–886.
[36]. Vajtai R., Wei B. Q., and Ajayan P. M., *Controlled growth of carbon nanotubes*, Philosophical transactions of the Royal society : A **362** (2004) 2143–2160.
[37]. Mizel A., Benedict L. X., Cohen M. L., Louie S .G., Zettl A., Budraa N. K., and Beyermann W. P., *Analysis of the low-temperature specific heat of multiwalled carbon nanotubes and carbon nanotube ropes*, Physical Review : B **60** (1999) 3264–3270.

[38]. Hone J., Batlogg B., Benes Z., Johnson A.T., and Fischer J.E., *Quantized phonon spectrum of single-wall carbon nanotubes*, Science **289** (2000) 1730–1733.
[39]. Lasjaunias J. C., Biljaković K., Benes Z., Fischer J. E., and Monceau P., *Low-temperature specific heat of single-wall carbon nanotubes*, Physical Review : B **65** (2002) 113409–113412.
[40]. Yi W., Lu L., Dian-lin Z., Pan Z. W., and Xie S.S., *Linear specific heat of carbon nanotubes*, Physical Review : B **59** (1999) 9015–9018.
[41]. Koo J.H., *Polymer nanocomposites. Processing, characterization and applications*, New York: McGraw-Hill; (2006) 272 p.
[42]. Harris P. J. F., *Carbon nanotubes and related structures:new materials for the twenty-first centur*, Cambridge: Cambridge University Press; (1999) 293 p.
[43]. Tanaka K., Yamabe T., and Fukui K., *The science and technology of carbon nanotubes*, Amsterdam: Elsevier; (1999) 199 p.
[44]. Saito R., Dresselhaus G., and Dresselhaus M. S., *Physical properties of carbon nanotubes*, London: Imperial College Press; (1998) 259 p.
[45]. Iijima S., *Helical microtubules of graphitic carbon*, Nature **354** (1991) 56–58.
[46]. Oberlin A., Endo M., and Koyama T., *High resolution electron microscope observations of graphitized carbon fibers*, Carbon **14** (1976) 133–135.
[47]. Buyanov R. A., Chesnokov V. V., Afanasiev A.D., and Babenko V. S., *Carbide mechanism of formation of carbon depositions and their properties on iron-chromium catalysts of dehydrogenation*, Kinetics and calalysis **18** (1977) 1021–1027. (in Russian).
[48]. Gibson J. A. E., *Early nanotubes*, Nature **359** (1992) 347–364.
[49]. Radushevich L. V. and Luk'yanovich V. M. *Structure of carbon formed at thermal decomposition of carbon oxide on iron contact*, Jurnal fizicheskoy khimii **26** (1952) 88–95. (in Russian).
[50]. Zhang Z. F., Liu T., Sreekumar T. V., Kumar S., Moore V. C., Hauge R. H., and Smalley R. E., *Poly(vinyl alcohol)/SWNT composite film*, Nano letters **3** (2003) 1285–1288.
[51]. Barber A. H., Cohen S. R. , and Wagner H. D., *Measurement of carbon nanotube-polymer interfacial strength*, Applied Physics Letters **82** (2003) 4140–4142.
[52]. Coleman J. N., Blau W. J., Dalton A. B., Munoz E., Collins S., Kim B. G., Razal J., Selvidge M., Vieiro G., and Baughman R.H., *Improving the Mechanical Properties of Single-Walled Carbon Nanotube Sheets by Intercalation of Polymeric Adhesives*, Applied Physics Letters **82** (2003) 1682–1684.
[53]. Freidrich K., Fakirov S., and Zhang Z., *Polymer composites. From nano- to macro-scale*, New York : Springer; (2005) 367 p.
[54]. Moniruzzaman M. and Winey K. I., *Review polymer nanocomposites containing carbon nanotubes*, Macromolecules **39** (2006) 5194–5205.
[55]. Yang J., Xu T., Lu A., Zhang Q., Tan H., and Fu Q., *Preparation and properties of poly (p-phenylene sulfide)/multiwall carbon nanotube composites obtained by melt compounding*, Composites science and technology **69** (2009) 147–153.
[56]. Han M. S., Lee Y. K. , Lee H. S., Yun C. H., and Kim W. N., *Electrical, morphological and rheological properties of carbon nanotube composites with polyethylene and poly(phenylene sulfide) by melt mixing*, Chemical engineering science **64** (2009) 4649–4656.
[57]. Zeng C., Hossieny N., Zhang C., and Wang B., *Synthesis and processing of PMMA carbon nanotube nanocomposite foams*, Polymer **51** (2010) 655–664.

[58]. Kim H. M., Kim K., Lee S. J., Joo J., Yoon H. S. , Cho S. J., Lyu S. C., and Lee C. J., *Charge transport properties of composites of multiwalled carbon nanotube with metal catalyst and polymer: application to electromagnetic interference*, Current Applied Physics **4** (2004) 577–580.

[59]. Socher R., Krause B., Boldt R., Hermasch S., Wursche R., and Pötschke P., *Melt mixed nano composites of PA12 with MWNTs: influence of MWNT and matrix properties on macrodispersion and electrical properties*, Composites Science and Technology **71** (2011). 306–314.

[60]. Li J., Tong L., Fang Z., Gu A., and Xu Z., *Thermal degradation behavior of multi-walled carbon nanotubes/polyamide 6 composites*, Polymer degradation and stability **91** (2006) 2046–2052.

[61]. McClory C., Pötschke P., and McNally T., *Influence of screw speed on electrical and rheological percolation of melt-mixed high-impact polystyrene/MWCNT nanocomposites*, Macromolecular Materials and Engineering **296** (2011) 59–69.

[62]. Huang C.L. and Wang C., *Rheological and conductive percolation laws for syndiotactic polystyrene composites filled with carbon nanocapsules and carbon nanotubes*, Carbon **49** (2011) 2334–2344.

[63]. Mamunya Y., Boudenne A., Lebovka N., Ibos L., Candau Y., and Lisunova M., *Electrical and thermophysical behaviour of PVC-MWCNT nanocomposites*, Composites Science and Technology **68** (2008) 1981–1988.

[64]. Mamunya Y. P., Levchenko V. V., Rybak A., Boiteux G., Lebedev E.V., Ulanski J., and Seytre G. *Electrical and thermomechanical properties of segregated nanocomposites based on PVC and multiwalled carbon nanotubes*, Journal of Non-Crystalline Solids **356** (2010) 635–641.

[65]. Levchenko V., Mamunya Ye., Boiteux G., Lebovka M., Alcouffe P., Seytre G., and Lebedev E., *Influence of organo-clay on electrical and mechanical properties of PP/MWCNT/OC nanocomposites,* European Polymer Journal **47** (2011) 1351-1360.

[66]. Thiébaud F., Gelin J. C., *Characterization of rheological behaviors of polypropylene/carbon nanotubes composites and modeling their flow in a twin-screw mixer*, Composites science and technology **70** (2010) 647–656.

[67]. Lisunova M. O., Mamunya Ye. P., Lebovka N. I., and MelezhykA.V., *Percolation behaviour of ultrahigh molecular weight polyethylene/multi-walled carbon nanotubes composites*, European Polymer Journal **43** (2007) 949–958.

[68]. Bocchini S., Frache A., Camino G., and Claes M., *Polyethylene thermal oxidative stabilisation in carbon nanotubes based nanocomposites*, European Polymer Journal **43** (2007) 3222–3235.

[69]. Li L., Li B., Hood M.A., Christopher Y., and Li C.Y., *Carbon nanotube induced polymer crystallization: the formation of nanohybrid shish–kebabs*, Polymer **50** (2009) 953–965.

[70]. Wu C.S., *Polyester and multiwalled carbon nanotube composites: characterization, electrical conductivity and antibacterial activity*, Polymer International **60** (2011) 807–815.

[71]. Kim J. Y., *The effect of carbon nanotube on the physical properties of poly(butylene terephthalate) nanocomposite by simple melt blending*, Journal of Applied Polymer Science **112** (2009) 2589–2600.

[72]. Broza G., Kwiatkowska M., Rosłaniec Z., and Schulte K., *Processing and assessment of poly(butylene terephthalate) nanocomposites reinforced with oxidized single wall carbon nanotubes*, Polymer **46** (2005) 5860–5867.

[73]. Chen H., Liu Z., and Cebe P., *Chain confinement in electrospun nanofibers of PET with carbon nanotubes*, Polymer **50** (2009) 872–880.
[74]. Li Z., Luo G., Wei F., and Huang Y., *Microstructure of carbon nanotubes/PET conductive composites fibers and their properties*, Composites science and technology **66** (2006) 1022–1029.
[75]. Dhand C., Arya S.K., Datta M., and Malhotra B. D., *Polyaniline–carbon nanotube composite film for cholesterol biosensor*, Analytical biochemistry **383** (2008) 194–199.
[76]. Srivastava S., Sharma S.S., Kumar S., Agrawal S., Singh M., and Vijay Y.K., *Characterization of gas sensing behavior of multi walled carbon nanotube Polyaniline composite films*, International Journal of Hydrogen Energy **34** (2009) 8444–8450.
[77]. Ramamurthy P. C., Malshe A. M., Harrell W. R., Gregory R. V., McGuire K., and Rao A. M., *Polyaniline/single-walled carbon nanotube composite electronic devices*, Solid-state electronics **48** (2004) 2019–2024.
[78]. Pötschke P., Brünig H., Janke A., Fischer D., and Jehnichen D., *Orientation of multiwalled carbon nanotubes in composites with polycarbonate by melt spinning*, Polymer **46** (2005) 10355–10363.
[79]. Hornbostel B., Pötschke P., Kotz J., and Roth S., *Mechanical properties of triple composites of polycarbonate, single-walled carbon nanotubes and carbon fibres*, Physica E : Low-dimensional systems and nanostructures **40** (2008) 2434–2439.
[80]. Show Y. and Itabashi H., *Electrically conductive material made from CNT and PTFE*, Diamond and related materials **17** (2008) 602–605.
[81]. Chameswary J., Jithesh K., George S., Raman S., Mohanan P., and Sebastian M.T., *PTFE–SWNT composite for microwave absorption application*, Materials letters **64** (2010) 743–745.
[82]. Wan J., Yan X., Ding J., and Ren R. A, *Simple method for preparing biocompatible composite of cellulose and carbon nanotubes for the cell sensor*, Sensors and actuators B : Chemical **146** (2010) 221–225.
[83]. Imai M., Akiyama K., Tanaka T., and Sano E., *Highly strong and conductive carbon nanotube/cellulose composite paper*, Composites Science and Technology **70** (2010) 1564–1570.
[84]. Tang C., Zhang Q., Wang K., Fu Q., and Zhan C., *Water transport behavior of chitosan porous membranes containing multi-walled carbon nanotubes (MWNTs)*, Journal of membrane science **337** (2009) 240–247.
[85]. Jung R., Park W. I., Kwon S. M., Kim H. S., and Jin H. J., *Location-selective incorporation of multiwalled carbon nanotubes in polycarbonate microspheres*, Polymer **49** (2008) 2071–2076.
[86]. Li Q., Xue Q.Z., Gao X. L., and Zheng Q. B., *Temperature dependence of the electrical properties of the carbon nanotube/polymer composites*, eXPRESS Polymer Letters **3** (2009) 769–777.
[87]. Pat. 5434244 USA (1995), C08G63/00, Warner G. L., Wilson P. R., and Bradt J. E. *Process for isolating macrocyclic polyester oligomers*.
[88]. Brunelle D. J., Bradt J. E., Serth-Guzzo J., Takekoshi T., Evans T. L., Pearce E. J., and Wilson P. R. *Semicristalline polymers via ring-opening polymerization: preparation and polymerization of alkylene phthalate cyclic oligomers*, Macromolecules **31** (1998) 4782–4790.
[89]. Brunelle D. J., *Cyclic oligomer chemistry*, Journal of Polymer Science A : Polymer Chemistry **46** (2008) 1151–1164.

[90]. Hall A.J. and Hodge P., *Recent research on the synthesis and applications of cyclic oligomers*, Reactive & Functional Polymers **41** (1999) 133–139.
[91]. Bryant J. J. L. and Semlyen J. A., *Cyclic polyesters: 7. Preparation and characterization of cyclic oligomers from solution ring-chain reactions of poly(butylene terephthalate)*, Polymer **38** (1997) 4531–4537.
[92]. Pat. 20090264611 USA (1995), AC08G63183FI, Hamano T., Yamamoto M., Matsuzono S., and Noda K., *Polybutylene Terephthalate*.
[93]. Burch R., Lustig S.R., and Spinu M., *Synthesis of cyclic oligoesters and their rapid polymerization to high molecular weight*, Macromolecules **33** (2000) 5053 – 5064.
[94]. Ungar G. and Zeng X. B., *Learning polymer crystallization with the aid of linear, branched and cyclic model compounds*, Chemical Reviews **101** (2001) 4157 –4188.
[95]. Ishak Z. A .M., Shang P., and Karger-Kocsis J., *A modulated DSC study on the in situ polymerization of cyclic butylene terephthalate oligomers*, Journal of Thermal Analysis and Calorimetry **84** (2006) 637–641.
[96]. Ishak Z. A. M., Gatos K. G., and Karger-Kocsis J., *On the in-situ polymerization of cyclic butylene terephthalate oligomers: DSC and rheological studies*, Polymer Engineering and Science **46** (2006) 743–750.
[97]. Parton H., Baets J., Lipnik P., Goderis B., Devaux J., and Verpoest I., *Properties of poly(butylene terephthatlate) polymerized from cyclic oligomers and its composites*, Polymer **46** (2005) 9871–9880.
[98]. Hakme C., Stevenson I., Maazouz A., Cassagnau P., Boiteux G., and Seytre G., *In situ monitoring of cyclic butylene terephtalate polymerization by dielectric sensing*, Journal of non-crystalline solids **353** (2007) 4362–4365.
[99]. Harsch M., Karger-Kocsis J., and Apostolov A. A., *Crystallization-induced shrinkage, crystalline and thermomechanical properties of in situ polymerized cyclic butylene terephthalate*, Journal of Applied Polymer Science **108** (2008) 1455–1461.
[100]. Pang K., Kotek R., Tonelli A., *Review of conventional and novel polymerization processes for polyesters*, Progress in Polymer Science **31** (2006) 1009–1037.
[101]. Tripathy R., Elmoumni A., Winter H. H., and MacKnight W. J., *Effects of catalyst and polymerization temperature on the in-situ polymerization of cyclic poly(butylene terephthalate) oligomers for composite applications*, Macromolecules **38** (2005) 709–715.
[102]. Garcia-Gutierrez M.C., Nogales A., Rueda D.R., Domingo C., Garcia-Ramos J. V., Broza G., Roslaniec Z., Schulte K., Davies R. J., and Ezquerra T. A., *Templating of crystallization and shear-induced self-assembly of single-wall carbon nanotubes in a polymer-nanocomposite*, Polymer **47** (2006) 341–345.
[103]. Wu D., Wu L., Yu G. Xu B., and Zhang M., *Crystallization and thermal behavior of multiwalled carbon nanotube/poly(butylene terephthalate) composites*, Polymer Engineering and Science **48** (2008) 1057–1067.
[104]. Nogales A., Broza G., Roslaniec Z., Schulte K., Sics I., Hsiao B. H., Sanz A., García Gutiérrez M. G., Rueda D. R., Domingo C., and Ezquerra T. A., *Low percolation threshold in nanocomposites based on oxidized single wall carbon nanotubes and poly(butylene terephthalate)*, Macromolecules **37** (2004) 7669–7672
[105]. Ania F., Broza G., Mina M. F., Schulte K., Roslaniec Z., and Balta-Calleja F. J., *Micromechanical properties of poly(butylene terephthalate) nanocomposites with single- and multi-walled carbon nanotubes*, *Composite Interfaces* **13** (2006) 33–45.

[106]. Kwiatkovska M., Broza G., Schulte K, and Roslaniec Z., *The in-situ synthesis of polybuthylene terephthalate/carbon nanotubes composites*, Reviews on Advanced Materials Science **12** (2006) 154–159.
[107]. Mathew G., Hong, J. P., Rhee J. M., Lee H. S. and Nah C., *Preparation and characterization of properties of electrospun poly(butylene terephthalate) nanofibers filled with carbon nanotubes*, Polymer testing **24** (2008) 712–717.
[108]. Baets J., Godara A., Devaux J., and Verpoest I., *Toughening of polymerized cyclic butylene terephthalate with carbon nanotubes for use in composites*, Composites : A **39** (2008) 1756–1761.
[109]. Baets J., Godara A., Devaux J., and Verpoest I., *Toughening of isothermally polymerized cyclic butylene terephthalate for use in composites*, Polymer Degradation and Stability **95** (2010) 346 – 352.
[110]. Wu F. and Yang G., *Synthesis and properties of poly(butylene terephthalate)/multiwalled carbon nanotube nanocomposites prepared by in situ polymerization and in situ compatibilization*, Journal of Applied Polymer Science **118** (2010) 2929–2938.
[111]. Wu F. and Yang G., *Poly(butylene terephthalate) functionalized MWNTs by in situ ring-opening polymerization of cyclic butylene terephthalate oligomers*, Polymers Advanced Technologies, doi/10.1002/pat.1762, **22** (2011).
[112]. Hopkins A. R. and Lipeles R., *Preparation and characterization of single wall carbon nanotube-reinforced polycyanurate nanocomposites*, Polymer Preprints **46** (2005) 787-793.
[113]. Fang Z., Wang J., and Gu A., *Structure and properties of multiwalled carbon nanotubes/cyanate ester composites*, Polymer Engineering & Science **46** (2006) 670–679.
[114]. Okotrub A. V., Yudantsov N. F., and Aleksashin V. M., *Study of thermal and mechanical properties of composites from electroarc carbon nanotubes and thermostable binder based on cyanate ester*, Vysokomol. Soed.: A. **49** (2007) 1049–1055. (in Russian).
[115]. Che J. and Chan-Park M. B., *Reactive spinning of cyanate ester fibers reinforced with aligned amino-functionalized single wall carbon nanotubes*, Advanced Functional Materials **18** (2008) 888–897.
[116]. Tang Y. S., Kong J., Gu J. W., and Liang G-Z., *Reinforced cyanate ester resins with carbon nanotubes: surface modification, reaction activity and mechanical properties analyses*, Polymer-Plastics Technology and Engineering **48** (2009) 359–366.
[117]. *Chemistry and Technology of Cyanate Ester Resins*, ed. I. Hamerton, Glasgow: Chaman & Hall; (1994) 254 p.
[118]. Latypov Z. Z., and Pozdnyakov O. F. *Determination of conditions of producing of polymer films containing ordered structure of carbon nanotubes and fullerenes*, Letters to JTF **32** (2006) 28–33. (in Russian).
[119]. McIntosh D., Khabashesku V. N., and Barrera E. V., *Processing and mechanical properties of continuous fiber systems made from fluorinated single-walled carbon nanotube-polypropylene composites* / D. McIntosh, // Chemistry of materials. – 2006. – Vol. 18. – pp. 4561–4569.
[120]. Miaudet P., Badaire S., Maugey M., Derré A., Pichot V., Launois P., Poulin P., and Zakri C., *Hot-drawing of single and multiwall carbon nanotube fibers for hightoughness and alignment*, Nano letters **5** (2005) 2212–2215.

[121]. Zussman E., Yarin A. L., Bazilevsky A. V., Avrahami R., and Feldman M., *Electrospun polyaniline/poly(methyl methacrylate)-derived turbostratic carbon micro-/nanotubes*, Advanced Materials **18** (2006) 348–353.

[122]. Moniruzzaman M. and Winey I. K., *Polymer nanocomposites containing carbon nanotubes*, *Macromolecules* **39** (2006) 5194–5205.

[123]. Tseng C. H., Wang C. C., and Chen C. Y., *Functionalizing Carbon Nanotubes by Plasma Modification for the Preparation of Covalent-Integrated Epoxy Composites*, Chemistry of Materials **19** (2007) 308–315.

[124]. Fiedler B., Gojny F. H., Wichmann M. H. G., Nolte M. C. M., and Schulte K., *Fundamental aspects of nano-reinforced composites*, Composites science and technology **66** (2006) 3115–3125.

[125]. Goh H.W., Goh S.H., Xu G.O. Pramoda K. P., and Zhang W. D., *Dynamic mechanical behavior of in situ functionalized multi-walled carbon nanotube/phenoxy resin composite*, Chemical Physics Letters **373** (2003) 277–283.

[126]. Gojny F. H. , Nastalczyk J., Roslaniec Z., and Schulte K., *Surface modified multi-walled carbon nanotubes in CNT/epoxy-composites*, Chemical Physics Letters **370** (2003) 820–824.

[127]. Gojny F. H., Schulte K., *Functionalisation effect on the thermo-mechanical behaviour of multi-wall carbon nanotube/epoxy-composites*, Composites Science and Technology **64** (2004) 2303–2308.

[128]. Fife C. A., Niu J., and Mok K. J., *Synthesis and characterization of polyfunctional crosslinking agents for cyanate resins*, Journal of Polymer Science A : Polymer chemistry **33** (1995) 1191–1202.

[129]. Flegler S. L., Heckman J. W., and Klomparens K. L., *Scanning and transmission electron microscopy: an introduction*, Oxford : Oxford University Press; (1993) 385 p.

[130]. Joy D. C., Romig A. D., and Goldstein J. I., *Principles of analytical electron microscopy*, New York : Plenum Press; (1986) 522 p.

[131]. Williams D. B. and Carter C. B., *Transmission electron microscopy*, New York : Plenum Press; **IV** (1996) 347 p.

[132]. Hunt B. J. and James M. I., *Polymer characterisation*, London: Blackie Academic & Professional; (1993) 336 p.

[133]. Bershtein V. A., and Egorov V. M. *Differential scanning Calorimetry in physical chemistry of polymers*, Leningrad : Khimiya; (1990) 256 p. (in Russian)

[134]. Smith E. and Dent G., *Modern Raman spectroscopy : a practical approach*, Chichester : John Wiley & Sons. Ltd; (2005) 222 p.

[135]. Rao A. M., Richter E., Bandow S., Chase B., Eklund P. C., Williams K. A., Fang S., Subbaswamy K. R., Menon M., Thess A., Smalley R. E., Dresselhaus G., and Dresselhaus M. S., *Diameter-selective Raman scattering from vibrational modes in carbon nanotubes*, Science **275** (1997) 187–191.

[136]. Costa S., Borowiak-Palen E. , Kruszyñska M., Bachmatiuk A., and Kalenczuk R. J., *Characterization of carbon nanotubes by Raman spectroscopy*, Materials Science–Poland **26** (2008) 433-441.

[137]. Nilsen L. *Mechanical properties of polymers and polymer compositions*, Moscow : Khimiya; (1978) 312 p. (in Russian).

[138]. Dresselhaus M. S, Dresselhaus G, Saito R, and Jorio A., *Raman spectroscopy of carbon nanotubes*, Physics Reports **409** (2005) 47-99.

[139]. Keszler A. M, Nemes L, Ahmada S. R, and Fanga X., *Characterisation of carbon nanotube materials by Raman spectroscopy and microscopy–a case study of*

multiwalled and single walled samples, Journal of Optoelectronics and Advanced Materials **6** (2004) 1269–1274.

[140]. Donato M. G, Galvagno S, Messina G, Milone C, Pistone A, and Santangelo S., *Raman analysis of MWCNTs produced by catalytic CVD: derivation of a scaling law for the growth Parameters*, J. Raman Spectroscopy **39** (2008) 141–146.

[141]. Skipa T., Lellinger D., Böhm W., Saphiannikova M., and Alig I., *Shear-stimulated formation of multi-wall carbon nanotube networks in polymer melts*, Physica status solidi : B **246** (2009) 2453–2456.

[142]. Skipa T., Lellinger D., Böhm W., Böhm W., Saphiannikova M., and Alig I., *Influence of shear deformation on carbon nanotube networks in polycarbonate melts: Interplay between build-up and destruction of agglomerates*, Polymer **51** (2010) 201–210.

[143]. Riddle R.W., Lemieux M.C., Cicero G., Artyukhin A. B., Tsukruk V. V., Grossman J. C., Galli G, and Noy A., *Single functional group interactions with individual carbon nanotubes*, Nature nanotechnology **2** (2007) 692–697.

[144]. Lorenzo M. L. D. and Righetti M. C., *Morphological analysis of poly(butylene terephtalate) SPH spherulites during fusion*, Polym. Bulletin **53** (2004) 53-62.

[145]. *Nanotechnologies. Alphabet for everyone*, ed. Tret'yakov D., Moscow: Fizmatlit; (2008) 368 p. (in Russian).

[146]. Lusenkov A., Gomza Yu. P., Davidenko V. V., and Klepko V.V., *Structure and properties of polymer electrolytes based on PEG300 and carbon nanotubes*, Fizika kondensovanykh vysokomolekulyarnykh system, **14** (2010) 15–20. (in Russian).

[147]. *Dynamic mechanical analiser: temperature-time superposition*, Mettler Toledo, On-line laboratory of Mettler Toledo in Russia (2008) http://www.mtrus.com/lab/ta/dma2/tts/

[148]. Collins P. and Hagerstrom J., *Creating high performance conductive composites with carbon nanotubes*, Hyperion Catalysis International, http://www.hyperioncatalysis.com/articles2.htm

[149]. Gibson R. F., Ayorinde E. O., and Wen Y. F., *Vibrations of carbon nanotubes and their composites: a review*, Composites Science and Technology **67** (2007) 1–28.

[150]. McNally T., Pötschke P., Halley P., Murphyc M., Martinc D., Belld S. E. J., Brennane G. P., Beinf D., Lemoineg P., and Quinng J. P., *Polyethylene multiwalled carbon nanotube composite*s, Polymer **46** (2005) 8222–8232.

[151]. Pötschke P., Bhattacharyya A. R. , and Janke A., *Morphology and electrical resistivity of melt mixed blends of polyethylene and carbon nanotube filled polycarbonate*, Polymer **44** (2003) 8061–8069.

[152]. Kymakis E. and Amaratunga G. A. J., *Electrical properties of single-wall carbon nanotube-polymer composite films*, Journal of Applied Physics **99** (2006) 084302.1 – 084302.7.

[153]. Kim H. M., Choi M. S., Joo J., Cho S. J., and Yoon H. S., *Complexity in charge transport for multiwalled carbon nanotube and poly(methyl methacrylate) composites*, Physical Review : B **74** (2006) 054202 – 054202-7.

[154]. Eletsky A.V. *Transport properties of carbon nanotubes*, Uspekhi fizicheskikh nauk **179** (2009) 225–242. (in Russian).

[155]. Mdarhri A., Carmona F., Brosseau C., and Delhaes, P.; *Direct current electrical and microwave properties of polymer-multiwalled carbon nanotubes composites*, Journal of Applied Physics **103** (2008) 054303 – 054303-9.

[156]. Simsek Y., Ozyuzer L., Seyhan A.T., Tanoglu M., and Schulte K., *Temperature dependence of electrical conductivity in double-wall and multi-wall carbon*

nanotube/polyester nanocomposites, Journal of Materials Science **42** (2007) 9689–9695.

[157]. Rahatekar S. S. , Hamm M., Shaffer M. S. P., and Elliott J. A., *Mesoscale modeling of electrical percolation in fiber-filled systems*, Journal of Chemical Physics **123** (2005) 134702-1 – 134702-5.

[158]. Stauffer D. and Aharony A., *Introduction to percolation theory,* London: Taylor & Francis; (1992) 181 p.

[159]. Balberg I., Anderson C.H., Alexander S., and Wagner N., *Excluded volume and its relation to the onset of percolation*, Physical Reviews : B **30** (1984) 3933–3943.

[160]. Kirkpatrick S., *Percolation and conduction*, Reviews of Modern Physics **45** (1973) 574–588.

[161]. Sahimi M., *Applications of percolation theory*, London: Taylor & Francis editor; (1994) 258 p.

[162]. Hu G., Zhao C., Zhang S., Yang M., Wang Z., *Low percolation thresholds of electrical conductivity and rheology in poly(ethylene terephthalate) through the networks of multi-walled carbon nanotubes*, Polymer **47** (2006) 480–488.

[163]. Ulanski J., and Kryszewski M., *Electrical conductivity in heterogeneous organic polymeric systems*, Polish Journal of Chemistry **69** (1995) 651-673.

[164]. Gibson R. F., Ayorinde E. O., and Wen Y.-F., *Vibrations of carbon nanotubes and their composites: A review*, Composites Science and Technology **67** (2007) 1-28.

[165]. Sheng P. L., *Fluctuation-Induced tunneling conduction in disordered materials*, Physical Review, B **21** (6) (1980) 2180-2195.

[166]. Zhang R., Baxendale M., and Peijs T., *Universal resistivity-strain dependence of carbon nanotube/polymer composites*, Physical Review, B **76** (2007) 195433.1-195433.5.

[167]. Reich S., Thomsen Ch., and Maultzsch J., *Carbon nanotubes*, Wiley-VCH: Darmstadt, Germany; (2004) 215 p.

[168]. Wilder J. W. G., Venema L. C., Rinzler A. G., and Smalley R. E. Dekker C., *Electronic structure of atomically resolved carbon nanotubes*, Nature **391** (1998) 59-62.

[169]. Yeletsky A.V. *Transport properties of carbon nanotubes*, Progresses in physical sciences, **179** (2009) 1775-1781. (in Russian).

[170]. Bockrath M., Cobden D. H., Andrew J. L., Rinzler G., Smalley R. E., Balents L., and McEuen P. L., *Luttinger-liquid behavior in carbon nanotubes*, Nature **397** (1998) 598.

[171]. Frank S., Poncharal P., Wang Z. L., and de Heer W. A., *Carbon Nanotube Quantum Resistors*, Carbon Nanotube Quantum Resistors Science **280** (1998) 1744.

[172]. Ahmad K., Pan W., *Dramatic effect of multiwalled carbon nanotubes on the electrical properties of alumina based ceramic nanocomposites*, Composites Science and Technology **69** (2009) 1016-1021.

[173]. Braun D., Gustafsson G., McBranch D., and Heeger A. J., *Electroluminescence and electrical transport in poly(3-octylthiophene) diodes*, Journal of Applied Physics **72** (2009) 564 – 568.

[174]. Li H. J., Lu W. G., Li J. J., Bai X. D., and Gu C. Z., *Multichannel Ballistic Transport in Multiwall Carbon Nanotubes*, Phys. Rev. Lett. **95** (2005) 086601.1-086601.4.

[175]. Lan C., Zakharov D. N., Reifenberger R. G., *Determining the optimal contact length for a metal/multiwalled carbon nanotube interconnect*, Appl. Phys. Lett. **92** (2008) 213112.1-213112.3.
[176]. Pat. 52506 Ukraine (2010), C08G 73/00, Fainleib O. M., Bardash L. V., Grigoryeva O. P., Boiteux G. , and Ulanski J., *Method of producing of polycyanurates*.
[177]. Fainleib A., Bardash L., and Boiteux G., *Catalytic effect of carbon nanotubes on polymerization of cyanate ester resins*, eXPRESS Polymer Letters **3** (2009) 477–482.
[178]. Li W. Ling G., Xin W., *Triazine reaction of cyanate ester resin systems catalyzed by organic tin compound: kinetics and mechanism*, Polymer International **53** (2004) 869–876.
[179]. Osei-Owusu A. and Martin G. C., *Catalysis of cyclotrimerization of cyanate ester resin systems*, Polymer Engineering and Science **32** (1992) 535–541.
[180]. Carey F. A. and Sundberg R. J., *Advanced organic chemistry A* : structure and mechanisms, Verlag: Springer; (2007) 1199 p.
[181]. *Thermostable polycyanurates: synthesis, modification, structure and properties*, ed. Fainleib A., New York : Nova Science Publishers Inc.; (2010) 370 p.
[182]. Hong W. T. and Tai N. H., *Investigations on the thermal conductivity of composites reinforced with carbon nanotubes*, Diamond & Related Materials **17** (2008) 1577–1581.
[183]. Chen Y. M. and Ting J. M., *Ultra high thermal conductivity polymer composites*, Carbon **40** (2002) 359–362.
[184]. Godovsky Yu. K., *Thermal physics of polymers*, Moscow : Khimiya; (1982) 280 p. (in Russian)
[185]. Jen P. D. *Ideas of scaling in physics of polymers* (translation from English, ed. I. M.Lifshits, Moscow : Mir; (1982) 368 p. (in Russian).
[186]. Cipriano B. H., Kota A. K., Gershon A. L., Laskowski C. J., Kashiwagi T., Bruck H. A., and Raghavan S. R., *Conductivity enhancement of carbon nanotube and nanofiber-based polymer nanocomposites by melt annealing*, Polymer **49** (2008) 4846–4851.
[187]. Xie S. S., Li W. Z., Pan Z. W., Chang B. H., and Sun L. F., *Carbon nanotube arrays*, Microstructure and Processing **286** (2000) 11–15.
[188]. Hammel E., Tang X., Trampert M., Schmitt T., Mauthner K., Eder A., and Pötschke P. , *Carbon nanofibers for composite applications*, Carbon **42** (2004) 1153–1158.
[189]. Georjon O., Galy J., and Pascault J.P., *Isothermal curing of an uncatalyzed dicyanate ester monomer: kinetics and modeling*, Journal of Applied Polymer Science **49** (1993) 1441–1452.
[190]. Georjon O. and Galy J., *Effects of crosslink density on the volumetric properties of high Tg polycyanurate networks*, Polymer **39** (1998) 339–345.

Publications

1. ***Electrical conductivity of polymer/carbon nanotubes nanocomposites at low temperatures***

L. Bardash, G. Boiteux, R. Grykien, I. Głowacki, J. Ulanski, A. Fainleib, G. Seytre *submitted to Composites and Science Technology* (2011)

2. ***Conductive polymer nanocomposites based on poly(butylene terephthalate) and multi-walled carbon nanotubes***

L. Bardash, G. Boiteux, G. Seytre, A. Fainleib

Ukr. Polym. J., **32** (2010) 51–55.

3. ***Nanocomposites based on polycyanurates filled by carbon nanotubes***

L. Bardash, A. Fainleib

Ukr. Polym. J., **32** (2010) 287–298.

4. ***Effect of small additions of carbon nanotubes on thermal conductivity of nanocomposites based on crosslinked polycyanurate***

V. Korskanov, L. Bardash, A. Fainleib

Reports of the National Academy of Sciences of Ukraine, № 9, (2009) 144-148.

5. ***Catalytic effect of carbon nanotubes on polymerization of cyanate ester resins***

A. Fainleib, L. Bardash, G. Boiteux

eXPRESS polymer letters, **3** (2009) 477–482.

6. ***Novel conductive polymer composites based on poly(butylene terephtalate) filled with carbon fibers***

L. Bardash, G. Boiteux, G. Seytre, C. Hakme, N. Dargère, A. Rybak, F. Melis

E-polymers, № 155 (2008) 1–6.

7. ***Patent of Ukraine,*** № 52506 (2010). ***Method of producing of polycyanurate***

A. Fainleib, L. Bardash, O. Grigoryeva, G. Boiteux, J. Ulanski

8. ***Patent of Ukraine,*** № 50520 (2010). ***Method of producing of polycyanurate***

A. Fainleib, O. Grigoryeva, K. Gusakova, I. Danilenko, L. Bardash, N. Lacoudre, D. Grande